ME 563
MECHANICAL VIBRATIONS

Fall 2010

Potter
MWF 4:30 p.m.-5:20 p.m.

Instructor: Prof. D. E. Adams
Room: ME 361
Email: deadams@purdue.edu
Phone: 496-6033

1 Introduction to Mechanical Vibrations

1.1 Bad vibrations, good vibrations, and the role of analysis

Vibrations are oscillations in mechanical dynamic systems. Although any system can oscillate when it is forced to do so externally, the term "vibration" in mechanical engineering is often reserved for systems that can oscillate freely without applied forces. Sometimes these vibrations cause minor or serious performance or safety problems in engineered systems. For instance, when an aircraft wing vibrates excessively, passengers in the aircraft become uncomfortable especially when the frequencies of vibration correspond to natural frequencies of the human body and organs. In fact, it is well known that the resonant frequency of the human intestinal tract (approx. 4-8 Hz) should be avoided at all costs when designing high performance aircraft and reusable launch vehicles because sustained exposure can cause serious internal trauma (Leatherwood and Dempsey, 1976 NASA TN D-8188). If an aircraft wing vibrates at large amplitudes for an extended period of time, the wing will eventually experience a fatigue failure of some kind, which would potentially cause the aircraft to crash resulting in injuries and/or fatalities. Wing vibrations of this type are usually associated with the wide variety of flutter phenomena brought on by fluid-structure interactions. The most famous engineering disaster of all time was the Tacoma Narrows Bridge disaster in 1940 (see Figure 1.1 below). It failed due to the same type of self-excited vibration behavior that occurs in aircraft wings.

Figure 1.1: (left) View of Tacoma Narrows Bridge along deck; (right) view of torsional vibration

In reading books and technical papers on vibration including the previous paragraph, engineering students are usually left with the impression that all vibrations are detrimental because most publicized work discusses vibration reduction in one form or another. But

vibrations can also be beneficial. For instance, many different types of mining operations rely on sifting vibrations through which different sized particles are sorted using vibrations. In nature, vibrations are also used by all kinds of different species in their daily lives. Orb web spiders, for example, use vibrations in their webs to detect the presence of flies and other insects as they struggle after being captured in the web for food. The reason that mechanical systems vibrate freely is because energy is exchanged between the system's inertial (masses) elements and elastic (springs) elements. Free vibrations usually cease after a certain length of time because damping elements in systems dissipate energy as it is converted back-and-forth between kinetic energy and potential energy.

The role of mechanical vibration analysis should be to use mathematical tools for *modeling* and *predicting* potential vibration problems and solutions, which are usually not obvious in preliminary engineering designs. If problems can be predicted, then designs can be modified to mitigate vibration problems before systems are manufactured. Vibrations can also be intentionally introduced into designs to take advantage of benefits of relative mechanical motion and to resonate systems (e.g., scanning microscopy). Unfortunately, knowledge of vibrations in preliminary mechanical designs is rarely considered essential, so many vibration studies are carried out only after systems are manufactured. In these cases, vibration problems must be addressed using passive or active design modifications. Sometimes a design modification may be as simple as a thickness change in a vibrating panel; added thickness tends to push the resonant frequencies of a panel higher leading to less vibration in the operating frequency range. Design modifications can also be as complicated as inserting magneto-rheological (MR) fluid dampers into mechanical systems to take energy away from vibrating systems at specific times during their motion. The point here is that design changes prior to manufacture are less expensive and more effective than design modifications done later on.

1.2 Modeling issues

Modeling is usually 95% of the effort in real-world mechanical vibration problems; however, this course will focus primarily on the derivation of equations of motion, free response and forced response analysis, and approximate solution methods for vibrating systems. Figure 1.2 illustrates one example of why modeling can be challenging in mechanical vibrating systems. A large crane on a shipping dock is shown loading/unloading packages from a cargo ship. In one possible vibration scenario, the cable might be idealized as massless and the crane idealized as rigid. In

this simple case, the package and crane both oscillate as rigid bodies; the package oscillates about the end of the crane and the crane oscillates about its base point of rotation as the two exchange energy. These vibrations would most likely correspond to relatively *low frequencies* and would take place in addition to the gross dynamical motion of the crane and package. Two coupled ordinary differential equations would be needed in this case to model the discrete, independent motions of the crane and package.

This model might be sufficient in some cases, but what if the mass of the cable is comparable to the mass of the package? In this case, the crane and package still behave like rigid bodies, but the cable will probably vibrate either transversely or longitudinally as a continuous body along its length. These *higher frequency* vibrations would require that both ordinary differential equations for the crane and package and partial differential equations of the cable be used to model the entire system. Furthermore, if the assumption of rigidity in the crane were also relaxed, then it too would need to be modeled with partial differential equations. All of these complications would be superimposed on top of the simple rigid body dynamics of the crane and package.

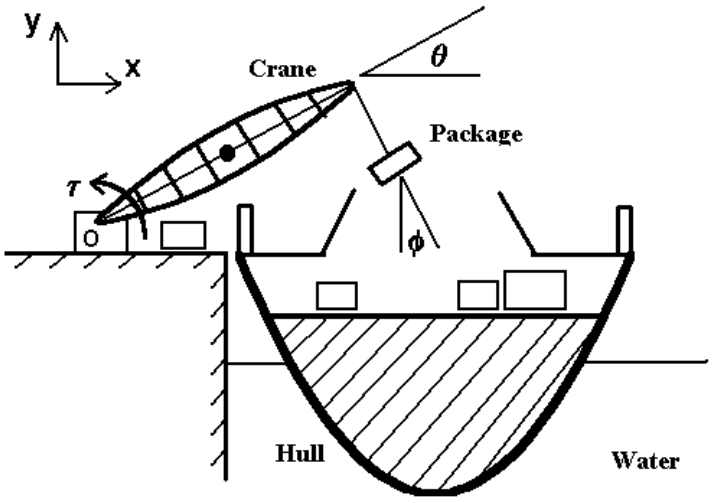

Figure 1.2: Crane for loading/unloading packages from cargo ship. Different regimes of operation require different levels of sophistication in the mechanical vibration model.

We will have the opportunity to discuss modeling considerations throughout the course when case studies of vibration phenomena are used to reinforce theoretical concepts and analysis procedures. Before starting to analyze systems, we must be able to derive differential equations

of motion that adequately describe the systems. There are many different methods for doing this; these are discussed in Chapter 2.

1.3 Linear superposition as a "working" principle

We cannot discuss everything in this course. In particular, there is not sufficient time to present linear and nonlinear methods of vibration analysis. Therefore, the course will primarily focus on linear vibrating systems and linear approaches to analysis. Only certain special characteristics of nonlinear systems will be introduced during the semester. Because the decision has been made to talk primarily about linear systems, the principle of superposition will hold in every problem that is discussed. Instead of stating this principle at the beginning of the course, and referencing it when it is needed in proofs and derivations, we will view it more as a "working" principle. In other words, linear superposition will guide us in our analysis of free and forced linear vibrations. When we begin to analyze vibrations, we will look to the principle of superposition to help us move forward in our analyses. Recall that a mathematical operator, $L[\bullet]$, which obeys the principle of linear superposition by definition satisfies the following two expressions:

$$L[ax] = aL[x] \tag{1.1}$$

and

$$L[ax + by] = L[ax] + L[by] \tag{1.2}$$

where L is said to operate on the two different functions, x and y, and a and b are constants. Eq. (1.1) is the principle of *homogeneity* and Eq. (1.2) is the principle of *additivity*. These two expressions may seem trivial or obvious, but they will in fact be extraordinarily useful later in the course. The important point to remember is that linear systems, which are governed by linear operators, $L[\bullet]$, are equal to the sum of their parts. Although this statement is profound and may even be fruit for philosophical discussions, the motivation for putting linear vibration into the context of linear superposition here is that it makes vibration analysis in free and forced systems much easier to develop and understand. More will be said about superposition in Chapter 3.

1.4 Review of kinematics and generalized coordinate descriptions

This section will review some of the fundamental techniques in particle kinematics. Note that this is only a review so no attempt is being made to cover everything here. Student should take this opportunity to refresh their memories of undergraduate courses in mechanics. *Generalized coordinates* are the basis for our *kinematic* description of vibrating bodies. Generalized coordinates are usually either position variables (e.g., x, y, z, and r), angular variables (e.g., ϕ, θ, and α), or a combination thereof (e.g., $r\cos\phi$). We must choose our set of generalized variables in each problem to adequately describe the *position* and *orientation* of all bodies in the mechanical system of interest. Note that the position and orientation are both important because both of these coordinates are associated with kinetic and potential energy storage. The minimum number of coordinates required is equal to the *degrees-of-freedom* (DOFs). Sometimes the number of DOFs is not obvious. For example, Figure 1.3 illustrates a pendulum-cart system that has many translating and rotating inertias. The question is: How many generalized coordinates are required to locate and orient all of the inertias?

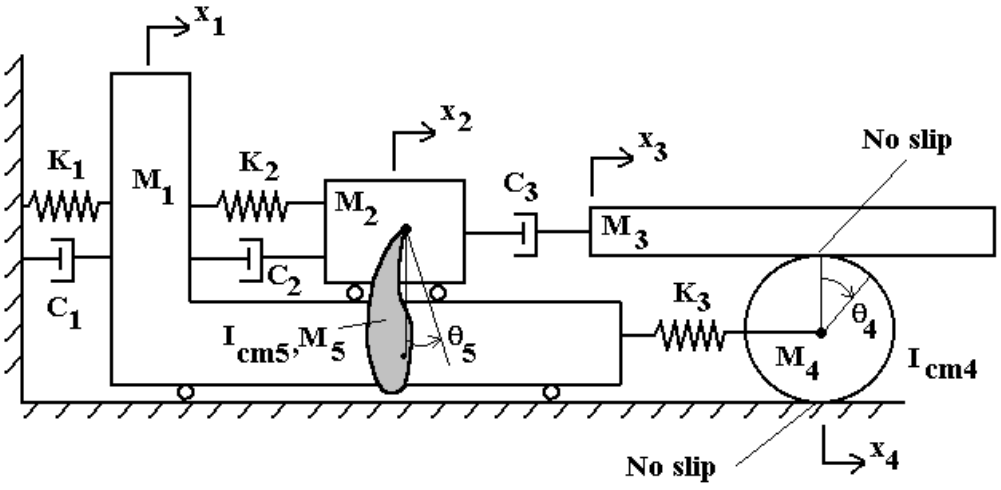

Figure 1.3: Mass-spring-damper-pendulum cart system

In order to locate and orient every body, it appears as if one coordinate is needed for M_1, one coordinate for M_2, one coordinate for M_3, two coordinates for M_4, and two coordinates for M_5: a total of seven coordinates are needed. But all of these coordinates are not actually required because there are some constraints between them. First, the translation of M_3 is equal to the

motion of the center-of-mass of M_4. Second, the translation of M_4 is proportional to its rotation, $x_4=R_4\theta_4$. Third, the translation of M_5 is equal to the translation of M_2 plus a component due to the rotation of M_5. With a total of three constraints, the number of DOFs is reduced as follows:

$$\begin{aligned} \#\,DOFs &= \#\begin{matrix}\text{coordinates}\\ \text{chosen}\end{matrix} - \#\begin{matrix}kinematic\,/\,geometric\\ \text{constraint equations}\end{matrix} \\ &= 7-3=4 \end{aligned}$$

Simply put, this statement implies that there should be four differential equations of motion for this system. The first step in any analytical vibrations problem should be to compute the number of DOFs. As an aside, the number of DOFs (i.e., ½ the order of the system) must also always be estimated prior to applying experimental vibration techniques.

There are many different common sets of generalized coordinates in use for mechanical vibration analysis. If a position vector, $\mathbf{r}$, of a particle (or center-of-mass) is written in terms of its associated generalized (possibly) curvilinear coordinates, q_i , as follows:

$$\mathbf{r} = \mathbf{r}(q_1, q_2, q_3) \tag{1.3}$$

then the differential tangent vector, $d\mathbf{r}$, is given by,

$$\begin{aligned} d\mathbf{r} &= \frac{\partial \mathbf{r}}{\partial q_1}dq_1 + \frac{\partial \mathbf{r}}{\partial q_2}dq_2 + \frac{\partial \mathbf{r}}{\partial q_3}dq_3 \\ &= h_{11}dq_1\left(\frac{1}{h_{11}}\frac{\partial \mathbf{r}}{\partial q_1}\right) + h_{22}dq_2\left(\frac{1}{h_{22}}\frac{\partial \mathbf{r}}{\partial q_2}\right) + h_{33}dq_3\left(\frac{1}{h_{33}}\frac{\partial \mathbf{r}}{\partial q_3}\right) \\ &= h_{11}dq_1\mathbf{e}_1 + h_{22}dq_2\mathbf{e}_2 + h_{33}dq_3\mathbf{e}_3 \end{aligned} \tag{1.4}$$

where the generalized coordinate unit vectors, $\mathbf{e}_k$, are given in parenthesis in the second of these equations and are chosen to be orthogonal in most vibration problems, and the h_{kk} are scale factors associated with the generalized coordinate differentials, dq_k. For example, the cylindrical coordinate system in terms of the Cartesian coordinate unit vectors is given by,

$$\mathbf{r} = r\cos\theta\mathbf{i} + r\sin\theta\mathbf{j} + z\mathbf{k}$$

(1.5)

so the differential position vector is,

$$d\mathbf{r} = (\cos\theta\mathbf{i} + \sin\theta\mathbf{j})dr + (-r\sin\theta\mathbf{i} + r\cos\theta\mathbf{j})d\theta + dz\mathbf{k}$$

(1.6)

with the following scale factors and orthogonal unit vectors:

$$h_{rr} = 1,\ h_{\theta\theta} = r,\ h_{zz} = 1$$
$$\mathbf{e}_r = \cos\theta\mathbf{i} + \sin\theta\mathbf{j},\ \mathbf{e}_\theta = -r\sin\theta\mathbf{i} + r\cos\theta\mathbf{j},\ \mathbf{e}_z = \mathbf{k}$$

(1.7)

The fundamental theorem of kinematics can now be used to compute the velocity vector directly (this equation is used later when computing velocity vectors for the kinetic energy terms). The general and specific forms (cylindrical coordinates) of the velocity, $d\mathbf{r}/dt$, are given below:

$$\begin{aligned}\dot{\mathbf{r}} &= h_{11}\dot{q}_1\mathbf{e}_1 + h_{22}\dot{q}_2\mathbf{e}_2 + h_{33}\dot{q}_3\mathbf{e}_3 \\ &= \dot{r}\mathbf{e}_1 + r\dot{\theta}\mathbf{e}_2 + \dot{z}\mathbf{e}_3\end{aligned}$$

(1.8)

There are other useful closed-form expressions for kinematic variables like acceleration, for example, which provide insight into various methods for deriving equations of motion in the next chapter. Moreover, we will see later that the acceleration in the $\mathbf{e}_k$ direction can be computed as follows:

$$a_k = \frac{1}{h_{kk}}\left[\frac{d}{dt}\left(\frac{\partial T}{\partial \dot{q}_k}\right) - \frac{\partial T}{\partial q_k}\right],\quad T = \frac{1}{2}\dot{\mathbf{r}}\cdot\dot{\mathbf{r}}$$
$$\text{e.g., cylindrical } a_\theta = \frac{1}{r}\left[\frac{d}{dt}\left(r^2\dot{\theta}\right) - 0\right] = r\ddot{\theta} + 2\dot{r}\dot{\theta}$$

(1.9)

which fits directly into Lagrange's approach for deriving differential equations of motion.

The important point to note here is that we must be able to describe how bodies move in order to derive physical equations of motion. Kinematics is the first essential element of vibration analysis. In the next chapter, methods for combining the kinematics and physics using Newtonian (vectorial) methods and analytical methods (e.g., energy/power, Lagrange) are discussed.

1.5 Review of energy and power expressions

This section will review some important ideas in energy and power in mechanical systems. These ideas are important because we will use analytical energy methods in many problems to derive equations of motion for vibrating systems. If an increment of mechanical work on a particle of mass M is denoted as ΔW, then this amount of work can be calculated using the force applied to the particle along the incremental change in path, $d\mathbf{r}$, of the particle as follows:

$$\Delta W = \mathbf{F} \cdot d\mathbf{r} \tag{1.10}$$

where the $\cdot$ denotes a dot product between the force and differential displacement vector. Note that the incremental amount of work is a scalar. Scalar quantities like this one will be used in Chapter 2 to develop elegant methods for deriving complicated equations of motion. Because the kinetic energy, T, of a particle is equal to the rate of change in ΔW with time, a convenient expression for T can be derived as follows:

$$\begin{aligned}
\frac{dT}{dt} &= \lim_{\Delta t \to 0} \frac{\Delta W}{\Delta t} = \mathbf{F} \cdot \frac{d\mathbf{r}}{dt} \\
T_2 - T_1 &= \int_1^2 \mathbf{F} \cdot \frac{d\mathbf{r}}{dt} dt \\
&= \int_1^2 \frac{d}{dt}\left(M \frac{d\mathbf{r}}{dt} \right) \cdot \frac{d\mathbf{r}}{dt} dt = \int_1^2 \frac{d}{dt}\left(\frac{1}{2} M \frac{d\mathbf{r}}{dt} \cdot \frac{d\mathbf{r}}{dt} \right) dt \\
&= \frac{1}{2} M \dot{\mathbf{r}} \cdot \dot{\mathbf{r}} \ \ (\text{for constant } M)
\end{aligned} \tag{1.11}$$

where the third equation in the sequence was obtained using Newton's second law (see Section 2.1 below). This expression for the kinetic energy of a particle works for any chosen set of coordinates with respect to an inertial reference frame. When using computer simulations to solve dynamics/vibrations problems, it is common practice to implement Eq. (1.8) in order to calculate the velocity vector.

For a rigid body, which is an infinite number of such particles, the kinetic energy can be found by summing the kinetic energies for all of the individual particles of mass, *dM*. This summation is performed using an integral over the entire body as follows

$$T = \frac{1}{2}\int_{Body} \dot{\mathbf{r}} \cdot \dot{\mathbf{r}} dM \qquad (1.12)$$

where the position vector, **r**, is the position of the mass particle, *dM* (see Figure 2.1). For reasons that will becomes clear later, it is best to write **r** with respect to the center of mass (CM) location, $\mathbf{R}_{CM}$, as follows:

$$\begin{aligned} \mathbf{r} &= \mathbf{R}_{CM} + \mathbf{r}_{CM/dM} \\ \dot{\mathbf{r}} &= \dot{\mathbf{R}}_{CM} + \frac{\partial \mathbf{r}_{CM/dM}}{\partial t} + \omega \times \mathbf{r}_{CM/dM} \\ &= \dot{\mathbf{R}}_{CM} + \omega \times \mathbf{r}_{CM/dM} \end{aligned} \qquad (1.13)$$

where $\mathbf{r}_{CM/dM}$ is the vector (constant length) drawn from CM to the infinitesimal particle *dM* and $\boldsymbol{\omega}$ is the angular velocity of the rigid body. Remember that the angular velocity of a rigid body does not depend on its translational motion. When Eq. (1.13) is substituted into Eq. (1.12), the following sequence of steps leads to a general expression for the kinetic energy of a rigid body:

$$
\begin{aligned}
T &= \frac{1}{2}\int_{Body}\left(\dot{\mathbf{R}}_{CM}+\omega\times\mathbf{r}_{CM/dM}\right)\cdot\left(\dot{\mathbf{R}}_{CM}+\omega\times\mathbf{r}_{CM/dM}\right)dM \\
&= \frac{1}{2}M\dot{\mathbf{R}}_{CM}\cdot\dot{\mathbf{R}}_{CM}+\mathbf{R}_{CM}\cdot\omega\times\int_{Body}\mathbf{r}_{CM/dM}dM+\frac{1}{2}\int_{Body}\left(\omega\times\mathbf{r}_{CM/dM}\right)\cdot\left(\omega\times\mathbf{r}_{CM/dM}\right)dM \\
&= \frac{1}{2}M\dot{\mathbf{R}}_{CM}\cdot\dot{\mathbf{R}}_{CM}+\frac{1}{2}\omega\cdot\mathbf{H}_{CM}
\end{aligned}
$$

(1.14)

where $\mathbf{H}_{CM}$ is the total angular momentum of the rigid body about the CM. For motions in the plane with angular velocity $\omega\mathbf{k}$ and velocity vector $\mathbf{V}_{CM}=V_x\mathbf{i}+V_y\mathbf{j}$, the total kinetic energy is,

$$
\begin{aligned}
T &= \frac{1}{2}M\mathbf{v}\cdot\mathbf{v}+\frac{1}{2}\omega\cdot\mathbf{H}_{CM} \\
&= \frac{1}{2}M\left(v_x^2+v_y^2\right)+\frac{1}{2}\left(\omega\mathbf{k}\right)\cdot\left(I_{CM}\omega\right)\mathbf{k} \\
&= \frac{1}{2}M\left(v_x^2+v_y^2\right)+\frac{1}{2}\left(I_{CM}\omega^2\right)
\end{aligned}
$$

(1.15)

where I_{CM} is the planar mass moment of inertia of the body about the *CM*.

The potential energy, V, of a particle or rigid body is also important in the work to follow. Consider cases where an external force vector, $\mathbf{F}$, can be written in terms of a special potential function, $V=V(\mathbf{r},t)$, which is only a function of the particle coordinates in an inertial reference frame, ($\mathbf{e}_1$, $\mathbf{e}_2$, $\mathbf{e}_3$), and possibly time,

$$
\begin{aligned}
\mathbf{F} &= -\nabla V \\
&= -\frac{\partial V}{\partial x_1}\mathbf{e}_1-\frac{\partial V}{\partial x_2}\mathbf{e}_2-\frac{\partial V}{\partial x_3}\mathbf{e}_3
\end{aligned}
$$

(1.16)

In this case, the total work done as the potential energy decreases is calculated as follows,

$$W_{1-2} = V_1 - V_2 + \int_1^2 \frac{\partial V}{\partial t} dt$$

(1.17)

For instance, in a linear spring that acts to oppose applied forces according to $\mathbf{F}=-Kx\mathbf{i}$, where K is the spring constant of the spring (force/displacement), the calculation in Eq. (1.17) is given by,

$$\begin{aligned} W_{1-2} &= V_1 - V_2 \\ \int_0^x -Kx\mathbf{i} \cdot dx\mathbf{i} &= 0 - V_2 \\ -\frac{1}{2}Kx^2 &= -V_2(x) \end{aligned}$$

(1.18)

Thus, the potential energy stored in a linear spring is $Kx^2/2$, where x is the final displacement of the end of a spring that is initially undeformed. The potential energy stored in the gravitational field between a mass M and the earth is given by $V(x)=Mgx$, where x is the vertical distance from an arbitrary datum or reference height to the mass. Note that in both the spring and the gravitational potential energies, a conservative force is associated with the stored energy. In the spring the conservative force is $\mathbf{F}=-Kx\mathbf{i}$, whereas in the gravitational field the force is $\mathbf{F}=-Mg\mathbf{j}$. We will see in the next Chapter that by extracting all conservative forces, $\mathbf{F}_c$, from the total external force on a body, $\mathbf{F}=\mathbf{F}_c+\mathbf{F}_{nc}$, and representing them with potential energy terms, energy/power methods for deriving equations of motion can be obtained quite easily. We will have many opportunities to compute potential energies in different problems in the next Chapter.

2 Equations of Motion

In order to discuss vibrations in mechanical systems, we must first derive mathematical equations, which can then be used to analyze the free and forced vibrations of interest. These equations that describe the physics and kinematics of systems are called the *equations of motion* (EOMs). There are many techniques for deriving these equations among them Newton's second law of motion and Euler's equation, the conservation of energy (first law of thermodynamics), Hamilton's principle, an array of analytical variational methods in dynamics (e.g., principles of

Jourdain, Gauss-Gibbs) including Lagrange's equations (class I and II), and others. We will only talk about a few of these. Students are encouraged to consult texts on dynamics by Greenwood, Crandall, Thompson, Tse, Richardson, and Moon for a thorough review of each technique.

The important thing to understand here is how these techniques are different. In other words, we want to know which method to choose for particular types of problems and why. For instance, Newton's second law and Euler's equation offer more insight in many cases because they involve vectors, which are often easily visualized in the course of solving the problem; unfortunately, that insight comes at price: all of the external forces on each free body diagram must be known or expressible in terms of the independent variables, and the accelerations for each free body must be computed. Forces in 'real-world' problems usually involve physics that are not well known (e.g., friction, aerodynamic boundary conditions, etc.), whereas accelerations involve extensive amounts of kinematic algebra, which can be complicated when rotating body coordinate systems are used.

The key to applying Newtonian methods is to select the generalized coordinates so as to balance the effort required to mathematically express the physics ($\Sigma\mathbf{F}$) and kinematics ($\mathbf{A}_{CM}=d\mathbf{V}_{CM}/dt$). During this course, we will attempt to illustrate good ways to choose methods for deriving EOMs in general.

2.1 Newton's second law and Euler's equation

Newton's second law of translational motion for a rigid body of (constant) mass M subjected to a resultant external force vector, $\mathbf{F}_{CM}$, is

$$\mathbf{F}_{CM} = \frac{d\mathbf{P}_{CM}}{dt} = M\ddot{\mathbf{R}}_{CM}, \text{ where } \mathbf{P}_{CM} = M\mathbf{V}_{CM} \tag{2.1}$$

where $\mathbf{R}_{CM}$ is the position vector of the CM with respect to an inertial reference frame. Euler's equation for the rotational motion of a rigid body is,

$$\mathbf{M}_{CM} = \frac{d\mathbf{H}_{CM}}{dt}, \text{ where } \mathbf{H}_{CM} = \mathbf{R}_{CM} \times \mathbf{P}_{CM} \tag{2.2}$$

where $\mathbf{F}_{CM}$ is the sum of all external forces acting on inertia M, $\mathbf{P}_{CM}$ is the total linear momentum of inertia M moving with velocity $\mathbf{V}_{CM}$, $\mathbf{H}_{CM}$ is the total angular momentum of inertia M about its own center of mass (CM), $\mathbf{R}_{CM}$ is the position of the center of mass in an inertial reference frame, and $\mathbf{V}_{CM}=d\mathbf{R}_{CM}/dt$ is the absolute velocity of the center of mass with respect to the inertial reference frame.

The first thing to remember about Eq. (2.1) is that the acceleration (velocity) must be calculated with respect to an *inertial reference frame*. NEWTON'S SECOND LAW IS NOT VALID FOR RELATIVE COORDINATES. The second thing to remember about Eq. (2.1) is that $\mathbf{F}_{CM}$ includes ALL external forces (conservative and non-conservative) on the body. Thus, the free body diagram (FBD), which shows all external forces and moments acting on the body, must be accurate or else the resulting EOM will be wrong. Always make sure that the EOMs match the FBDs. We will have many opportunities to enforce these two rules.

Although the form of Euler's equation in Eq. (2.2) is correct and always works, there are alternative forms, which are easier to apply in many cases. If a point A is chosen around which to develop Euler's equation instead of CM, then the moment equation can be written in several other forms as follows:

$$\begin{aligned}\mathbf{M}_A &= \frac{d\mathbf{H}_A}{dt} + \dot{\mathbf{R}}_A \times M\dot{\mathbf{R}}_{CM} \\ &= \frac{d\mathbf{H}_{CM}}{dt} + \mathbf{r}_{A/CM} \times M\ddot{\mathbf{R}}_{CM} \\ &= \frac{d\mathbf{H}_A}{dt} + \mathbf{r}_{A/CM} \times M\ddot{\mathbf{R}}_A\end{aligned} \qquad (2.3a,b,c)$$

where the vectors in these equations are defined in Figure 2.1.

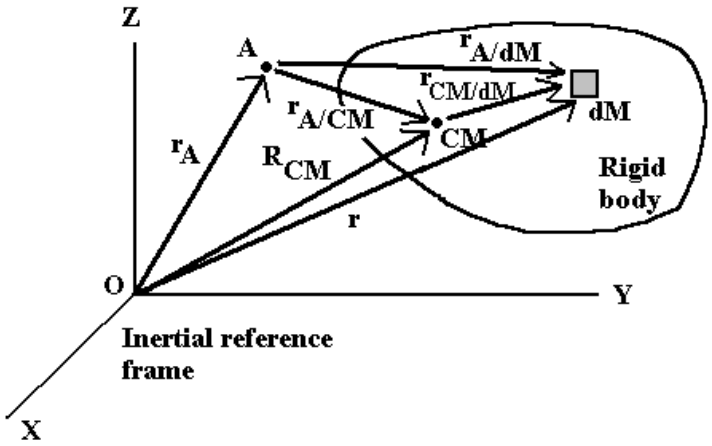

Figure 2.1: Coordinate system for developing various forms of Euler's equation

The reason Eqs. (2.3a,b,c) are all useful is because they simplify the kinematics tremendously in certain cases. Consider the system in Figure 2.2 below. A disk rolls on an incline as it is pulled down the incline by gravity and up the incline by the linear spring, *K*. The corresponding FBD is shown in the right of the figure. We will now illustrate the method for deriving EOMs using Newtonian (vectorial) techniques.

1. First, draw a schematic of the system if one is not provided. Assign as many coordinates as you need to define the position and orientation of all bodies in the system; make sure to label the positive directions for all coordinates and define any unit vectors you feel are appropriate to solve the problem. We are allowed to use relative coordinates in the problem; however, we must remember that the acceleration terms in Newton's equation and Euler's equation must be absolute (i.e., with respect to an inertial reference frame). The minimum number of coordinates needed to locate and orient all bodies in the system is by definition the number of DOFs; you should always state this in your solution. The number of DOFs in the system in Figure 2.2 is one because only x or ϕ is needed to locate and orient the disk. If you are not absolutely sure about the number of DOFs, the following formula may help you to find your redundant coordinates:

$$\#\,DOFs = \#\begin{matrix}\text{coordinates}\\ \text{chosen}\end{matrix} - \#\begin{matrix}kinematic\,/\,geometric\\ \text{constraint equations}\end{matrix} \qquad (2.4)$$

For example, if we choose both x or ϕ to locate and orient the disk, then we can use Eq. (2.4) to obtain the number of DOFs with the single constraint, $x=-a\phi$: #DOFs=#coord.-#constraints=2-1=1. We will choose the phase angle, ϕ, as our main coordinate. This means we will need to use the constraint equation, $x=-a\phi$, to eliminate all occurrences of x in our equations. Step 1 is primarily concerned with the kinematics of the system.

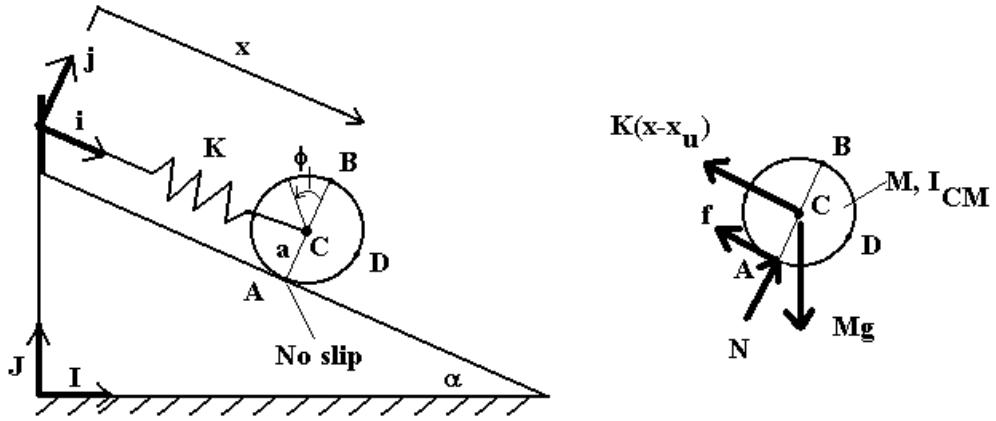

Figure 2.2: (Left) Sprung disk on incline and (right) free body diagram (FBD)

2. State any assumptions you made in drawing the schematic or any assumptions you will make in deriving the EOMs. For instance, the no slip condition in Figure 2.2 means that the velocity of the disk's point of contact with the surface is zero (i.e., the velocity of the disk relative to the surface is zero, $\mathbf{V}_{contact/A}=\mathbf{0}$, where A is a point inside the incline at the point of contact). This assumption is important and must be stated.

3. Draw the FBDs for every body in the system. Draw FBDs even for those bodies that you believe are not needed. We must put a lot of thought into FBDs because they will determine whether we get the correct EOMs in the end. It is usually best to re-draw coordinate systems with each FBD corresponding to individual bodies in the system. Compute forces in springs and dampers by using the relative motion across the element; the directions of these forces are determined by remembering that forces and dampers oppose increases in relative displacement or velocity across them. When we draw vectors on the FBD, we label vectors with magnitudes – the vectors take care of directionality.

4. Spend a few moments thinking about how you will write down only as many equations as you need to find the EOMs. We could write down every equation we think of, but this is usually not as effective as thinking about which equations we need and why. For example, we could write down both the force and moment equations for the inclined rolling disk in Figure 2.2. The force equation in the *x* direction will involve the friction force (unknown in terms of coordinates), gravity (known), and the restoring force in the spring (known). The force equation in the *y* direction will involve the normal force (unknown) and a gravitational component (known). The moment equation could be written around several different reference points:

Around point CM (center of mass):

$$\mathbf{M}_{CM} = \frac{d\mathbf{H}_{CM}}{dt}$$
$$(-a\mathbf{j})\times(-f\mathbf{i}) = \frac{d}{dt}\left(I_{CM}\dot{\phi}\mathbf{k}\right)$$
$$-af\mathbf{k} = I_{CM}\ddot{\phi}\mathbf{k} \Rightarrow I_{CM}\ddot{\phi} = -af$$

(2.5)

Around point A (point of contact inside the incline):

$$\mathbf{M}_A = \frac{d\mathbf{H}_A}{dt} + \dot{\mathbf{r}}_A \times M\dot{\mathbf{R}}_{CM} = \frac{d\mathbf{H}_A}{dt}$$
$$(a\mathbf{j})\times(-Mg\mathbf{J}) + (a\mathbf{j})\times\left(-K(x-x_u)\mathbf{i}\right) = \frac{d}{dt}\left(I_A\dot{\phi}\mathbf{k}\right)$$
$$-aMg\sin\alpha\mathbf{k} + aK(x-x_u)\mathbf{k} = I_{CM}\ddot{\phi}\mathbf{k} \Rightarrow I_A\ddot{\phi} = -aMg\sin\alpha + aK(x-x_u)$$

(2.6)

Around point B (point on perpendicular to point of contact):

$$\mathbf{M}_B = \frac{d\mathbf{H}_B}{dt} + \dot{\mathbf{r}}_B \times M\dot{\mathbf{R}}_{CM} = \frac{d\mathbf{H}_B}{dt}$$
$$(-2a\mathbf{j})\times(-f)\mathbf{i} + (-a\mathbf{j})\times\left(-Mg\mathbf{J} - K(x-x_u)\mathbf{i}\right) = \frac{d}{dt}\left(I_B\dot{\phi}\mathbf{k}\right)$$
$$-2af\mathbf{k} + aMg\sin\alpha\mathbf{k} - aK(x-x_u)\mathbf{k} = I_{CM}\ddot{\phi}\mathbf{k} \Rightarrow I_B\ddot{\phi} = -2af + aMg\sin\alpha - aK(x-x_u)$$

(2.7)

In this case, the moment equation about CM was the easiest to apply; however, it leaves us with an unknown, f, which can be found using Newton's second law in the x direction:

$$\begin{aligned}\mathbf{F}_{CM} &= M\mathbf{A}_{CM}\\ (\cdot)\mathbf{j} + \left(-K(x-x_u) - f + Mg\sin\alpha\right)\mathbf{i} &= M(\ddot{x})\mathbf{i}\\ -M\ddot{x} + Mg\sin\alpha - K(x-x_u) &= f\end{aligned}$$

(2.8)

5. Solve the resulting equations to obtain the EOMs; there should be as many EOMs as there are DOFs from Step 1. Upon substituting Eq. (2.8) into Eq. (2.5), the following EOM is obtained:

$$\left(I_{CM} + Ma^2\right)\ddot{\phi} + Ka^2\phi = -Mga\sin\alpha - aKx_u$$

(2.9)

Note that the only forces that do work on the body are the spring force and the gravitational force. This means that the friction force and normal force are both extraneous in our analysis. We only used them to solve for the EOM; they do not really play a role in our EOM. We will study other methods for deriving EOMs later that do not use extraneous forces like this one (called ideal forces of constraint).

6. Check to see if the EOM makes physical sense. Do not forget this step; it is probably the most important step for graduate students to perform. There are a few things we can check: Is the inertia positive? Are the stiffness and damping positive (stability)? Do the forces push or pull the system in the proper directions? etc. We will see later that there are several more checks for multiple DOF systems with more than one EOM.

7. Solve for the free and forced response characteristics (see Chapters 3 and 4). Check to make sure these characteristics and solutions make physical sense.

Step 5 above mentioned that Newtonian techniques require that all forces on each body are included; however, not all of the forces generally do work on the system. In fact, some of the forces simply hold the system together (i.e., no slip constraint, normal forces between smooth

surfaces, etc.). For instance, the normal force in Figure 2.2 does no work on the system because the disk does not move in the **j** direction. If we could ignore all of these so-called *idealized constraint forces* and only include the forces that do work (i.e., active forces), then it would be easier to derive the EOMs in many circumstances.

What if we just project the EOM onto the direction perpendicular to the constraint force? This projection would effectively eliminate the constraint but retain the active forces as desired. For example, if we projected Newton's second law of motion for the rolling disk onto the direction of motion, $\delta x\mathbf{i}$, then we could eliminate all but the "important" forces as follows:

$$
\begin{aligned}
&\left(\mathbf{F}_{CM} - M\mathbf{A}_{CM}\right)\cdot\delta\mathbf{r} = 0\\
&\left(\mathbf{F}_{active} + \mathbf{F}_{constr} - M\mathbf{A}_{CM}\right)\cdot\delta\mathbf{r} = 0\\
&\left(\left(N - Mg\cos\alpha\right)\mathbf{j} - f\mathbf{i} + \left(-K\left(x - x_u\right) + Mg\sin\alpha\right)\mathbf{i} - M\ddot{x}\mathbf{i}\right)\cdot\delta\mathbf{r} = 0\\
&\left(\left(N - Mg\cos\alpha\right)\mathbf{j} + \frac{I_{CM}\ddot{\phi}}{a}\mathbf{i} + \left(-K\left(x - x_u\right) + Mg\sin\alpha\right)\mathbf{i} - M\ddot{x}\mathbf{i}\right)\cdot\left(\delta x\mathbf{i}\right) = 0\\
&\left(\frac{I_{CM}\ddot{\phi}}{a} - M\ddot{x} - K\left(x - x_u\right) + Mg\sin\alpha\right)\delta x = 0\\
&\left(M + \frac{I_{CM}}{a^2}\right)\ddot{x} + K\left(x - x_u\right) - Mg\sin\alpha = 0 \text{ for arbitrary } \delta x
\end{aligned}
$$

(2.10)

where $\delta\mathbf{r} = \partial\mathbf{r}/\partial x\cdot\delta x + \partial\mathbf{r}/\partial\phi\cdot\delta\phi = \delta x\mathbf{i}$ is called the *total variation* of **r** with respect to the coordinates x and ϕ. We see that by projecting Newton's second law onto $\delta\mathbf{r}$ we were able to remove the normal force of constraint. Note that we substituted the other force of constraint, f, from Eq. (2.8). When we recognize ahead of time that the constraints will fall out of the equation with no effect, we can write the so-called d'Alembert-Lagrange principle for a single particle, M_i, as follows,

$$\left(\mathbf{F}_{active,i} - M_i\mathbf{A}_i\right)\cdot\delta\mathbf{r}_i = 0$$

(2.11)

where $\mathbf{A}_i$ is the absolute acceleration of the particle, $\mathbf{F}_{active,i}$ is the total active force on the particle, and $\delta\mathbf{r}_i$ is variation of the position vector of the particle. It is also sometimes more convenient to

replace the variation, $\delta\mathbf{r}_i$, with the first or second derivative of the variation to produce the generalized d'Alembert-Lagrange principle for a particle. This technique can be extended to multiple particles or rigid bodies, but we prefer to discuss an energy method first as follows.

2.2 Conservation of energy (first law of thermodynamics)

Energy principles are always applicable in vibrations so long as the necessary kinetic and potential energies can be calculated. Furthermore, energy methods only take into account active forces; idealized forces of constraint, which do no work, are ignored. This simplification is a significant advantage in systems with many components (i.e., DOFs). For a single degree-of-freedom (SDOF) system, the power equation is equal to the first law of thermodynamics,

$$\frac{d}{dt}(T+V)=\frac{dW_{nc}}{dt} \tag{2.12}$$

where W_{nc} is the work done by non-conservative (dissipative) forces during the motion, T is the kinetic energy, and V is the potential energy of the particle or body. For instance, the system in Figure 2.2 has $T=M(dx/dt)^2/2+I_{CM}(d\phi/dt)^2/2$, $V=-Mg(x-x_u)\sin\alpha$ (note V decreases for increasing x), and no non-conservative forces. With these energy expressions, Eq. (2.18) yields,

$$\begin{aligned}\frac{d}{dt}\left(\frac{1}{2}M\dot{x}^2+\frac{1}{2}I_{CM}\frac{\dot{x}^2}{a^2}-Mg(x-x_u)\sin\alpha+\frac{1}{2}K(x-x_u)^2\right)&=\frac{dW}{dt}\\ \left(M\ddot{x}+\frac{I_{CM}}{a^2}\ddot{x}-Mg\sin\alpha+K(x-x_u)\right)\dot{x}&=0\\ \left(M+\frac{I_{CM}}{a^2}\right)\ddot{x}-Mg\sin\alpha+K(x-x_u)&=0\end{aligned} \tag{2.13}$$

Note that in moving from the third to the fourth equation, there were two options for satisfying the equation, but the zero velocity condition is trivial and only a special case. Also note that before proceeding to take derivatives, the rotational kinetic energy was expressed in terms of the translational coordinate using the kinematic constraint. We will usually carry out this step when

applying the power method and when applying generalized energy methods in the next section; we will apply the constraints before taking derivatives to simplify the calculus.

Eq. (2.13) was relatively easy to obtain in comparison to any of the Newtonian-based EOMs. Of course, it is identical to Eq. (2.10) and to Eq. (2.9) when the kinematic constraint is enforced; however, there was no need to include either of the constraint forces because neither one of them does work on the disk. Likewise, the conservative forces due to gravity and the spring are accounted for by the potential energy expression, V. When there are non-conservative forces acting, then the work done by those forces must be computed. This calculation is performed using variational calculus, which simply projects the forces onto differential changes in the position vector. Assume that the non-conservative force is given by,

$$\mathbf{F} = F_1\mathbf{e}_1 + F_2\mathbf{e}_2 \tag{2.14}$$

where $\mathbf{e}_1$ and $\mathbf{e}_2$ are unit coordinate vectors and F_1 and F_2 are the components of the force. Also, assume that the position vector of application of the force is,

$$\mathbf{r}_A = x_1\mathbf{e}_1 + x_2\mathbf{e}_2 \tag{2.15}$$

where both x_1 and x_2 are functions of some generalized variable, q. Then the *spatial variation* of the position vector is given by,

$$\begin{aligned}\delta\mathbf{r}_A &= \frac{d\mathbf{r}_A}{dq}dq \\ &= \left(\frac{dx_1}{dq}\mathbf{e}_1 + \frac{dx_2}{dq}\mathbf{e}_2\right)dq\end{aligned} \tag{2.16}$$

Finally, the work done by the non-conservative force is found by projecting the force onto the differential in Eq. (2.16):

$$
\begin{aligned}
dW &= \mathbf{F}\cdot\delta\mathbf{r}_A \\
&= \left(F_1\mathbf{e}_1 + F_2\mathbf{e}_2\right)\cdot\left(\frac{dx_1}{dq}\mathbf{e}_1 + \frac{dx_2}{dq}\mathbf{e}_2\right)dq \\
&= \left(F_1\frac{dx_1}{dq} + F_2\frac{dx_2}{dq}\right)dq
\end{aligned}
$$

(2.17)

For example, if a force $f(t)=F_o\cos\omega_o t$ acts on the disk in the positive x direction (Figure 2.2), then the increment of work done on the disk is given by,

$$
\begin{aligned}
dW &= \mathbf{F}\cdot\delta\mathbf{r}_A \\
&= f(t)\mathbf{i}\cdot\left(\frac{dx}{dx}\mathbf{i}\right)dx \\
&= f(t)dx \\
&= F_o\cos\omega_o t dx
\end{aligned}
$$

(2.18)

and therefore the power equation in Eq. (2.12) becomes,

$$
\begin{aligned}
&\frac{d}{dt}\left(\frac{1}{2}M\dot{x}^2 + \frac{1}{2}I_{CM}\frac{\dot{x}^2}{a^2} - Mgx\sin\alpha + \frac{1}{2}K\left(x-x_u\right)^2\right) = \frac{dW}{dt} \\
&\left(M\ddot{x} + \frac{I_{CM}}{a^2}\ddot{x} - Mg\sin\alpha + K\left(x-x_u\right)\right)\dot{x} = F_o\cos\omega_o t\dot{x} \\
&\Rightarrow \left(M + \frac{I_{CM}}{a^2}\right)\ddot{x} - Mg\sin\alpha + K\left(x-x_u\right) = F_o\cos\omega_o t
\end{aligned}
$$

(2.19)

The important thing to remember about the energy method using the power equation, Eq. (2.12), is that the forces of constraint do no work and are not included in the analysis. Also, note that the technique as presented only produces one EOM and, consequently, only works for SDOF systems. Next, we will talk about a general energy method in analytical dynamics that can be used for any number of DOFs. This technique still requires us to find the kinetic and potential

energy expressions and to calculate the work done by external non-conservative forces, but it is generally simpler to apply than Newton's method in complicated problems.

2.3 Lagrange's equations of class II (holonomic form)

The energy method is Section 2.2 worked well and was simple to apply, but it was only valid for SDOF systems; i.e., we only produced one EOM. *Lagrange's equations* simply extend the energy method to accommodate multiple degree-of-freedom (MDOF) systems. Recall from Section 2.2 that if we want to ignore the ideal forces of constraint, then we can project Newton's second law of motion onto the variational displacement of the system – this operation eliminates the constraints and maintains the forces that do work on the system. If there are *N* particles, then Eq. (2.12) is repeated *N* times:

$$\sum_{i=1}^{N} \left(\mathbf{F}_{active,i} - M_i \ddot{\mathbf{r}}_i \right) \cdot \delta \mathbf{r}_i^{(k)} = 0 \qquad (2.20)$$

where $\mathbf{A}_i = d^2\mathbf{r}_i/dt^2$ is the absolute acceleration of the i^{th} particle, $\mathbf{F}_{active,i}$ is the total active force on that particle, and $\delta\mathbf{r}_i^k$ is the k^{th} order derivative of the variation of the position vector, $\mathbf{r}_i$. The definition of the variation is,

$$\delta \mathbf{r}_i^{(k)} = \sum_{r=1}^{n} \frac{\partial \mathbf{r}_i^{(k)}}{\partial q_r^{(k)}} \delta q_r^{(k)} \qquad (2.21)$$

where q_r is the r^{th} generalized coordinate and n is the total number of generalized coordinates. Each of the $\delta q^{(k)}_r$ variations is called an *arbitrary kinematic variation*; these variations must always satisfy the constraints on the system.

Lagrange's equations of class II follow directly from Eq. (2.20) after some variational calculus. First we make the following substitution,

$$\ddot{\mathbf{r}}_i \cdot \frac{\partial \mathbf{r}_i}{\partial q_r} = \frac{d}{dt}\left(\frac{\partial}{\partial \dot{q}_r}\left(\frac{1}{2}\dot{\mathbf{r}}_i \cdot \dot{\mathbf{r}}_i \right) \right) - \frac{\partial}{\partial q_r}\left(\frac{1}{2}\dot{\mathbf{r}}_i \cdot \dot{\mathbf{r}}_i \right)$$

(2.22)

into Eq. (2.20). Recall the similarity of this result to that in Eq. (1.9) for the acceleration computation in the generalized coordinate direction, q_r. Also, note that Eq. (2.22) is equal to the rate of change in T within a differential, which affords a different methodology for deriving Lagrange's equations. Then we decompose the resultant active force vectors on each particle into conservative (lamellar) and non-conservative components, $\mathbf{F}_{\text{active,i}}=\mathbf{F}_{\text{i,c}}+\mathbf{F}_{\text{i,nc}}$, and project them onto the corresponding variations to obtain the so-called generalized forces as described in the first term of Eq. (2.20) given Eq. (2.21):

$$\begin{aligned} Q_r &= \sum_{i=1}^{N} \left(\mathbf{F}_{active,i} \right) \cdot \frac{\partial \mathbf{r}_i^{(k)}}{\partial q_r^{(k)}} \\ &= \sum_{i=1}^{N} \left(\mathbf{F}_{i,c} + \mathbf{F}_{i,nc} \right) \cdot \frac{\partial \mathbf{r}_i^{(k)}}{\partial q_r^{(k)}} \\ &= \sum_{i=1}^{N} \left(-\nabla_i V + \mathbf{F}_{i,nc} \right) \cdot \frac{\partial \mathbf{r}_i^{(k)}}{\partial q_r^{(k)}} \\ &= -\frac{\partial V}{\partial q_r} + Q_r^* \end{aligned}$$

(2.23)

where Q_r is the r^{th} generalized force, Q_r^* is the r^{th} generalized non-conservative force, V is the potential function corresponding to the conservative forces, and $\nabla_i V$ is the gradient of the potential function. Lastly, Eq. (2.23) is substituted into Eq. (2.20) along with Eq. (2.22) to obtain the following:

$$\sum_{i=1}^{N}\left(M_i\ddot{\mathbf{r}}_i - \mathbf{F}_{active,i}\right)\cdot\delta\mathbf{r}_i^{(k)} = 0$$

$$\sum_{i=1}^{N}\left(M_i\ddot{\mathbf{r}}_i - \mathbf{F}_{active,i}\right)\cdot\sum_{r=1}^{n}\frac{\partial\mathbf{r}_i^{(k)}}{\partial q_r^{(k)}}\delta q_r^{(k)} = 0$$

$$\sum_{r=1}^{n}\sum_{i=1}^{N}\left(M_i\ddot{\mathbf{r}}_i - \mathbf{F}_{i,c} - \mathbf{F}_{i,nc}\right)\cdot\frac{\partial\mathbf{r}_i^{(k)}}{\partial q_r^{(k)}}\delta q_r^{(k)} = 0$$

$$\sum_{r=1}^{n}\left(\frac{d}{dt}\frac{\partial T}{\partial\dot{q}_r} - \frac{\partial T}{\partial q_r} + \frac{\partial V}{\partial q_r} - Q_r^*\right)\delta q_r^{(k)} = 0$$

$$\sum_{r=1}^{n}\left(\frac{d}{dt}\frac{\partial L}{\partial\dot{q}_r} - \frac{\partial L}{\partial q_r} - Q_r^*\right)\delta q_r^{(k)} = 0$$

(2.24)

where $L=T-V$ is called the *Lagrangian*. If all of the generalized coordinates are independent of one another, which they can sometimes be if we are careful about choosing generalized coordinates, then the (holonomic) form of the Lagrange equations of class two are given by,

$$\frac{d}{dt}\frac{\partial L}{\partial\dot{q}_r} - \frac{\partial L}{\partial q_r} = Q_r^*$$

(2.25)

If Eq. (2.25) is applied to the system in Figure 2.2 when a force, $f(t)=F_o\cos\omega_o t$, is applied to the mass in the x direction and a viscous damper, C, is placed in parallel with the spring, then the kinetic and potential energy expressions are the same as before in Eq. (2.13) and Q_r^* is calculated as in Eq. (2.23):

$$\begin{aligned} Q_r^* &= \sum_{i=1}^{N}\left(\mathbf{F}_{i,nc}\right)\cdot\frac{\partial\mathbf{r}_i^{(k)}}{\partial q_r^{(k)}} \\ &= \sum_{i=1}^{N}\left(F_o\cos\omega_o t - C\dot{x}\right)\mathbf{i}\cdot\frac{\partial\mathbf{r}_i^{(k)}}{\partial q_r^{(k)}} \\ &= \left(F_o\cos\omega_o t - C\dot{x}\right)\mathbf{i}\cdot\mathbf{i} \\ &= F_o\cos\omega_o t - C\dot{x} \end{aligned}$$

(2.26)

The kinetic and potential energies can then be substituted into Eq.(2.25):

$$\begin{aligned}
&\frac{d}{dt}\frac{\partial}{\partial \dot{x}}\left(\frac{1}{2}M\dot{x}^2+\frac{1}{2}I_{CM}\frac{\dot{x}^{\,2}}{a^2}+Mg\left(x-x_u\right)\sin\alpha-\frac{1}{2}K\left(x-x_u\right)^2\right)\\
&\qquad-\frac{\partial}{\partial x}\left(\frac{1}{2}M\dot{x}^2+\frac{1}{2}I_{CM}\frac{\dot{x}^{\,2}}{a^2}+Mg\left(x-x_u\right)\sin\alpha-\frac{1}{2}K\left(x-x_u\right)^2\right)=Q_r^*\\
&\frac{d}{dt}\left(M\dot{x}+I_{CM}\frac{\dot{x}}{a^2}\right)-\left(Mg\sin\alpha-K\left(x-x_u\right)\right)=F_o\cos\omega_o t-C\dot{x}\\
&\left(M+\frac{I_{CM}}{a^2}\right)\ddot{x}+C\dot{x}+K\left(x-x_u\right)-Mg\sin\alpha=F_o\cos\omega_o t
\end{aligned}$$

(2.27)

This equation has the same form as the EOMs obtained in the previous sections. It might be helpful at this point to reflect on what we just did. We applied Lagrange's equations of class II to a system where the (holonomic) constraints had already been applied to remove dependencies between the generalized coordinates. This procedure gave us an EOM that was identical to the EOM we derived using Newton-Euler vectorial techniques. The question we should answer now is: Why do these two seemingly different techniques yield the same equation? First of all, we used Newton's second law in the absence of ideal constraints to derive Lagrange's equations (recall Eq. (2.20)), so they should be the same. Second, we can associate terms as follows in the two techniques to convince ourselves that the two techniques must give the same EOM:

$$\begin{aligned}
M\ddot{\mathbf{r}} &\Leftrightarrow \frac{d}{dt}\frac{\partial T}{\partial \dot{q}}-\frac{\partial T}{\partial q}\\
\mathbf{F}_{active,i} &\Leftrightarrow -\frac{\partial V}{\partial q_r}+Q_r^*
\end{aligned}$$

(2.28)

2.4 Multiple degree-of-freedom (MDOF) systems

Up to this point, we have only discussed EOMs of SDOF systems. We follow the same procedure in this section as in Sections 2.1-2.3 to apply Newtonian, energy/power, and Lagrangian techniques to multiple degree-of-freedom (MDOF) systems. Each DOF in the system

will require another EOM and all of these EOMs will in general be coupled in some way. For example, the EOMs of the simple system in Figure 2.3 with viscous damping can be derived using Newtonian or Lagrangian techniques. The FBDs of this system are shown in the bottom of the figure.

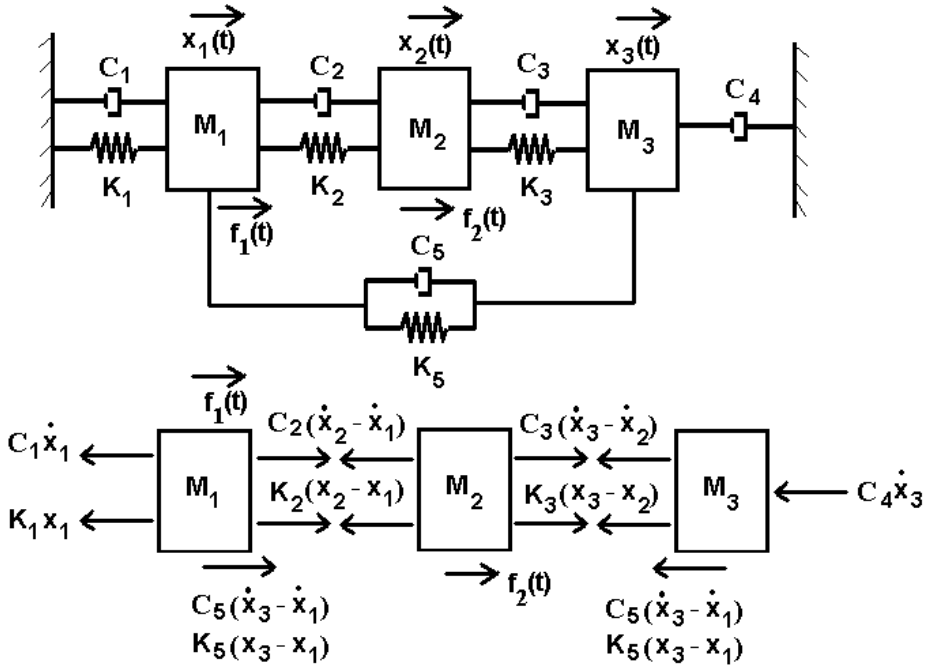

Figure 2.3: (Top) three degree-of-freedom vibrating system and (bottom) FBDs

When applying any EOM derivation technique, we first find the number of DOFs. In this case, three coordinates are required to locate and orient all masses in the system: #DOFs=3. The coordinate definitions are given in the figure. Then for Newton's second law, the following sequence of equations is obtained:

$$
\begin{aligned}
M_1\ddot{x}_1 &= f_1(t) - K_1x_1 - C_1\dot{x}_1 + C_2\left(\dot{x}_2 - \dot{x}_1\right) + K_2\left(x_2 - x_1\right) + C_5\left(\dot{x}_3 - \dot{x}_1\right) + K_5\left(x_3 - x_1\right) \\
M_2\ddot{x}_2 &= f_2(t) - C_2\left(\dot{x}_2 - \dot{x}_1\right) - K_2\left(x_2 - x_1\right) + C_3\left(\dot{x}_3 - \dot{x}_2\right) + K_3\left(x_3 - x_2\right) \\
M_3\ddot{x}_3 &= -C_4\dot{x}_3 - C_3\left(\dot{x}_3 - \dot{x}_2\right) - K_3\left(x_3 - x_2\right) - C_5\left(\dot{x}_3 - \dot{x}_1\right) - K_5\left(x_3 - x_1\right)
\end{aligned}
\qquad (2.29)
$$

This sequence can then be rearranged and placed into matrix form as follows:

$$\begin{bmatrix} M_1 & 0 & 0 \\ 0 & M_2 & 0 \\ 0 & 0 & M_3 \end{bmatrix}\begin{Bmatrix} \ddot{x}_1 \\ \ddot{x}_2 \\ \ddot{x}_3 \end{Bmatrix} + \begin{bmatrix} C_1 + C_2 + C_5 & -C_2 & -C_5 \\ -C_2 & C_2 + C_3 & -C_3 \\ -C_5 & -C_3 & C_5 + C_3 + C_4 \end{bmatrix}\begin{Bmatrix} \dot{x}_1 \\ \dot{x}_2 \\ \dot{x}_3 \end{Bmatrix} + \begin{bmatrix} K_1 + K_2 + K_5 & -K_2 & -K_5 \\ -K_2 & K_2 + K_3 & -K_3 \\ -K_5 & -K_3 & K_5 + K_3 \end{bmatrix}\begin{Bmatrix} x_1 \\ x_2 \\ x_3 \end{Bmatrix} = \begin{Bmatrix} f_1(t) \\ f_2(t) \\ 0 \end{Bmatrix} \quad (2.30)$$

There are three equations because there are three DOFs. This set of equations has some important properties that are common in systems of this type where absolute coordinates are used to derive the EOMs. First, note that the mass, damping, and stiffness matrices are all symmetric; this symmetry changes when relative coordinates are used. Second, note that the off-diagonals of the mass matrix are zero. Because the mass matrix is diagonal, we say there is no *dynamic coupling* in this system through these coordinates. Dynamic coupling implies that the inertia associated with one coordinate directly produces inertia in another coordinate. Because the stiffness matrix is not diagonal, we say that the system is *statically coupled* through these coordinates. Static coupling implies that a deflection of one coordinate causes deflections in other coordinates. Third, note that the force vector only has two nonzero entries (first and second) because the third DOF has no exogenous force applied.

There are an infinite number of other EOMs for this system depending on the choice of coordinates. Students are encouraged to define their own set of coordinates and derive the EOMs to demonstrate this point for themselves. For example, if x_2 is replaced with x^*_2, where $x^*_2 = x_2 - x_1$, a relative coordinate, then the EOM matrix becomes:

$$\begin{bmatrix} M_1 & 0 & 0 \\ M_1 & M_2 & 0 \\ 0 & 0 & M_3 \end{bmatrix}\begin{Bmatrix} \ddot{x}_1 \\ \ddot{x}^*_2 \\ \ddot{x}_3 \end{Bmatrix} + \begin{bmatrix} C_1 + C_5 & -C_2 & -C_5 \\ C_3 & C_2 + C_3 & -C_3 \\ -C_5 - C_3 & -C_3 & C_5 + C_3 + C_4 \end{bmatrix}\begin{Bmatrix} \dot{x}_1 \\ \dot{x}^*_2 \\ \dot{x}_3 \end{Bmatrix} + \begin{bmatrix} K_1 + K_2 + K_5 & -K_2 & -K_5 \\ K_3 & K_2 + K_3 & -K_3 \\ -K_5 - K_3 & -K_3 & K_5 + K_3 \end{bmatrix}\begin{Bmatrix} x_1 \\ x^*_2 \\ x_3 \end{Bmatrix} = \begin{Bmatrix} f_1(t) \\ f_2(t) \\ 0 \end{Bmatrix} \quad (2.31)$$

Note that the symmetry in the mass, damping, and stiffness matrices has disappeared and the coordinates have become dynamically coupled as well as statically coupled.

We can also use Lagrange's equations from Eq. (2.25) to derive the EOMs of the system in Figure 2.3. To do this, we first compute the kinetic and potential energy functions and the so-called *Rayleigh dissipation function*, *R*:

$$
\begin{aligned}
T &= \frac{1}{2} M_1 \dot{x}_1^2 + \frac{1}{2} M_2 \dot{x}_2^2 + \frac{1}{2} M_3 \dot{x}_3^2 \\
V &= \frac{1}{2} K_1 x_1^2 + \frac{1}{2} K_2 (x_2 - x_1)^2 + \frac{1}{2} K_3 (x_3 - x_2)^2 + \frac{1}{2} K_5 (x_3 - x_1)^2 \\
R &= \frac{1}{2} C_1 \dot{x}_1^2 + \frac{1}{2} C_2 (\dot{x}_2 - \dot{x}_1)^2 + \frac{1}{2} C_3 (\dot{x}_3 - \dot{x}_2)^2 + \frac{1}{2} C_5 (\dot{x}_3 - \dot{x}_1)^2 + \frac{1}{2} C_4 \dot{x}_3^2
\end{aligned}
$$

(2.32)

The Rayleigh dissipation function is a common means for simplifying the derivation of EOMs in damped systems. In a sense, damping is treated just like kinetic and potential energy analytically. When *R* is included in Lagrange's equation, Eq. (2.25) is modified somewhat to,

$$
\frac{d}{dt} \frac{\partial L}{\partial \dot{q}_r} - \frac{\partial L}{\partial q_r} + \frac{\partial R}{\partial \dot{q}_r} = Q_r^*
$$

(2.33)

where Q_r^* is now understood to be the remainder of the r^{th} generalized force when viscous damping has been accounted for with the dissipation function, *R*.

In summary, to derive Lagrange's EOMs for a system, follow Steps 1 through 3 in Section 2.1 and then continue with the steps below:

1) After defining the coordinate system, finding the number of DOFs, and drawing the FBDs, calculate the potential and kinetic energy functions as well as the Rayleigh dissipation function (*V*, *T*, and *R*). ENFORCE THE CONSTRAINTS at this point to eliminate dependencies in the selected generalized coordinates.

2) Form the Lagrangian, L. This step is really not necessary if we choose to leave Eq. (2.33) in the expanded form, second to the last line in Eq. (2.24), involving V and T instead.
3) Take the necessary partial derivatives of V, T, and R with respect to the generalized coordinates and velocities and then take the time derivative of the kinetic energy partials.
4) Find the generalized forces, Q_r^*, as in Eq. (2.23) by projecting the non-conservative forces not already accounted for in Rayleigh's function onto the variational coordinates.
5) Substitute the results from Steps 3 and 4 into Lagrange's equations, Eq. (2.33).

2.5 Linearizing the differential equations of motion

The differential EOMs of typical real-world vibrating systems are nonlinear. Mechanical systems can contain many different types of nonlinearities including geometric, kinematic, material, and other less common types. Although there are powerful techniques for analyzing nonlinear vibrating systems, this course will largely ignore those techniques and focus instead on linear techniques. Thus, we must start with linear differential EOMs by linearizing nonlinear EOMs. There are two approaches for doing this: 1) we can derive the full EOMs and then linearize them; or 2) we can linearize the necessary energy functions before applying Lagrange's approach to derive the final linearized EOMs. We will discuss both of these techniques, but we choose to focus on the first method because it is slightly more intuitive for introductory material.

Consider the unforced and undamped simple pendulum, which has the following EOM:

$$ML^2\ddot{\theta} + MgL\sin\theta = 0 \qquad (2.34)$$

where M is the lumped mass of the pendulum, g is the gravitational acceleration constant, L is the distance from the center of rotation to the lumped mass, and θ is the angular coordinate that the pendulum makes with the vertical. In order to linearize Eq. (2.34), we look to the nonlinear function, $\sin\theta$. Figure 2.4 shows that when the pendulum oscillates closely around the downward equilibrium position (i.e., near $\theta = 0$ *rad*), $\sin\theta$ is approximated well by the dotted straight line that

passes through the origin. If the pendulum oscillates too far away from the origin (i.e., if θ is too large), then the straight line does not accurately describe the pendular motion. We can use Taylor series (Maclaurin series) to mathematically linearize the EOM using these arguments. The Taylor series of $\sin\theta$ about $\theta=0$ (Maclaurin series) is,

$$\sin\theta = \sin\theta_o + \sum_{n=1}^{\infty} \frac{1}{n!}\left[\frac{d^{(n)}}{d\theta^{(n)}}(\sin\theta)\right]\Bigg|_{\theta=\theta_o} (\theta-\theta_o)^n = \theta - \frac{1}{6!}\theta^3 + \cdots \qquad (2.35)$$

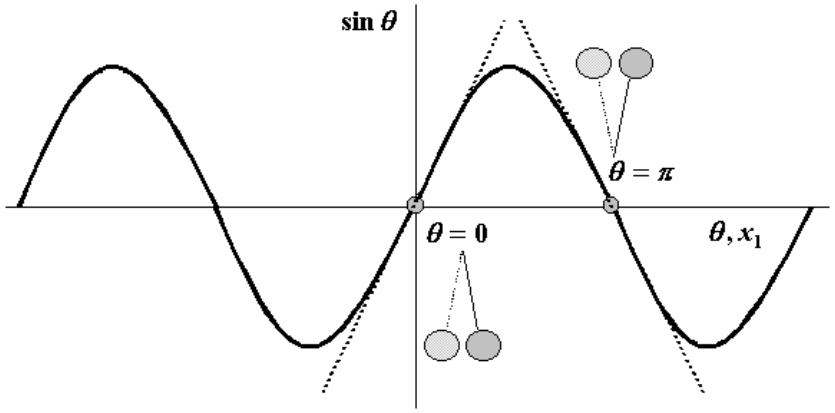

Figure 2.4: Nonlinear function with two equilibrium points and associated linear characteristics

The form of Eq. (2.35) confirms our discussion above; as long as the angular rotation is small, the third and higher order terms are "negligible" compared to the first order linear term. Thus, if we are just interested in how the pendulum moves in the neighborhood of the origin for $|\theta|<<1$ *rad*, then we can define a new coordinate, $\theta_d=\theta-\theta_o=\theta-0$, and then linearize Eq. (2.34) as follows,

$$\begin{aligned} ML^2\ddot{\theta} + MgL\sin\theta &= 0 \\ ML^2\ddot{\theta}_d + MgL\sin(\theta_d + 0) &= 0 \\ \ddot{\theta}_d + \frac{g}{L}\theta_d &\cong 0 \end{aligned} \qquad (2.36)$$

We see then that the goal of linearization is to approximate nonlinear functions in EOMs with linear terms near certain operating points (i.e., equilibrium states) of interest. We could just as easily have linearized Eq. (2.34) about $\theta=\pi$ *rad* as well:

$$\begin{aligned} ML^2\ddot{\theta} + MgL\sin\theta &= 0 \\ ML^2\ddot{\theta} + MgL\sin(\theta_d + \pi) &= 0 \\ ML^2\ddot{\theta} - MgL\sin(\theta_d) &= 0 \\ \ddot{\theta}_d - \frac{g}{L}\theta_d &\cong 0 \end{aligned}$$

(2.37)

which of course describes the unstable nature of the equilibrium point at $\theta=\pi$ *rad*. In summary, all of the analysis techniques we will use in this course are based on the assumption that the EOM is linear. We usually have to linearize the EOM before applying these techniques by defining our operating point of interest and then approximating nonlinear functions in the EOMs with linear functions in the neighborhood of our chosen operating point.

Although the technique presented above for linearizing "after the fact" in the final EOMs is useful in relatively simple problems, it will become unwieldy for more significant problems. In those cases, we can use the Lagrange solution procedure as follows: first, we calculate the energy expression for T, V, and R in addition to the generalized forces, Q^*_r as before; second, we linearize the energy expressions; lastly, we write down the linearized EOMs directly. We begin by examining the holonomic Lagrange equation of class II at an equilibrium point where $d^{(n)}q_r/dt^{(n)}=0$ for $n>0$. At the equilibrium point, the values of the generalized coordinates are placed in the vector, $\mathbf{q}_o$. From the form of Lagrange's equations, we have

$$\begin{aligned} \frac{d}{dt}\left(\frac{\partial L}{\partial \dot{q}_r}\right) - \frac{\partial L}{\partial q_r} + \frac{\partial R}{\partial \dot{q}_r} &= 0 \\ \left.\frac{\partial V}{\partial q_r}\right|_{Eq.Pt.} &= 0 \end{aligned}$$

(2.38)

If we are again only interested in small motions around the equilibrium point, then we can expand the potential energy function using a multi-variable Taylor series to third order in $\Delta\mathbf{q}$:

$$V(\mathbf{q}) = V(\mathbf{q}_o) + \sum_{r=1}^{n} \left.\frac{\partial V}{\partial q_r}\right|_{\mathbf{q}=\mathbf{q}_o} (q_r - q_{ro}) + \frac{1}{2}\sum_{r=1}^{n}\sum_{m=1}^{n} \left.\frac{\partial^2 V}{\partial q_r \partial q_m}\right|_{\mathbf{q}=\mathbf{q}_o} (q_r - q_{ro})(q_m - q_{mo}) + O(\Delta q^3)$$

$$= V(\mathbf{q}_o) + \frac{1}{2}\sum_{r=1}^{n}\sum_{m=1}^{n} K_{rm} q_{dr} q_{dm}, \text{ where } K_{rm} \stackrel{\Delta}{=} \left.\frac{\partial^2 V}{\partial q_r \partial q_m}\right|_{\mathbf{q}=\mathbf{q}_o} \text{ and } q_{dr} = q_r - q_{ro},\ q_{dm} = q_m - q_{mo}$$

(2.39)

Note that we used Eq. (2.38) in addition to the conditions on the derivatives of the generalized coordinates. Because Eq.
(2.39) is a quadratic form (i.e., $q_{dr}q_{dm}$), we can immediately write down the partial derivatives that we need for Lagrange's equations:

$$\frac{\partial V}{\partial q_p} = \frac{\partial}{\partial q_p}\left(V(\mathbf{q}_o) + \frac{1}{2}\sum_{r=1}^{n}\sum_{m=1}^{n} K_{rm} q_{dr} q_{dm} \right)$$

$$= \sum_{p=1}^{n} K_{pr} q_{dr}$$

(2.40)

which will provide the linear stiffness to ground and all the coupling stiffnesses for the linearized EOMs. As for the kinetic energy, we can obtain a similar expression by computing the two sets of partial derivatives we need for Lagrange's equations:

$$\frac{\partial T}{\partial \dot{q}_p} = \frac{\partial}{\partial \dot{q}_p}\left(\frac{1}{2}\sum_{r=1}^{n}\sum_{m=1}^{n} M_{rm} \dot{q}_{dr} \dot{q}_{dm} \right)$$

$$= \sum_{p=1}^{n} M_{pr} \dot{q}_{dr}$$

$$\text{with } M_{pr} = M_{pr}\big|_{\mathbf{q}_o} + \sum_{j=1}^{n} \frac{\partial}{\partial q_j} M_{pr}\big|_{\mathbf{q}_o} q_{dj} + O(q_d^2)$$

(2.41)

and

$$\frac{\partial T}{\partial q_p} = \frac{\partial}{\partial q_p}\left(\frac{1}{2}\sum_{r=1}^{n}\sum_{m=1}^{n} M_{rm}\dot{q}_{dr}\dot{q}_{dm}\right) \cong 0 \text{ near } \mathbf{q}_o \tag{2.42}$$

Rayleigh's dissipation function is handled in the same way as in the previous section.

Consider the simple pendulum again with the potential and kinetic energies as follows:

$$V = MgL(1-\cos\theta)$$
$$T = \frac{1}{2}ML^2\dot{\theta}^2 \tag{2.43}$$

The following procedure is used below to develop the linearized EOM for the simple pendulum:

1) Find the potential energy function, $V(\mathbf{q})$. Note that this procedure assumes that all restoring forces are accounted for in V. Find the equilibrium point, $\mathbf{q}_o$, such that Eq. (2.38) is satisfied. Calculate the symmetric stiffness coefficients, K_{rm}, using the formula in Eq. (2.39) and find the stiffness matrix.
2) Find the kinetic energy function, T, and expand it into a quadratic form involving products of the generalized coordinate velocities, $(dq_r/dt)\cdot(dq_m/dt)$. Evaluate the coefficients of these quadratic terms at $\mathbf{q}_o$ and calculate the mass matrix of the linearized EOMs.
3) Find the Rayleigh dissipation function, R, expand it in quadratic forms, identify the viscous damping coefficients and create the viscous damping matrix.
4) Write down the linearized EOMs in terms of the dynamic coordinates (i.e., variation of coordinates away from the equilibrium point) using the calculated mass, damping, and stiffness matrices computed in Steps 1-3.

Simple pendulum example:

$$V = MgL(1-\cos\theta), \text{ where } \theta_o = 0$$

$$\text{so } V = 0 + MgL\left(\frac{1}{2!}\theta^2 - \frac{1}{4!}\theta^4 + O(\theta^6)\right)$$

$$\left.\frac{\partial^2 V}{\partial \theta^2}\right|_{\theta=\theta_o} = MgL = K_{11}$$

$$\text{Since } T = \frac{1}{2}(ML^2)\dot{\theta}^2, \text{ then } M_{11} = ML^2$$

$$\frac{d}{dt}\left(\frac{\partial T}{\partial \dot{\theta}}\right) - \frac{\partial T}{\partial \theta} + \frac{\partial V}{\partial \theta} = 0$$

$$M_{11}\ddot{\theta}_d + K_{11}\theta_d = 0, \text{ where } \theta_d = \theta - \theta_o = \theta$$

(2.44)

Note that the terms of order two and lower (quadratic and linear) are kept in the potential energy because these are the terms that will produce linear terms in the EOMs. We will apply this procedure in more complicated examples throughout the course.

2.6 Continuous systems of second and fourth-order

So far in these notes we have only discussed discrete systems: masses, dampers, and springs, which were all lumped elements. Next, we treat continuous systems by allowing the system mass, damping, and stiffness to vary as continuous functions of the generalized coordinates. Most systems are in reality continuous systems, but we are often interested to know how discrete models can be used to get accurate approximate solutions? We will discuss this point later, but for now we start with a relatively simple example of transverse vibrations along a string and then move on to a more complicated example. Results here will parallel those in acoustics. The process of deriving EOMs for continuous systems is identical to that for discrete systems in Sections 2.1-2.4; however, the FBDs will look more complicated when in reality they are not.

Consider the continuous string shown in Figure 2.5 below with mass density, $\rho(x)$ (mass/length) and tension, $T(x)$ (force). Note that the density and tension are both allowed to vary with x, the longitudinal position of the small piece of mass along the string in contrast to the fixed mass and spring coefficients in the previous sections.

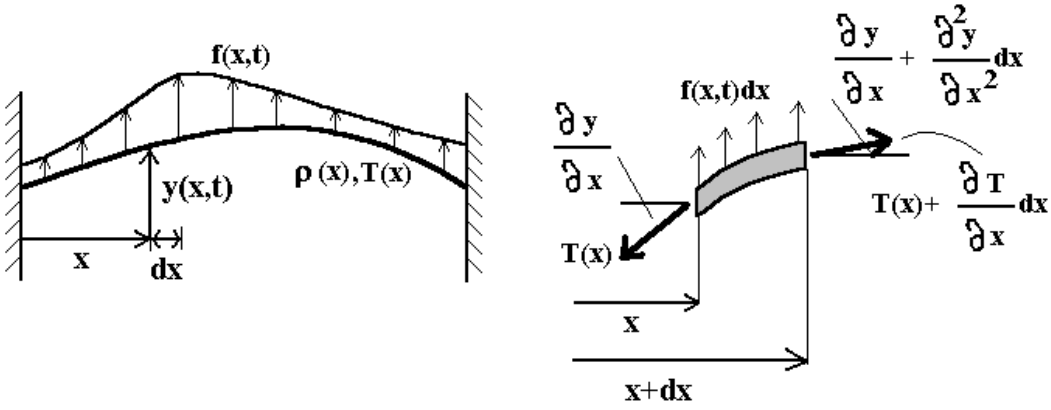

Figure 2.5: (Left) String fixed on both ends (right) FBDs of infinitesimal string element

The FBD of an infinitesimal string element is shown on the right of the figure. Note that changes in both the tension and slope along the string are expressed using a two term Taylor series; terms of higher order than one are neglected assuming small deflections. Newton's second law applied to the FBD in Figure 2.5 yields the following:

$$(\rho(x)dx)\frac{\partial^2 y(x,t)}{\partial t^2} = \left(T(x)+\frac{\partial T(x)}{\partial x}dx\right)\left(\frac{\partial y(x,t)}{\partial x}+\frac{\partial^2 y}{\partial x^2}dx\right) - T(x)\frac{\partial y(x,t)}{\partial x} + f(x,t)dx$$

$$\rho(x)\frac{\partial^2 y(x,t)}{\partial t^2}dx = \frac{\partial T(x)}{\partial x}\frac{\partial y(x,t)}{\partial x}dx + T(x)\frac{\partial^2 y}{\partial x^2}dx + \frac{\partial T(x)}{\partial x}\frac{\partial^2 y}{\partial x^2}(dx)^2 + f(x,t)dx$$

$$\rho(x)\frac{\partial^2 y(x,t)}{\partial t^2} = \frac{\partial}{\partial x}\left(T(x)\frac{\partial y(x,t)}{\partial x}\right) + f(x,t) + O(dx)$$

(2.45)

The second order terms in this last equation can be ignored just as they were ignored in calculating the slope of the string at both ends of the infinitesimal segment in Figure 2.5. Of course, this equation is only valid along the length of the string ($0<x<L$) and must be accompanied by two boundary conditions at its end points to have physical meaning. Because the equation is of second order in $y(x,t)$, it requires two boundary conditions. In the case shown in Figure 2.5, both ends are fixed so,

$$y(0,t) = 0 = y(L,t)$$

(2.46)

Other possible boundary conditions would be computed similarly in terms of the displacement, y, at the end points of the string. For example, if the left end is fixed and the right end is made to oscillate according to the function $g(t)$, then the boundary conditions would be $y(0,t)=0$ and $y(L,t)=g(t)$.

Before proceeding with the derivation of other EOMs for continuous systems, we should reflect on the meaning of Eq. (2.45). Recall that one of the steps in deriving EOMs is to verify that the resultant equations make physical sense. If we rewrite that equation in the following form:

$$\rho(x)\frac{\partial^2 y(x,t)}{\partial t^2} - \frac{\partial}{\partial x}\left(T(x)\frac{\partial y(x,t)}{\partial x}\right) = f(x,t)$$

(2.47)

then it is relatively clear that the EOM for a string describes a balance between inertial, tension, and external (exogenous) forces. For example, if the string is massless and the external force is zero, then $\rho(x)=0$ and $f(x,t)=0$. In this special case,

$$\frac{\partial}{\partial x}\left(T(x)\frac{\partial y(x,t)}{\partial x}\right) = 0 \Rightarrow T(x)\frac{\partial y(x,t)}{\partial x} = \text{constant}(t)$$

(2.48)

which means that for constant tension strings, $T(x)=constant$, the slope of the string is the same all along its length at each moment in time. Does this make sense? Prove to yourself that it does by conducting an experiment of some kind. Also, in the steady state when $f(x,t)=constant$ (and there is a small amount of damping in the string) the inertial force goes to zero along with the acceleration because the motions cease and the tension force balances the external force:

$$-\frac{\partial}{\partial x}\left(T(x)\frac{\partial y(x,t)}{\partial x}\right) = f(x,t) \text{ at steady state}$$

(2.49)

As in Eq. (2.48), this equation shows that for static forces (i.e., gravity) and constant tension strings, the rate of change in slope with distance along the string is proportional to *f(x,t)*.

We can also derive EOMs for bars experiencing bending. Figure 2.5 shows the system and FBD for this type of system. In this type of problem, the linear mass density, *m(x)*, and flexural (bending) stiffness, *EI(x)*, are given as functions of position along the bar, *x*, and the loading distribution, *f(x,t)*, is given as well. The deflection at a position *x* along the bar is the deflection of the neutral axis of the beam, which is assumed to experience negligible shear deformations and rotations along its length. Application of Newton's second law in the vertical direction and Euler's equation about the left end of the infinitesimal element yields the following two equations:

$$\begin{aligned} (m(x)dx)\frac{\partial^2 y(x,t)}{\partial t^2} &= \left(Q(x,t)+\frac{\partial Q}{\partial x}dx\right)-Q(x,t)+f(x,t)dx \\ 0 &= \left(M(x,t)+\frac{\partial M}{\partial x}dx\right)-M(x,t)+\left(Q(x,t)+\frac{\partial Q}{\partial x}dx\right)dx+f(x,t)dx\frac{dx}{2} \end{aligned}$$

(2.50 a,b)

By ignoring second order terms as in the string case and substituting the result from the second of Eqs. (2.50 a,b), $\partial M/\partial x+Q=0$, into the first , the following EOM is obtained:

$$m(x)\frac{\partial^2 y(x,t)}{\partial t^2} = -\frac{\partial^2 M}{\partial x^2}+f(x,t)$$

(2.51)

Because our goal is to find an EOM for the deflection, *y(x,t)*, we now have to eliminate *M(x,t)* in terms of *y* by using the standard moment equation from elementary B-E bending theory:

$$M(x,t) = EI(x)\frac{\partial^2 y(x,t)}{\partial x^2}$$

(2.52)

which gives the final EOM in terms of *y(x,t)*:

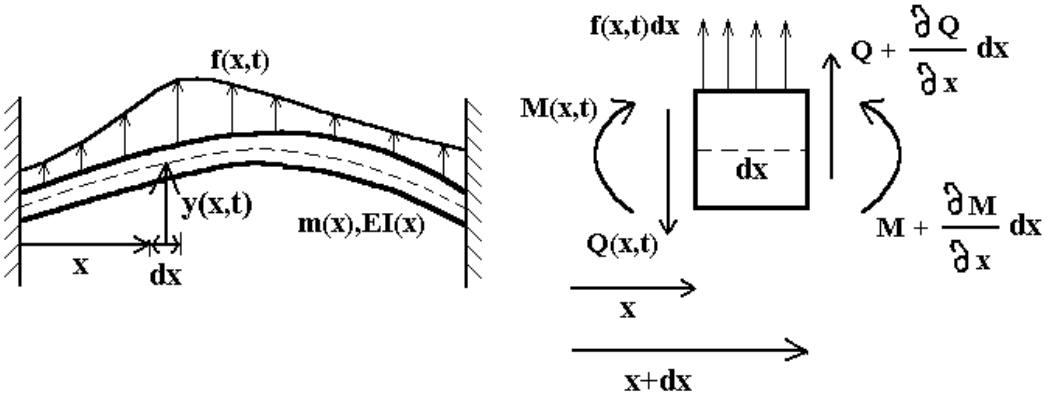

Figure 2.4: (Left) Bending bar fixed on both ends (right) FBDs of infinitesimal bar element

$$m(x)\frac{\partial^2 y(x,t)}{\partial t^2} = -\frac{\partial^2}{\partial x^2}\left(EI(x)\frac{\partial^2 y(x,t)}{\partial x^2}\right) + f(x,t) \tag{2.53}$$

Note that this is a fourth order partial differential equation, which requires four boundary conditions (two on each end) for physical applications. In Figure 2.5, with clamped ends on the left and right of the bar, the boundary conditions are given by,

$$y(0,t) = 0, \left.\frac{\partial y(x,t)}{\partial x}\right|_{x=0} \text{ and } y(L,t) = 0, \left.\frac{\partial y(x,t)}{\partial x}\right|_{x=L} \tag{2.54}$$

Other types of boundary conditions include hinges (zero deflection and moment) and free ends (zero moment and shearing force). When the boundary conditions are determined by the geometry of the problem, they are called *geometric boundary conditions*. When the boundary conditions are determined by the physics of the problem at the boundaries, they are called *natural*. Again, we should interpret Eq. (2.53) to ensure that it makes physical sense. First, note that Eq. (2.53) essentially describes a balance between inertial, stiffness, and external (exogenous) forces. Second, note that the EOM describes a system undergoing static bending deflections when the inertial term is ignored. We can perform various other simple thought experiments to verify the correctness of Eq. (2.53).

Although we used Newton's second law to derive both Eq. (2.45) and Eq. (2.53), we can also use Hamilton's method (energy methods) to obtain the same results. To do this, we must formulate the kinetic and potential energy expressions for continuous systems. All of these expressions are based on the corresponding discrete versions, but involve integrals. The kinetic energy of a continuous system can be found as follows:

$$T(t) = \frac{1}{2}\int_0^L m(x)\left(\frac{\partial y(x,t)}{\partial t}\right)^2 dx$$

(2.55)

The potential energy of a longitudinally vibrating rod with displacement, *u(x,t)*, is given by,

$$V(t) = \frac{1}{2}\int_0^L EA(x)\left[\frac{\partial u(x,t)}{\partial x}\right]^2 dx$$

(2.56)

and the potential energy of a bar in bending with transverse deflection, *y(x,t)*, is given by,

$$V(t) = \frac{1}{2}\int_0^L EI(x)\left[\frac{\partial^2 y(x,t)}{\partial x^2}\right]^2 dx$$

(2.57)

These expressions can be used in conjunction with Hamilton's principle to derive the EOMs; however, this technique will not be presented here because it requires a clear working knowledge of variational calculus, which is beyond the scope of this course.

3 Free Vibrations

Free vibrations occur without the aid of external forces. Now that we have derived EOMs for some common vibrating systems, we are ready to analyze the free response behavior of these systems. Recall that response analysis was the next step in the EOM procedure given in Section

2.1. The rationale for studying the free response behavior first and then the forced response behavior is provided by the principle of superposition, i.e., the total response (solution) is equal to the sum of the homogeneous solution and the non-homogeneous solution. We will begin by studying the free response of undamped and damped SDOF systems. Different types of damping and their effects on response characteristics will then be discussed. Then we will study how MDOF systems can be treated in similar ways using the notion of linear superposition as a working principle. After discussing the importance of eigenvalues and eigenvectors in discrete linearized MDOF systems, we will study eigenvalues and eigenfunctions in the free response of continuous systems.

3.1 Free response of single degree-of-freedom systems with viscous damping

Consider the SDOF differential equation model (Eq. (2.29)) of the system in Figure 2.4 (the rolling disk on an incline – repeated below for reference). If we set the input to zero, *f(t)=0*, as it must be in free vibration problems, then the EOM becomes:

$$\left(M + \frac{I_{CM}}{a^2}\right)\ddot{x} + C\dot{x} + K\left(x - x_u\right) - Mg\sin\alpha = 0 \qquad (3.1)$$

This equation is called the *homogeneous*, or *unforced*, EOM. We can see immediately that the steady state response of this system, x_{ss}, after the initial transient has decayed due to damping, is found by setting $dx/dt=0=d^2x/dt^2$ (i.e., the rate of change of position and velocity are zero):

$$K\left(x_{ss} - x_u\right) - Mg\sin\alpha = 0$$

$$x_{ss} = x_u + \frac{Mg}{K}\sin\alpha \qquad (3.2)$$

Does this result make sense? Because gravity is acting down the incline, the steady state position of the disk is equal to the position of the disk CM when the spring is undeformed (i.e., no *V*) plus the deformation in the spring when it is balancing the force due to gravity on the disk. This steady state value is important in many applications; for instance, the static deflection in an

automobile suspension system might be important because it indicates how much working space is left for dynamic deflections in the strut for potholes and other road inputs. However, it is very common in vibrations to remove the static (steady state) part of the response by redefining the coordinate system. In our case, Eq. (3.2) suggests that the new coordinate, x_d ("*d*" denotes the dynamic coordinate) should be defined as follows:

$$x_d \overset{\Delta}{=} x - x_{ss} \tag{3.3}$$

When this substitution is made in the EOM (Eq. (3.1)), only the vibrational aspects of the response are retained:

$$\left(M + \frac{I_{CM}}{a^2}\right)\ddot{x}_d + C\dot{x}_d + Kx_d = 0 \tag{3.4}$$

We will now analyze the free response described by this EOM. (What is the steady state solution of this EOM?) There are many different ways to solve Eq. (3.4). We can guess a solution of the form,

$$x_d = Ae^{st} \tag{3.5}$$

substitute this guess into Eq. (3.4),

$$\left(M + \frac{I_{CM}}{a^2}\right)s^2 Ae^{st} + CsAe^{st} + KAe^{st} = 0$$

$$\left[\left(M + \frac{I_{CM}}{a^2}\right)s^2 + Cs + K\right]Ae^{st} = 0 \tag{3.6}$$

and then select the only non-trivial solution that satisfies the resulting *characteristic*, or *subsidiary*, equation, Eq. (3.6):

$$x_d(t) = A_1 e^{s_1 t} + A_2 e^{s_2 t} \quad \text{where} \quad s_{1,2} = \frac{-C}{2\left(M + \frac{I_{CM}}{a^2}\right)} \pm \frac{\sqrt{C^2 - 4\left(M + \frac{I_{CM}}{a^2}\right)K}}{2\left(M + \frac{I_{CM}}{a^2}\right)}$$

(3.7)

The constants s_1 and s_2 are called the roots, poles, or modal frequencies of the system described by Eq. (3.4). They depend directly on the mass, damping, and stiffness parameters; in other words, *the roots of a system are determined solely by the system*. They will not depend on what kind of input we measure or even what type of output we measure. There are two unknown constants in this solution, A_1 and A_2, which are determined by the initial conditions on x_d and its derivative (velocity):

$$x_d(0) = A_1 + A_2$$
$$\dot{x}_d(0) = s_1 A_1 + s_2 A_2$$

(3.8)

Only the initial conditions on position and velocity are needed because this is a second order system, which has by definition two states of importance. If we know these states at time zero and have a valid EOM, then we can always find the free vibration response (solution). This approach is fairly easy to apply and always works as long as we remember how to deal with systems involving repeated roots (i.e., $s_1=s_2$). Recall from the variation of parameters that if we insert an extra factor of time, t, we can retain two independent solutions as in Eq. (3.7).

In order to find the solution to Eq. (3.4), which is linear, we could also take the Laplace transform of that equation and solve for the Laplace transform of the response, $X_d(s)$, as follows:

$$\left[\left(M+\frac{I_{CM}}{a^2}\right)s^2-\left(M+\frac{I_{CM}}{a^2}\right)sx_d(0)-\left(M+\frac{I_{CM}}{a^2}\right)\dot{x}_d(0)\right]X_d(s)+$$
$$\left[Cs-Cx_d(0)\right]X_d(s)+KX_d(s)=0$$
$$\left[\left(M+\frac{I_{CM}}{a^2}\right)s^2+Cs+K\right]X_d(s)=\left(M+\frac{I_{CM}}{a^2}\right)sx_d(0)+Cx_d(0)+\left(M+\frac{I_{CM}}{a^2}\right)\dot{x}_d(0)$$
$$X_d(s)=\frac{\left(M+\frac{I_{CM}}{a^2}\right)s+C}{\left(M+\frac{I_{CM}}{a^2}\right)s^2+Cs+K}x_d(0)+\frac{\left(M+\frac{I_{CM}}{a^2}\right)}{\left(M+\frac{I_{CM}}{a^2}\right)s^2+Cs+K}\dot{x}_d(0)$$

(3.9)

Eq. (3.9) is the solution for the frequency domain response (s is sometimes called the *complex frequency*). This procedure has the advantage that the initial conditions appear automatically in the solution, but has the disadvantage that we must factor the denominator of both terms (i.e., the characteristic polynomial) and then carry out a partial fraction expansion to obtain the time domain response. Regardless of which method we use to obtain the response, will need to find the roots (modal frequencies) and then apply the initial conditions. Therefore, it makes sense to study s_1 and s_2 first. We can do this by plotting the two roots in the complex plane as shown in Figure 3.1. Representative time domain free responses are also shown at the right of the figure. We will now analyze the roots in Eq. (3.7) to better understand and explain Figure 3.1.

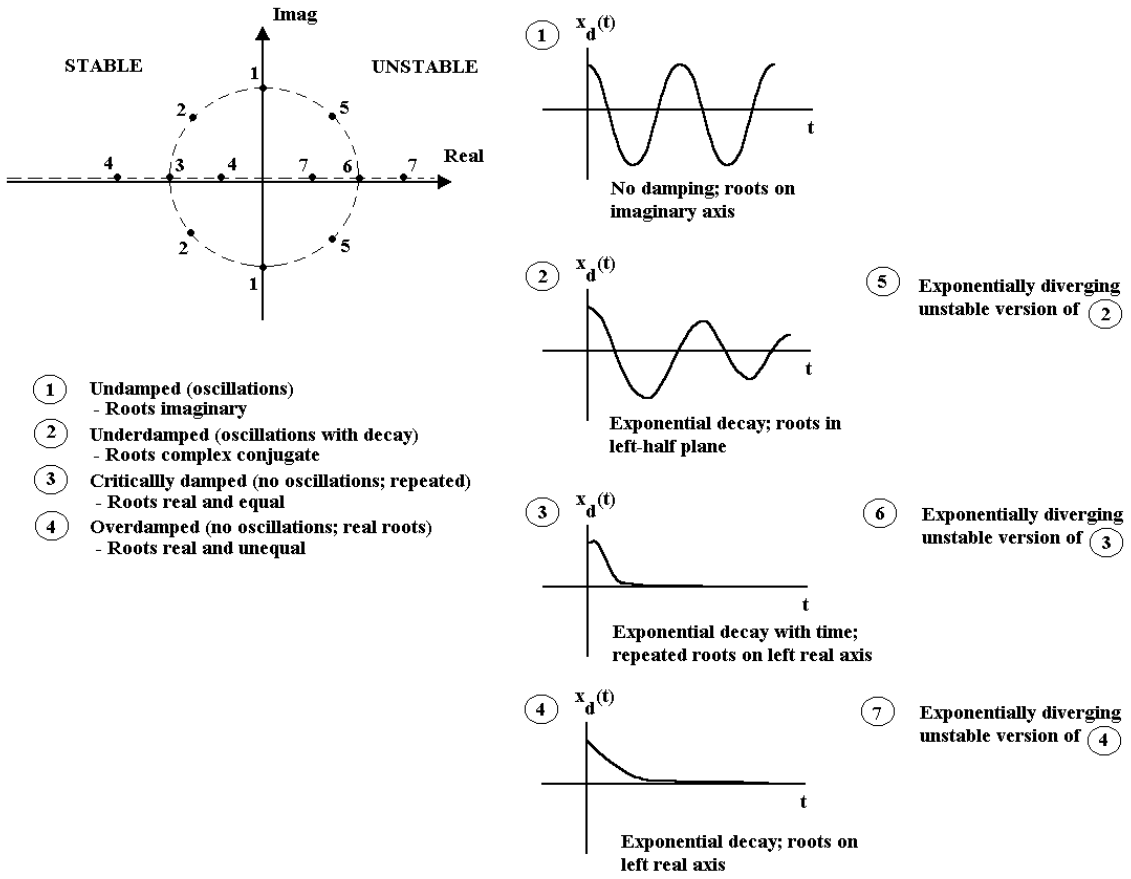

Figure 3.1: (Left) Plot of several pairs of roots in the complex plane (right) corresponding time domain free responses illustrating the natural response behavior of second order systems for undamped, underdamped, critically damped, and overdamped cases.

If we examine the roots in Eq. (3.7) closely, we notice the following:

1) Roots in second order systems come in pairs. Furthermore, whenever the roots are complex (real and imaginary parts) or imaginary, they must be complex conjugates of one another: *(a+bj,a-bj)* and *(bj,-bj)*. Can you see this in Eq. (3.7)? Look at the +- sign.

2) The real part of the root, which we will call σ, the *damping factor*, determines the rate of decay (or growth) of the free response. The imaginary part of the root, which we will call the *damped natural frequency*, ω_d, determines the frequency of oscillation. This terminology is appropriate because when we substitute the roots into the exponential solution, the real part is factored out and the imaginary part (via Euler's formula) produces oscillations between a sinusoid and cosinusoid as shown below:

$$\text{If } s_1 = \sigma + j\omega_d = s_2^{\,*}, \text{ then}$$
$$e^{s_1 t} = e^{(\sigma + j\omega_d)t} = e^{\sigma t} e^{j\omega_d t} = e^{\sigma t}\left(\cos\omega_d t + j\sin\omega_d t\right), \text{ and}$$
$$e^{s_2 t} = e^{(\sigma - j\omega_d)t} = e^{\sigma t} e^{-j\omega_d t} = e^{\sigma t}\left(\cos\omega_d t - j\sin\omega_d t\right)$$

(3.10)

We also note that the units of σ and ω_d correspond to those of a circular frequency, *rad/s*. We can find the actual values of the damping factor and damped natural frequency using Eq. (3.7):

$$s_{1,2} = \frac{-C}{2\left(M + \frac{I_{CM}}{a^2}\right)} \pm \frac{\sqrt{C^2 - 4\left(M + \frac{I_{CM}}{a^2}\right)K}}{2\left(M + \frac{I_{CM}}{a^2}\right)} = \sigma \pm j\omega_d$$

$$\text{where } \sigma = \frac{-C}{2\left(M + \frac{I_{CM}}{a^2}\right)} = \frac{damping}{inertia}$$

$$\omega_d = \frac{\sqrt{4\left(M + \frac{I_{CM}}{a^2}\right)K - C^2}}{2\left(M + \frac{I_{CM}}{a^2}\right)}$$

(3.11)

3) Roots with positive real parts are unstable whereas roots with negative real parts are stable. This result makes sense because $e^{\sigma t}$ determines the decay/growth of the free response. When the damping is positive ($C>0$), the roots are in the left half plane, and when damping is negative ($C<0$), the roots are in the right half plane. Recall that damping determines the rate at which energy is dissipated and also determines the rate at which energy is absorbed by the system.

4) Purely imaginary roots produce pure harmonic solutions; these solutions have a constant amplitude and do not decay or grow. This characteristic makes sense because the exponential part of the solution, $e^{\sigma t}$, is equal to one when the damping factor is zero, σ=0. Also, when the damping factor is zero there is no damping ($C=0$), and so the roots and undamped natural frequency from Eq. (3.11) are found as follows:

$$s_{1,2} = 0 \pm j\frac{\sqrt{4\left(M + \frac{I_{CM}}{a^2}\right)K}}{2\left(M + \frac{I_{CM}}{a^2}\right)}$$

$$= \pm j\sqrt{\frac{K}{M + \frac{I_{CM}}{a^2}}} = \pm j\sqrt{\frac{stiffness}{inertia}}$$

where $\omega_n \overset{\Delta}{=} \sqrt{\frac{stiffness}{inertia}}$ is the undamped natural frequency

(3.12)

5) When the roots are complex or imaginary, the constants A_1 and A_2 (called the *residues*) must be complex conjugates of one another just as the roots are complex conjugates. Why is this true? If they are not complex conjugates, then when we substitute Eqs. (3.10) into the solution, $x_d(t)$, we produce a complex solution. This result does not make physical sense. The only way to obtain a real solution for the free response is to satisfy the condition: $A_1 = A_2^*$. Real solutions require complex conjugate residues. We also note that in general the roots can be rewritten in terms of other more phenomenologically meaningful parameters, the damping ratio and undamped natural frequency from Eq. (3.12), as given below:

$$s_{1,2} = \frac{-C}{2\left(M + \frac{I_{CM}}{a^2}\right)} \pm j\frac{\sqrt{4\left(M + \frac{I_{CM}}{a^2}\right)K - C^2}}{2\left(M + \frac{I_{CM}}{a^2}\right)} = \sigma \pm j\omega_d = -\varsigma\omega_n \pm j\sqrt{1-\varsigma^2}\,\omega_n$$

where $\sigma = -\varsigma\omega_n$

$$\omega_d = \sqrt{1-\varsigma^2}\,\omega_n$$

$$\varsigma = \frac{C}{2\sqrt{K\left(M + \frac{I_{CM}}{a^2}\right)}} = \frac{C}{C_c} = \frac{Damping\ ratio}{}, \text{ where } C_c = \text{Critical damping coefficient}$$

(3.13)

Eq. (3.13) shows that the type of free responses in Figure 3.1 can be classified in terms of their corresponding damping ratios, ζ. When ζ=0, the response is *undamped*, when ζ<1, the response is *underdamped*, and when ζ>1, the response is *overdamped*. When ζ<0, the roots are in the right half plane, which indicates that the response is unstable.

6) Given the relationships developed in comments 1) through 5), it is often best to plot roots in terms of their so-called *modal parameters* (e.g., damping factors, damped natural frequencies, and undamped natural frequencies) as shown in Figure 3.2 below. The student is encouraged to prove that the equations following the figure are true.

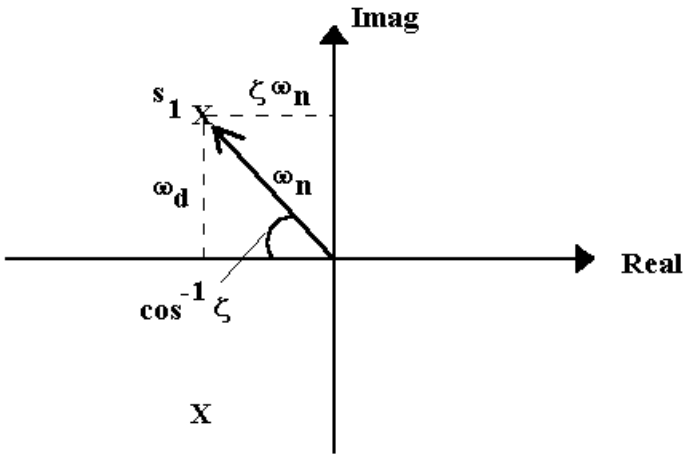

Figure 3.3: Plot of root locations in complex plane using modal parameters

$$\begin{aligned} \text{Given } s_{1,2} &= \sigma \pm j\omega_d = -\varsigma\omega_n \pm j\sqrt{1-\varsigma^2}\,\omega_n \\ \operatorname{Re} s_{1,2} &= -\varsigma\omega_n, \operatorname{Im} s_{1,2} = \pm j\sqrt{1-\varsigma^2}\,\omega_n \\ \text{(Modulus) } \left\|s_{1,2}\right\| &= \sqrt{\sigma^2+\omega_d^2} \\ \text{(Argument) } \angle s_{1,2} &= \pm\cos^{-1}\varsigma \end{aligned} \qquad (3.14)$$

Therefore, roots that are far away from the origin correspond to large undamped natural frequencies, roots close to the imaginary axis correspond to lightly damped (underdamped) responses, and roots close to the real axis correspond to heavily damped responses.

In summary, the complex plane is a simple way to visual free responses in linear vibrating systems. By plotting the roots of the characteristic equation, and studying their real and imaginary parts, we can immediately determine whether the response exhibits oscillations and to what degree. We can also determine whether the response is stable or unstable. Students are encouraged to review Figure 3.1 thoroughly; a good knowledge of how pole locations determine free response characteristics is indispensable in mechanical vibration analysis.

The solution of a SDOF system is rarely written in the form given in Eq.(3.7), rather it is usually written in the following simplified manner:

$$\begin{aligned} x_d(t) &= X_o e^{\sigma t}\cos(\omega_d t + \phi_o) \\ &= X_o e^{-\zeta\omega_n t}\cos\left(\sqrt{1-\zeta^2}\,\omega_n t + \phi_o\right) \\ \text{where } x_d(0) &= X_o\cos\phi_o \\ \dot{x}_d(0) &= \sigma X_o\cos\phi_o - \omega_d X_o\sin\phi_o \end{aligned}$$

(3.15)

This form is obtained using Euler's formula with the complex conjugate constants A_1 and A_2 in Eq. (3.7). After applying the initial conditions, the following values of X_o and ϕ_o are obtained:

$$\begin{aligned} \phi_o &= \tan^{-1}\frac{-\dot{x}_d(0) + \sigma x_d(0)}{\omega_d} \\ X_o &= \sqrt{\left(\frac{-\dot{x}_d(0) + \sigma x_d(0)}{\omega_d}\right)^2 + \left(x_d(0)\right)^2} \end{aligned}$$

(3.16)

Note that just as the constants A_1 and A_2 in Eq. (3.7) were determined by the initial conditions, so to are the constants X_o and ϕ_o in Eq. (3.15).

3.2 Free response of single degree-of-freedom systems for arbitrary damping

The SDOF system in Eq. (3.1) had viscous damping, which is rare. Systems usually have more arbitrary linear or even nonlinear types of damping mechanisms. For instance, when we model a system with wheels, we usually need to model the Coulomb damping/friction in the bearings to account for surface-to-surface dissipation during oscillation. When we model structural vibrations within fluids (i.e., off-shore oil rigs), we usually include nonlinear quadratic damping to account for dissipation due to momentum transfer in the fluid. We can also model structural or hysteretic (material) damping in problems with harmonic inputs by using a complex stiffness parameter. Structural damping occurs as material layers slide over one another during vibration. It is important to remember that damping is one of the most difficult phenomena to model in vibrating systems. In fact, in the twenty years from 1945 to 1965, 2000 papers were published in the area of damping technology. Mass and stiffness can both be approximated rather accurately using finite element models, for instance; however, damping estimates are notoriously inaccurate because dissipation is difficult to quantify analytically. Damping is usually best estimated experimentally.

Although damping mechanisms in real systems are rarely viscous, the "nice" analytical properties of vibrating systems with viscous damping are worth exploiting if possible. In fact, the concept of equivalent viscous damping is in wide use within the noise & vibration engineering community. The *equivalent viscous damping* in a model is defined such that the total energy dissipated per cycle in the model is the same as in the true physical vibrating system under harmonic excitation (forced response to be addressed in the next chapter). More specifically, if W_{nc} is the amount of energy dissipated per cycle, then the equivalent viscous damping, C_{eq}, is defined as follows:

$$\begin{aligned} dW_{nc} &= F_{viscous} \cdot dx, \quad \text{given } x(t) = X_o \cos \omega t \\ \frac{W_{nc}}{cycle} &= \int_{cycle} -C_{eq}\dot{x}dx = \int_0^{2\pi/\omega} -C_{eq}\dot{x}^2 dt \\ &= \int_0^{2\pi/\omega} -C_{eq}X_o{}^2 \cos^2 \omega t dt \\ &= -\pi\omega C_{eq}X_o^2 \end{aligned}$$

(3.17)

The equivalent viscous damping is chosen such that for oscillation amplitudes X_o, the energy dissipated in the viscous damper is the same as that dissipated in the arbitrary damper within the system. Note that we are prematurely introducing forced SDOF responses to harmonic excitations in order to talk about the following most common damping mechanisms.

For example, a system with Coulomb friction is governed by the type of damping characteristic shown in Figure 3.4. Recall that the idealized static Coulomb friction force is equal to the product of the static friction coefficient between two surfaces, μ, and the normal force between the surfaces, N. A viscous damping characteristic is also shown in the figure for reference. Note that Coulomb friction is a nonlinear kind of damping; i.e., the qualitative nature of the damping characteristic is a function of the relative velocity between the two surfaces. For positive velocities, the friction/damping force is positive and opposes the motion whereas for negative velocities this force is negative and again opposes the motion. In these two vibration regimes, a SDOF system model is given by the following two equations, where the normal force has been assumed to be equal to the gravitational force on the mass:

$$M\ddot{x} + Kx = -\mu Mg \text{ for } \dot{x} > 0$$
$$M\ddot{x} + Kx = +\mu Mg \text{ for } \dot{x} < 0$$

(3.18 a,b)

By solving each of these equations in succession using the SDOF forced response solution techniques discussed in the next chapter, we can show that the rate of decay of the peak amplitudes is linear with time rather than exponential as with viscous damping. It may also be clear from Eqs. (3.18 a,b) that the frequency of oscillation/vibration does not depend on the friction force or coefficient of friction; it is always equal to $\sqrt{(K/M)}$. As long as the restoring force in the spring is large enough to overcome the friction force, the mass will continue to oscillate as shown in Figure 3.4.

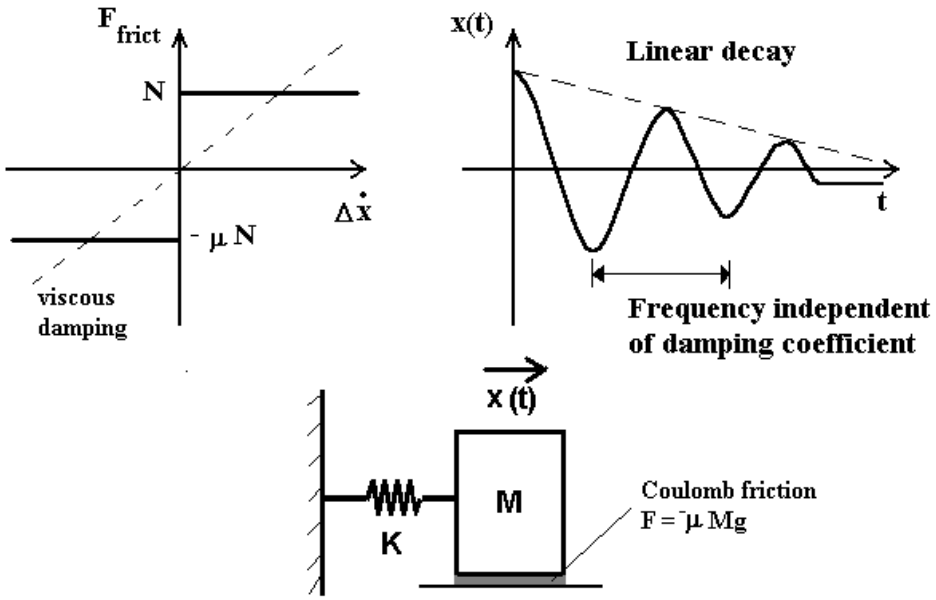

Figure 3.4: (Top left) Coulomb friction characteristic and (right) free vibration response

As a second example of non-viscous damping, consider the common case of *hysteretic* or *structural damping*. Recall that viscous damping forces are proportional to the velocity across the damper; in other words, if a SDOF system is made to oscillate at a certain frequency, ω, according to $x(t)=X_o\cos(\omega t+\phi)$, then the viscous damping force is:

$$\begin{aligned} F_{viscous} &= C\dot{x} \\ &= \omega C X_o \sin(\omega t + \phi) \end{aligned} \qquad (3.19)$$

which means the force is in phase with the velocity and proportional to the frequency. Recall from Eq. (3.17) that the energy dissipated in the viscous damper in one cycle is also proportional to the frequency. It is widely known that energy dissipation in many kinds of materials and structural joints is not proportional to frequency but instead to the amplitude of oscillation. These damping mechanisms are at the same time in phase with the velocity (i.e., 90 deg out of phase with the displacement). In order to satisfy these two observed phenomena, the viscous damping model can be used to describe structural damping so long as the damping coefficient is chosen such that $C=h/\omega$, where h is the hysteretic damping coefficient. This choice of C leads to the following hysteresis damping force under harmonic excitation:

$$\begin{aligned} F_{hysteresis} &= C\dot{x} \\ &= \omega C X_o \sin(\omega t + \phi) \\ &= h X_o \sin(\omega t + \phi) \end{aligned}$$

(3.20)

In most applications, hysteretic or structural damping is usually incorporated into models by defining a so-called *complex modulus*, $K(1+j\eta)$, where $\eta=h/K$ is called the *loss coefficient*. It should be noted at this point most material dampers provide less energy dissipation for higher frequencies, which is inconsistent with both the viscous and hysteretic models. Figure 3.5 shows a typical plot of a loss coefficient in a viscoelastic material, which is by far the most common damping material in use today. Note that there is an optimum frequency and temperature at which the viscoelastic should be used to dissipate energy.

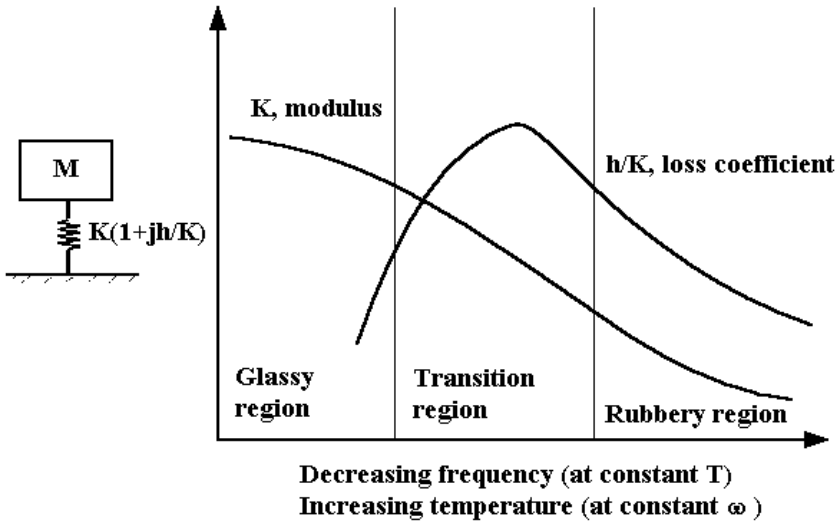

Figure 3.5: Characteristics of complex modulus in viscoelastic damping material

3.3 Free response of multiple degree-of-freedom systems

Although many applications can be modeled with a single degree-of-freedom, most systems contain multiple degrees-of-freedom (MDOF). Sometimes we do not need to include all of these DOFs. For instance, an offshore oil platform (Figure 3.6) vibrates as if it were a SDOF system in

many circumstances because the support acts largely as a stiffness element and the platform acts like an inertia in the frequency range associated with typical waves. For higher frequencies associated with pressure surges or pulsations in the oil delivery pipelines, the tower behaves more like a collection of oscillating bodies with different components in the platform participating in the modes of vibration. This type of transition from low-order (SDOF-like) to high-order (MDOF-like) vibrations is common in most applications. We should always think about the *frequency range of interest* before we begin to model or analyze a vibrating system.

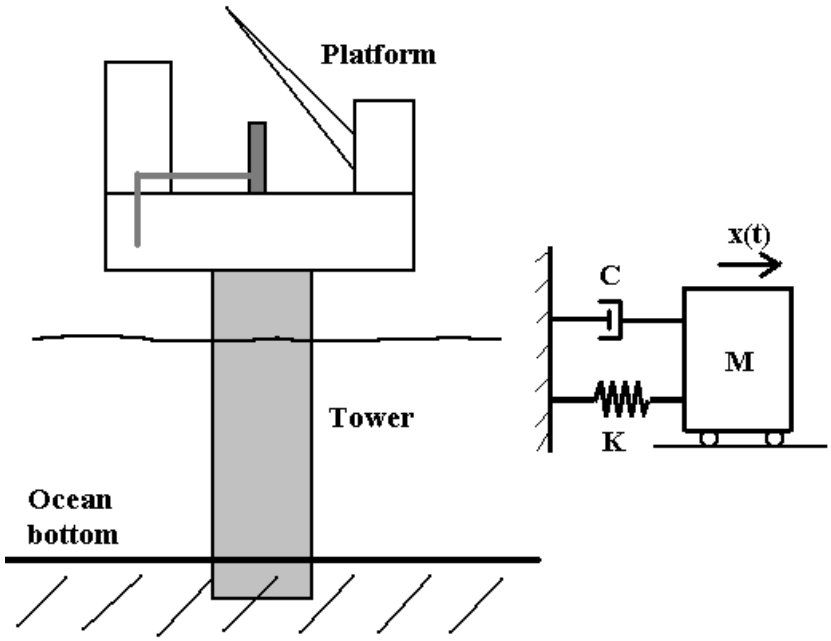

Figure 3.6: Offshore oil platform with SDOF model

The basis of our analysis of free response in MDOF systems is the principle of linear superposition. Recall from Section 3.1 that the free response of a SDOF system occurs at the damped natural frequency of oscillation. When we look at the free response of a MDOF system (Figure 3.7), we find that each DOF response contains several frequencies. Each of these frequencies can be associated with a SDOF system. By adding the free responses from all of the SDOF systems, the MDOF system response is obtained. These SDOF systems that make up the MDOF system are called *normal modes* (for special types of damping) or just *modes of vibration*. Each mode has a temporal component, the modal frequency $\sigma_r+j\omega_r$, and a spatial component, the modal vector ψ_r. Figure 3.7 shows that in general the modal frequencies are different as are the modal vectors. In this particular case, the two DOF system is decomposed into two SDOF

systems with an in-phase lower frequency mode of vibration (lower-left) and out-of-phase higher frequency mode of vibration (lower-right). Our goal in this section is to justify this proposed SDOF method of analysis with MDOF analytical techniques. We will be using eigen-solution methods for obtaining the modal properties, so students are encouraged to review their previous experience with methods in linear algebra.

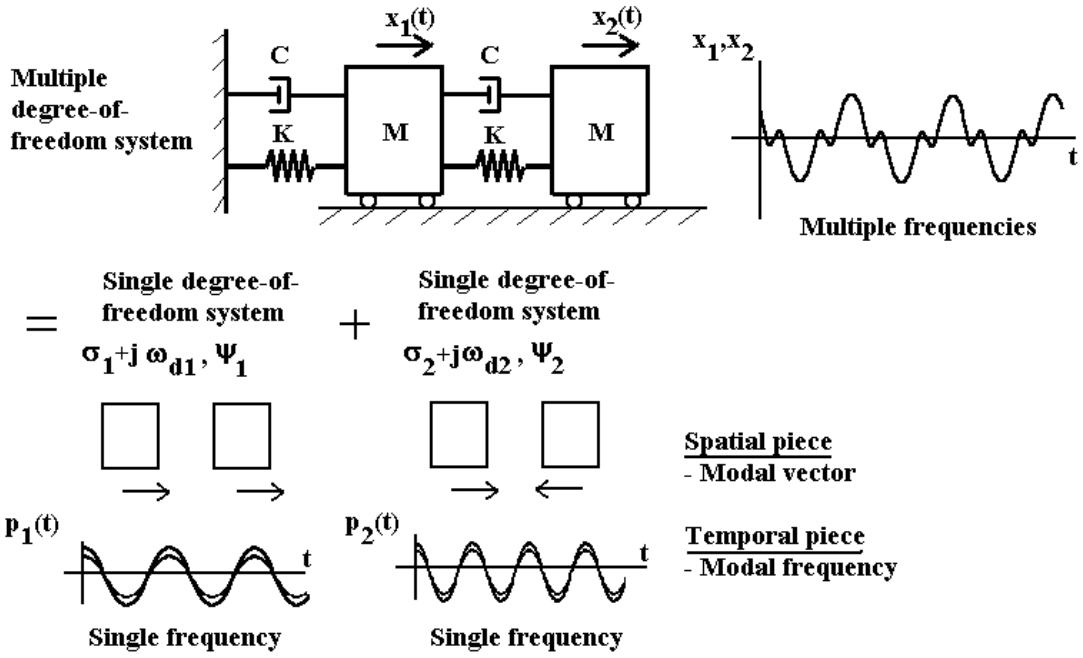

Figure 3.7: MDOF system described as a superposition of SDOF modes of vibration

We will start by writing down the EOM for the simple two DOF shown in Figure 3.7:

$$\begin{bmatrix} M & 0 \\ 0 & M \end{bmatrix} \begin{Bmatrix} \ddot{x}_1 \\ \ddot{x}_2 \end{Bmatrix} + \begin{bmatrix} 2C & -C \\ -C & C \end{bmatrix} \begin{Bmatrix} \dot{x}_1 \\ \dot{x}_2 \end{Bmatrix} + \begin{bmatrix} 2K & -K \\ -K & K \end{bmatrix} \begin{Bmatrix} x_1 \\ x_2 \end{Bmatrix} = \begin{Bmatrix} 0 \\ 0 \end{Bmatrix} \tag{3.21}$$

Note that the external (exogenous) forces are zero in this case as they must be in a free vibration problem. There are two ways to proceed from here: we can use physical arguments to find the modal properties or we can use mathematical eigen-methods to calculate the modal properties. Both approaches offer insight into general MDOF vibrating systems, so we will discuss both of

them. We will begin with the first approach because it is a more physical and intuitive approach to free vibration analysis in MDOF systems.

The model in Eq. (3.21) admits a wide variety of solutions. Because our argument above in Figure 3.7 is based on the premise that MDOF systems are actually a combination of SDOF normal modes, we will proceed in exactly the same way as we did to find the free response of SDOF systems. First, we make a guess of the form,

$$\begin{Bmatrix} x_1 \\ x_2 \end{Bmatrix} = \begin{Bmatrix} X_1 \\ X_2 \end{Bmatrix} e^{st} \tag{3.22}$$

substitute our guess into the EOM,

$$\begin{bmatrix} Ms^2 + 2Cs + 2K & -Cs - K \\ -Cs - K & Ms^2 + Cs + K \end{bmatrix} \begin{Bmatrix} X_1 \\ X_2 \end{Bmatrix} e^{st} = \begin{Bmatrix} 0 \\ 0 \end{Bmatrix} \tag{3.23}$$

and pick the only non-trivial solutions. It is these non-trivial solutions that will make up the normal modes we talked about in Figure 3.7. For non-trivial solutions of Eq. (3.23), $X_1 \neq 0$ and $X_2 \neq 0$, the matrix on the left hand side must be singular (i.e., it must have a non-zero null space). This constraint gives us the characteristic equation of the two DOF system:

$$\left(Ms^2 + 2Cs + 2K\right)\left(Ms^2 + Cs + K\right) - \left(Cs + K\right)^2 = 0 \tag{3.24}$$

which has four solutions, $s_1=\sigma_1+j\omega_1$, $s_2=\sigma_1-j\omega_1$, $s_3=\sigma_2+j\omega_2$, and $s_4=\sigma_2-j\omega_2$. The real parts of these solutions determine the decay/growth rate of the free responses whereas the imaginary parts determine the frequencies of oscillation (recall the discussion surrounding Eq. (3.10) in Section 3.1). For simplicity in notation, we have suppressed the subscript "*d*" that indicates that the imaginary parts of the roots are damped natural frequencies. Note that each complex conjugate pair of roots (modal frequencies) is associated with a different solution vector (modal vector) in

Eq. (3.23). From the form of the original guess, the solution can now be written in either of the following ways using Euler's formula ($e^{\pm ja}=cosa \pm jsina$):

$$\begin{Bmatrix} x_1 \\ x_2 \end{Bmatrix} = \begin{Bmatrix} X_{11} \\ X_{21} \end{Bmatrix} e^{s_1 t} + \begin{Bmatrix} X^*_{11} \\ X^*_{21} \end{Bmatrix} e^{s_2 t} + \begin{Bmatrix} X_{12} \\ X_{22} \end{Bmatrix} e^{s_3 t} + \begin{Bmatrix} X^*_{12} \\ X^*_{22} \end{Bmatrix} e^{s_4 t}$$

$$= X_1 \begin{Bmatrix} \psi_{11} \\ \psi_{21} \end{Bmatrix} e^{\sigma_1 t} \cos(\omega_1 t + \phi_1) + X_2 \begin{Bmatrix} \psi_{12} \\ \psi_{22} \end{Bmatrix} e^{\sigma_2 t} \cos(\omega_2 t + \phi_2)$$

(3.25 a,b)

These equations are in the form we discussed previously; two modes of vibration are used to describe the total solution. The constant vectors, $\{X_{1r} \;\; X_{2r}\}^T$ and $\{X^*_{1r} \;\; X^*_{2r}\}^T$, are complex conjugates of one another and are associated with mode *r*. They correspond to the constants, A_1 and A_2, in the SDOF free response solution. The modal vectors, $\{\psi_{1r} \;\; \psi_{2r}\}^T$, in the second of Eqs. (3.25 a,b) are determined to within a scale factor; these vectors describe how the DOFs move relative to one another at the two modes of vibration, *r=1* and *r=2*. It is important to note that the modal vectors are not unique. The $e^{\sigma r t}cos(\omega_r t+\phi_r)$ factors in Eqs. (3.25 a,b) are determined by the modal frequencies/roots from Eq. (3.24); they describe the frequency and damping characteristics of each of the modal responses. Just as we argued in Figure 3.7, the modal frequencies from the characteristic equation determine the *temporal* characteristics of the solution and the modal vectors from the nullspace calculation in Eq. (3.23) determine the *spatial* characteristics in the solution. This decomposition of the MDOF response into temporal and spatial pieces is only possible with linear systems thanks to the principle of linear superposition.

The second equation in Eqs. (3.25 a,b) is the form we will use in this course because it is most easily applied to satisfy the initial conditions. How many initial conditions do we need? Because there are four constants to determine, X_1, X_2, ϕ_1 and, ϕ_2, we need four initial conditions on the displacements and velocities of the two coordinates. These four conditions are satisfied as follows:

$$\begin{Bmatrix} x_1(0) \\ x_2(0) \end{Bmatrix} = A_1 \begin{Bmatrix} \psi_{11} \\ \psi_{21} \end{Bmatrix} \cos(\phi_1) + A_2 \begin{Bmatrix} \psi_{12} \\ \psi_{22} \end{Bmatrix} \cos(\phi_2)$$

$$\begin{Bmatrix} \dot{x}_1(0) \\ \dot{x}_2(0) \end{Bmatrix} = \sigma_1 A_1 \begin{Bmatrix} \psi_{11} \\ \psi_{21} \end{Bmatrix} \cos(\phi_1) - \omega_1 A_1 \begin{Bmatrix} \psi_{11} \\ \psi_{21} \end{Bmatrix} \sin(\phi_1) + \sigma_2 A_2 \begin{Bmatrix} \psi_{12} \\ \psi_{22} \end{Bmatrix} \cos(\phi_2) - \omega_2 A_2 \begin{Bmatrix} \psi_{12} \\ \psi_{22} \end{Bmatrix} \sin(\phi_2)$$

OR

$$\begin{Bmatrix} x_1(0) \\ x_2(0) \end{Bmatrix} = \begin{bmatrix} \psi_{11} & \psi_{12} \\ \psi_{21} & \psi_{22} \end{bmatrix} \begin{Bmatrix} A_1 \cos(\phi_1) \\ A_2 \cos(\phi_2) \end{Bmatrix}$$

$$\begin{Bmatrix} \dot{x}_1(0) \\ \dot{x}_2(0) \end{Bmatrix} = \begin{bmatrix} \sigma_1\psi_{11} & \sigma_2\psi_{12} \\ \sigma_1\psi_{21} & \sigma_2\psi_{22} \end{bmatrix} \begin{Bmatrix} A_1 \cos(\phi_1) \\ A_2 \cos(\phi_2) \end{Bmatrix} + \begin{bmatrix} -\omega_1\psi_{11} & -\omega_2\psi_{12} \\ -\omega_1\psi_{21} & -\omega_2\psi_{22} \end{bmatrix} \begin{Bmatrix} A_1 \sin(\phi_1) \\ A_2 \sin(\phi_2) \end{Bmatrix}$$

(3.26 a,b,c,d)

In order to make this discussion less abstract, consider the special case when *K=1 N/m*, *C=0.1 Ns/m*, and *M=1 kg*. Then the solution in Eq. (3.25 a,b) is given by,

$$\begin{Bmatrix} x_1 \\ x_2 \end{Bmatrix} = X_1 \begin{Bmatrix} 0.618 \\ 1.000 \end{Bmatrix} e^{-0.019t} \cos(0.618t + \phi_1) + X_2 \begin{Bmatrix} 1.000 \\ -0.618 \end{Bmatrix} e^{-0.131t} \cos(1.613t + \phi_2)$$

(3.27 a,b)

These two modes of vibration are illustrated in Figure 3.8 below. Note that the first mode is at a lower frequency than the second mode and is more lightly damped as well. Also note that in the first mode, the x_1 coordinate (solid line) has lower relative amplitude than the x_2 coordinate (dotted line). Finally, it is important to note that the amplitude of the modal components shown in Figure 3.8 are arbitrary. They were selected so that the largest amplitude would have a value of unity. In order to obtain the exact amplitudes, initial conditions must be applied and Eqs. (3.26 a,b,c,d) must then be solved to obtain the constants in the solution. The relative amplitudes shown in Figure 3.8 would still apply in this case.

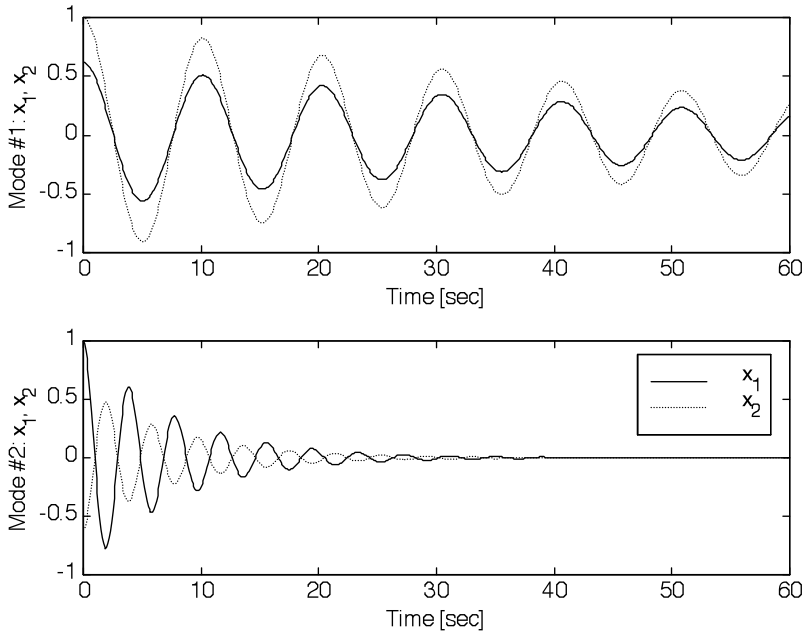

Figure 3.8: Two modes of vibration in two DOF system

We can also use eigen-analysis techniques to find the modal frequencies and vectors as follows. If the system has no damping, then Eq. (3.23) reduces to the following:

$$\begin{bmatrix} Ms^2 + 2K & -K \\ -K & Ms^2 + K \end{bmatrix} \begin{Bmatrix} X_1 \\ X_2 \end{Bmatrix} e^{st} = \begin{Bmatrix} 0 \\ 0 \end{Bmatrix} \tag{3.28}$$

which can be easily reformulated into the following standard eigen-problem,

$$[A] \begin{Bmatrix} X_1 \\ X_2 \end{Bmatrix} = \lambda \begin{Bmatrix} X_1 \\ X_2 \end{Bmatrix} \tag{3.29}$$

by moving the inertia terms to the right and the stiffness terms to the left.

$$\begin{bmatrix} 2K & -K \\ -K & K \end{bmatrix} \begin{Bmatrix} X_1 \\ X_2 \end{Bmatrix} = -s^2 \begin{bmatrix} M & 0 \\ 0 & M \end{bmatrix} \begin{Bmatrix} X_1 \\ X_2 \end{Bmatrix}$$

$$\begin{bmatrix} M & 0 \\ 0 & M \end{bmatrix}^{-1} \begin{bmatrix} 2K & -K \\ -K & K \end{bmatrix} \begin{Bmatrix} X_1 \\ X_2 \end{Bmatrix} = \lambda \begin{Bmatrix} X_1 \\ X_2 \end{Bmatrix}$$

$$\begin{bmatrix} 2K/M & -K/M \\ -K/M & K/M \end{bmatrix} \begin{Bmatrix} X_1 \\ X_2 \end{Bmatrix} = \lambda \begin{Bmatrix} X_1 \\ X_2 \end{Bmatrix}$$

(3.30)

Now we just solve for the eigenvalues and eigenvectors of the matrix on the left hand side of this equation. The values we obtain are given below:

$$\lambda_1 = -s_{1,2}^2 = 0.382, \lambda_2 = -s_{3,4}^2 = 2.618$$

$$\begin{Bmatrix} X_1 \\ X_2 \end{Bmatrix}_1 = \begin{Bmatrix} 0.618 \\ 1.000 \end{Bmatrix}, \begin{Bmatrix} X_1 \\ X_2 \end{Bmatrix}_2 = \begin{Bmatrix} 1.000 \\ -0.618 \end{Bmatrix}$$

$$\text{which yields } s_{1,2} = \pm j0.618 = \pm j\omega_{n1} \text{ and } s_{3,4} = \pm j1.618 = \pm j\omega_{n2}$$

(3.31)

Note how the eigenvalues of the system in Eq. (3.30) are related to the modal frequencies of the system. For every pair of modal frequencies, we have one eigenvalue. Since we ignored the damping to formulate the eigenvalue problem, we ended up with purely imaginary modal frequencies, which correspond to the undamped natural frequencies of the system. The undamped natural frequencies in Eq. (3.31) are very close to the damped natural frequencies that were found in Eq. (3.27 a,b) because the system is lightly damped (i.e., $\zeta << 1$) with the selected value of C. In large problems, we often carry out the procedure above to find the modal frequencies. That is, we ignore damping temporarily to formulate the eigenvalue problem, compute the eigenvalues and eigenvectors, compute the undamped modal frequencies, and then estimate the damping factors for each pole. In fact, this technique is the most common one applied in standard finite element software.

If we preferred to retain damping throughout the eigenvalue problem, then we must reformulate the EOMs in Eq. (3.21) in the state space. In other words, we define two of the state

variables as the displacements of the two DOFs and the other two as the derivatives of these variables. This produces the *Duncan-Collar formulation* and is given below:

$$\begin{bmatrix} 1 & 0 & 0 & 0 \\ 0 & M & 0 & 0 \\ 0 & 0 & 1 & 0 \\ 0 & 0 & 0 & M \end{bmatrix} \begin{Bmatrix} \dot{y}_1 \\ \dot{y}_2 \\ \dot{y}_3 \\ \dot{y}_4 \end{Bmatrix} + \begin{bmatrix} 0 & -1 & 0 & 0 \\ 2K & 2C & -K & -C \\ 0 & 0 & 0 & -1 \\ -K & -C & K & C \end{bmatrix} \begin{Bmatrix} y_1 \\ y_2 \\ y_3 \\ y_4 \end{Bmatrix} = \begin{Bmatrix} 0 \\ 0 \\ 0 \\ 0 \end{Bmatrix}$$

where $y_1 = x_1, y_2 = \dot{x}_1 = \dot{y}_1, y_3 = x_2, y_4 = \dot{x}_2 = \dot{y}_3$

(3.32)

The eigenvalues and eigenvectors of the system can then be computed as before except now there is no need to perform the subsidiary calculation with s^2 because the system is formulated as first order rather than second order. Students are encouraged to attempt this calculation and compare their results with the ones given in Eqs. (3.27 a,b).

3.4 Principal coordinates and modal transformations

The techniques described above for treating discrete MDOF systems like a collection of SDOF systems, each with their own associated modal frequencies and vectors, can be formulated in a more systematic way. Consider again the two DOF system from Eq. (3.21), repeated below for convenience:

$$\begin{bmatrix} M & 0 \\ 0 & M \end{bmatrix} \begin{Bmatrix} \ddot{x}_1 \\ \ddot{x}_2 \end{Bmatrix} + \begin{bmatrix} 2C & -C \\ -C & C \end{bmatrix} \begin{Bmatrix} \dot{x}_1 \\ \dot{x}_2 \end{Bmatrix} + \begin{bmatrix} 2K & -K \\ -K & K \end{bmatrix} \begin{Bmatrix} x_1 \\ x_2 \end{Bmatrix} = \begin{Bmatrix} 0 \\ 0 \end{Bmatrix}$$

If we ignore damping again, for convenience only, then our goal in this section will be to find a new set of coordinates defined by the transformation, $\mathbf{x}(t)=\mathbf{\Psi}\mathbf{p}(t)$, where $\mathbf{p}(t)$ is the vector of *principal coordinates*. Note that we are prompted to use a linear transformation here because the system obeys the principle of superposition. We want to choose the transformation, $\mathbf{\Psi}$, such that the resulting EOMs in terms of principal coordinates are as "simple" as possible. Recall from Figure 3.7 that our ideal description of a MDOF system is a collection of SDOF systems. Furthermore, we want these SDOF systems to be *uncoupled* from one another so that we can solve each of them independently and then add the results to produce the total solution for the

MDOF system. This transformation will be called a *modal transformation* for the reasons explained below.

Fortunately, we have already achieved this kind of transformation in Eq. (3.25 a,b), which is repeated below and re-written using the notation above:

$$\begin{aligned}\begin{Bmatrix} x_1 \\ x_2 \end{Bmatrix} &= X_1 \begin{Bmatrix} \psi_{11} \\ \psi_{21} \end{Bmatrix} e^{\sigma_1 t} \cos(\omega_{d1} t + \phi_1) + X_2 \begin{Bmatrix} \psi_{12} \\ \psi_{22} \end{Bmatrix} e^{\sigma_2 t} \cos(\omega_{d2} t + \phi_2) \\ &= \begin{bmatrix} \psi_{11} & \psi_{12} \\ \psi_{21} & \psi_{22} \end{bmatrix} \begin{Bmatrix} X_1 e^{\sigma_1 t} \cos(\omega_{d1} t + \phi_1) \\ X_2 e^{\sigma_2 t} \cos(\omega_{d2} t + \phi_2) \end{Bmatrix} \\ \mathbf{x}(t) &= \Psi \mathbf{p}(t)\end{aligned}$$

(3.33)

Thus, the principal coordinates we seek are precisely the same as the temporal components in the free response solution, which we already obtained in Eq. (3.25 a,b). The transformation matrix, $\boldsymbol{\Psi}$, was also obtained previously and is simply the matrix of modal vectors. Again we see that the principle of linear superposition is at work: the free response of a MDOF system is the superposition of the free responses of the individual modes of vibration (principal coordinates). If we substitute the modal vectors from Eq. (3.27 a,b) into the undamped version of the two DOF system, then we can carry out the following simplifications using linear algebra:

$$\begin{aligned}&\begin{bmatrix} M & 0 \\ 0 & M \end{bmatrix} \begin{Bmatrix} \ddot{x}_1 \\ \ddot{x}_2 \end{Bmatrix} + \begin{bmatrix} 2K & -K \\ -K & K \end{bmatrix} \begin{Bmatrix} x_1 \\ x_2 \end{Bmatrix} = \begin{Bmatrix} 0 \\ 0 \end{Bmatrix} \\ &\begin{bmatrix} M & 0 \\ 0 & M \end{bmatrix} \begin{bmatrix} \psi_{11} & \psi_{12} \\ \psi_{21} & \psi_{22} \end{bmatrix} \begin{Bmatrix} \ddot{p}_1 \\ \ddot{p}_2 \end{Bmatrix} + \begin{bmatrix} 2K & -K \\ -K & K \end{bmatrix} \begin{bmatrix} \psi_{11} & \psi_{12} \\ \psi_{21} & \psi_{22} \end{bmatrix} \begin{Bmatrix} p_1 \\ p_2 \end{Bmatrix} = \begin{Bmatrix} 0 \\ 0 \end{Bmatrix} \\ &\begin{bmatrix} \psi_{11} & \psi_{12} \\ \psi_{21} & \psi_{22} \end{bmatrix}^T \begin{bmatrix} M & 0 \\ 0 & M \end{bmatrix} \begin{bmatrix} \psi_{11} & \psi_{12} \\ \psi_{21} & \psi_{22} \end{bmatrix} \begin{Bmatrix} \ddot{p}_1 \\ \ddot{p}_2 \end{Bmatrix} + \begin{bmatrix} \psi_{11} & \psi_{12} \\ \psi_{21} & \psi_{22} \end{bmatrix}^T \begin{bmatrix} 2K & -K \\ -K & K \end{bmatrix} \begin{bmatrix} \psi_{11} & \psi_{12} \\ \psi_{21} & \psi_{22} \end{bmatrix} \begin{Bmatrix} p_1 \\ p_2 \end{Bmatrix} = \begin{Bmatrix} 0 \\ 0 \end{Bmatrix} \\ &\Psi^T \mathbf{M} \Psi \ddot{\mathbf{p}} + \Psi^T \mathbf{K} \Psi \mathbf{p} = \mathbf{0} \\ &\mathbf{M}_r \ddot{\mathbf{p}} + \mathbf{K}_r \mathbf{p} = \mathbf{0}\end{aligned}$$

(3.34)

If we want the principal coordinates to decouple the MDOF system into two SDOF systems, then the two coefficient matrices, the so-called *modal mass* and *modal stiffness matrices*, in Eq.

(3.34) must be diagonal. We can prove that they are by reconsidering our eigen-system analysis of this system. First, recall from Eq. (3.30) that each set of eigenvalues and eigenvectors, $\lambda=-s^2$ and $\{X_1 \; X_2\}^T$, satisfy the following equation:

$$\mathbf{K}\begin{Bmatrix} X_1 \\ X_2 \end{Bmatrix} = \lambda\mathbf{M}\begin{Bmatrix} X_1 \\ X_2 \end{Bmatrix}$$

(3.35)

Next, write this relationship for the two different sets of eigenvalues and eigenvectors, pair *r* and pair *s*:

$$\begin{aligned} \mathbf{K}\psi_r &= \lambda_r\mathbf{M}\psi_r \\ \mathbf{K}\psi_s &= \lambda_s\mathbf{M}\psi_s \end{aligned}$$

(3.36)

Now we perform an inspired sequence of linear algebra operations: we pre-multiply the first equation by the transpose of the *s* eigenvector and the second by the transpose of the *r* eivenvector, and then subtract these two results to obtain the following result:

$$\begin{aligned} \psi_s^T\mathbf{K}\psi_r &= \lambda_r\psi_s^T\mathbf{M}\psi_r \\ \psi_r^T\mathbf{K}\psi_s &= \lambda_s\psi_r^T\mathbf{M}\psi_s \\ 0 &= (\lambda_r - \lambda_s)\psi_r^T\mathbf{M}\psi_s \quad \text{for } r \neq s \end{aligned}$$

(3.37)

The last of these equations proves that if the two eigenvalues are distinct, then the corresponding eigenvectors are orthogonal with respect to the mass matrix. Likewise, they are also orthogonal with respect to the stiffness matrix:

$$0 = (\lambda_r - \lambda_s)\psi_r^T\mathbf{K}\psi_s \quad \text{for } r \neq s$$

(3.38)

Of course, when r=s, Eqs. (3.37) and (3.38) are not satisfied, rather, they produce the modal mass and modal stiffness, respectively. Armed with this information, we can revisit Eq. (3.34) and discover that we were successful in transforming the MDOF system into uncoupled SDOF systems of the following form:

$$\mathbf{M}_r\ddot{\mathbf{p}} + \mathbf{K}_r\mathbf{p} = \mathbf{0} \Rightarrow M_r\ddot{p}_r + K_r p_r = 0 \text{ for } r = 1,2$$
$$\text{where } \psi_r^T\mathbf{M}\psi_r = M_r \text{ and } \psi_r^T\mathbf{K}\psi_r = K_r \qquad (3.39)$$

The principal coordinate solutions to these equations are those given in Eq. (3.33). In summary, we used a coordinate transformation from physical (x) to principal or modal (p) coordinates to decouple the MDOF system into a collection of SDOF systems. The solutions to each of these SDOF EOMS are then combined using linear superposition according to Eq. (3.33).

The modal analysis described above and resulting in Eq. (3.39) was only valid for undamped systems; however, similar analyses can also be carried out for damped systems with special classes of damping. For example, *proportionally damped* systems have viscous damping matrices of the following form:

$$\mathbf{C} = \alpha\mathbf{M} + \beta\mathbf{K} \qquad (3.40)$$

where α and β are real constants. Systems with damping of this type afford the same sort of modal decomposition as in Eq. (3.39) with the addition of an extra damping term:

$$\mathbf{M}_r\ddot{\mathbf{p}} + \mathbf{C}_r\mathbf{p} + \mathbf{K}_r\mathbf{p} = \mathbf{0} \Rightarrow M_r\ddot{p}_r + C_r\dot{p}_r + K_r p_r = 0 \text{ for } r = 1,2 \qquad (3.41)$$

When systems are *non-proportionally damped* (viscous), then the Duncan-Collar formulation in Eq. (3.32) is used to perform the modal transformation in a subsidiary first order vector space. When other arbitrary forms of damping (e.g., structural) are encountered, then the equivalent

viscous damping can be computed for harmonic inputs as described previously in Section 3.2, and then the Duncan-Collar formulation can be used to perform the modal transformation.

In the interest of clarity, we should pause for a moment and consider some of the variations in terminology that we see in the literature. Sometimes the components in $\mathbf{p}(t)$ will be called the *natural coordinates* instead of the principal coordinates, and, in a similar way, we will call the vectors in $\boldsymbol{\Psi}$ the *natural modes* instead of the modal vectors. Furthermore, if the natural modes/modal vectors are normalized in any consistent way (e.g., unity modal mass) with respect to the mass and stiffness matrices as in Eq. (3.39) then we replace the word "natural" with "normal" – i.e., normal coordinates and normal modes. We will see this same terminology in the analysis of free response in continuous systems.

3.5 Boundary conditions and rigid body modes in semi-definite MDOF systems

There are many topics to discuss in this course, but two of the most important are boundary conditions and their effects on mechanical vibration characteristics. What do we mean by boundary conditions? Consider the two DOF system in Figure 3.7 and recall that there are two sets of springs and dampers. One set couples the two inertias (i.e., the two DOFs) together whereas the other set holds the two DOFs in the same general area as they vibrate. In this case, the spring and damper to ground at the left of DOF 1 form the boundary condition of this system. Of course, the surface below the two DOFs is also a boundary condition, but in this case it is not very interesting because the wheels are frictionless and massless and experience no slip. We will now consider how the boundary condition to the left of mass 1 affects the free response of the two DOF system.

Physically, we see that if the stiffness, K, to ground becomes very, very large ($\rightarrow\infty$), then the two DOF system becomes a SDOF system because mass 1 is no longer able to move; it is fixed to ground. Does our analysis above reveal this sensitivity to the boundary conditions? From Eq. (3.30), the modified eigen-problem for variable stiffness at the boundary condition is,

$$\begin{bmatrix} \left(K_{boundary}+K\right)/M & -K \\ -K & K/M \end{bmatrix} \begin{Bmatrix} X_1 \\ X_2 \end{Bmatrix} = \lambda \begin{Bmatrix} X_1 \\ X_2 \end{Bmatrix} \qquad (3.42)$$

The undamped modal frequencies corresponding to this eigenvalue problem are shown below in Figure 3.8. Note from the equation above that as the boundary stiffness increases, the modal frequency for the second mode grows and the frequency for the first mode levels out. This result makes physical sense because if the stiffness becomes large enough, the first DOF will remain stationary as the second mass vibrates at $\sqrt{(K/M)}$ according to the schematic in Figure 3.7.

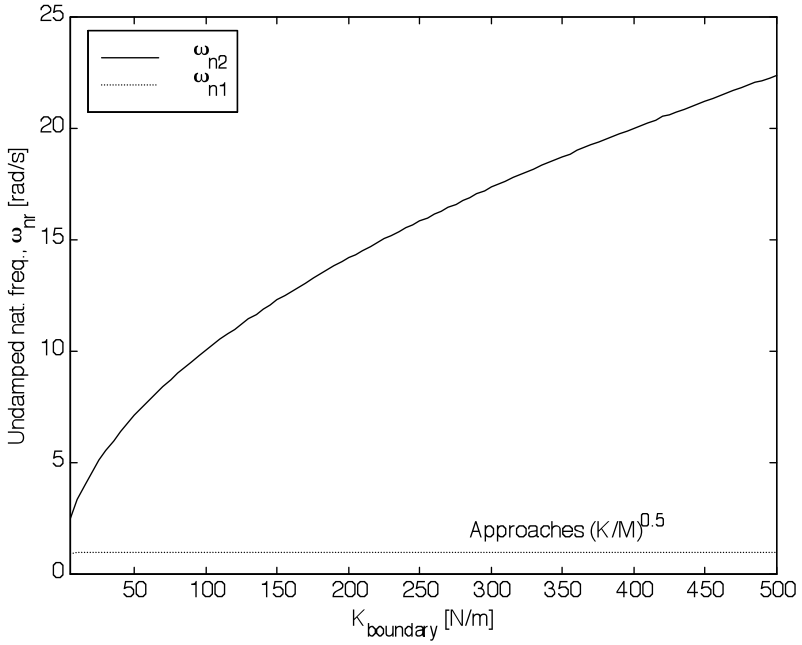

Figure 3.8: Effects of BC stiffness on undamped modal frequencies in two DOF system

What happens to the modal frequencies if we reduce the boundary stiffness to zero? Figure 3.9 shows the same modal frequency sensitivity plot for this case as in Figure 3.8. Note that the first modal frequency, the one which corresponds to the mode of vibration where the two DOFs move in phase, approaches zero. When there is a mode of vibration at zero like this, it is called a *rigid body mode* and the system is said to be *semi-definite*. Physically, it means that the system does not oscillate at all for this modal vector. This result should not surprise us because the system in Figure 3.7 is free to move to any position along the *x* direction and then can oscillate around that position. From Eq. (3.21), when the boundary stiffness goes to zero, the stiffness matrix actually becomes singular. This result also makes physical sense because we should not

be able to solve for a unique steady state (equilibrium point) in this case because the system is unrestrained (free-free BCs).

Rigid body modes are essential in analytical and experimental vibrations because when systems vibrate, they also usually experience rigid body motions. For instance, passenger cars in trains can move as rigid bodies along the track to carry passengers from one place to another, but they can also vibrate as energy is exchanged between the cars. Both types of motion are needed to describe the general motions of the train. In terms of potential energy, the train at one position can have the same potential energy stored in the springs/links between the cars as at any other position of the train along the track. The most common real-world application in which rigid body modes are important is in rotating systems (e.g., stages in gas turbine engine, drive-train in vehicles). In these applications, large rigid body motions of the inertia-shaft assemblies are prevented by bearings.

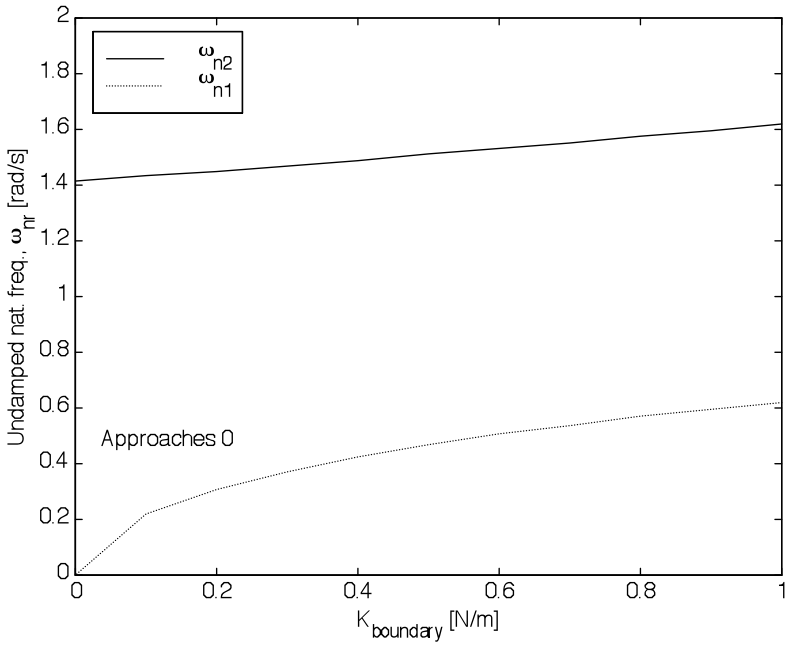

Figure 3.9: Effects of BC stiffness on undamped modal frequencies in two DOF system

3.6 Second order continuous systems and separation of variables

In the discrete MDOF eigen-system/modal analysis described above, we were able to decompose the total free response into two components: a temporal piece (the principal coordinates) and a spatial piece (the modal vectors). We found that this decomposition greatly simplified the EOMs because it effectively decoupled the equations, leaving us only with simple second order (SDOF) equations to solve for the modal responses (normal modes in the undamped case). We would like to exploit the same sort of "separation" of the temporal and spatial pieces in the free responses of second order continuous systems like the string EOM in Eq. (2.36) (homogeneous equation is repeated below for convenience). Boundary conditions will be included below.

$$\rho(x)\frac{\partial^2 y(x,t)}{\partial t^2} - \frac{\partial}{\partial x}\left(T(x)\frac{\partial y(x,t)}{\partial x}\right) = 0 \qquad (3.43)$$

Because the response, *y(x,t)*, is a function of both space and time, this problem could be potentially very difficult to solve when time and space are coupled. Fortunately, our approach so far using linear superposition has been to decouple the temporal and spatial components by thinking in terms of *synchronous* modes of vibration, in which all elements of a system oscillate together (in phase) at certain special frequencies (modal frequencies). With this approach in mind, we can separate the two variables by assuming that the response is of the following form:

$$y(x,t) = Y(x)\cdot G(t) \qquad (3.44)$$

It is instructive to compare Eq. (3.44) with Eq. (3.33): the spatial function, *Y(x)*, is directly analogous to the matrix of modal vectors/natural modes, $\boldsymbol{\Psi}$, and the temporal function, *G(t)*, is directly analogous to the principal coordinates/natural coordinates, $\mathbf{p}(t)$. In fact, if we just allow the number of DOFs to approach infinity, then the modal vectors should turn into *Y(x)* and the principal coordinates should turn into *G(t)*. Other analogies between discrete and continuous free vibrations will emerge as we proceed. When we substitute Eq. (3.44) into Eq. (3.43), we convert the partial derivatives into ordinary derivatives to arrive at the expression below:

$$\rho(x)\frac{\partial^2[Y(x)G(t)]}{\partial t^2} - \frac{\partial}{\partial x}\left(T(x)\frac{\partial[Y(x)G(t)]}{\partial x}\right) = 0$$

$$\rho(x)Y(x)\frac{\partial^2[G(t)]}{\partial t^2} - G(t)\frac{\partial}{\partial x}\left(T(x)\frac{\partial[Y(x)]}{\partial x}\right) = 0$$

$$\frac{1}{G(t)}\frac{\partial^2[G(t)]}{\partial t^2} = \frac{1}{\rho(x)Y(x)}\frac{\partial}{\partial x}\left(T(x)\frac{\partial[Y(x)]}{\partial x}\right)$$

(3.45)

Now we make an inspired observation: because the left hand side of this equation is only a function of *t* and the right hand side is only a function of *x*, the only way to have equality is for both sides to equal the same constant. Our inspired substitution for this constant will be $-\omega^2$:

$$\ddot{G}(t) + \omega^2 G(t) = 0$$

$$\frac{d}{dx}\left(T(x)\frac{dY(x)}{dx}\right) = -\omega^2\rho(x)Y(x)$$

(3.46 a,b)

We have achieved exactly what we had hoped to achieve in Eqs. (3.46 a,b) in that the temporal and spatial components in the free response are decoupled. For instance, we can immediately write down the form of *G(t)*, the principal coordinates:

$$G(t) = G_r\cos(\omega t + \phi_r)$$

(3.47)

in which the constants, G_r and ϕ_r, are associated with the form of *Y(x)*. As for *Y(x)*, we must apply the boundary conditions to find the possible natural modes by solving the continuous eigen-problem. Once we obtain the infinite number of natural modes, $Y_r(x)$, then the solution, *y(x,t)*, can be written down in terms of the principal coordinates and natural modes:

$$y(x,t) = \sum_{r=1}^{\infty} Y_r(x)G_r(t) = \sum_{r=1}^{\infty} Y_r(x)G_r\cos(\omega t + \phi_r)$$

(3.48)

We sometimes use normal modes and normal coordinates to expand the free response. These normal modal properties are obtained by performing continuous versions of the discrete orthogonality calculations in the previous Section 3.4. More specifically, unit orthogonality of the natural modes with respect to the density function is expressed as follows:

$$\int_0^L \rho(x) Y_r(x) Y_s(x) dx = \delta_{rs} = \begin{cases} 0 \text{ for } r \neq s \\ 1 \text{ for } r = s \end{cases}$$

(3.49)

where δ_{rs} is the binary Kronecker delta function, and the corresponding orthogonality of the natural modes with respect to the tension is expressed as follows:

$$\int_0^L T(x) \frac{dY_r(x)}{dx} \frac{dY_s(x)}{dx} dx = \omega_r^2 \delta_{rs}$$

(3.50)

When these normal modes are used to expand the free vibration response, we can rewrite Eq. (3.48) as follows:

$$y(x,t) = \sum_{r=1}^{\infty} Y_r(x) g_r(t) = \sum_{r=1}^{\infty} Y_r(x) g_r \cos(\omega_r t + \phi_r)$$
$$\text{where } \ddot{g}_r(t) + \omega_r^2 g_r(t) = 0 \text{ and } Y_r(x) \text{ is normalized as above}$$

(3.51)

The discussion above can be made less abstract by solving for the free response of the string shown in Figure 2.5; that string is fixed on both ends. We can also assume that the string has a constant density and tension if it is taut. These simplifications to the second of Eqs. (3.46 a,b) yield the following second order differential equation:

$$\frac{d^2 Y(x)}{dx^2} + \omega^2 \frac{\rho}{T} Y(x) = 0 \quad \text{with } Y(0) = 0 \text{ and } Y(L) = 0$$

(3.52)

which admits the following set of harmonic solutions:

$$\frac{d^2Y(x)}{dx^2} + \omega^2 \frac{\rho}{T} Y(x) = 0 \quad \text{with } Y(0) = 0 \text{ and } Y(L) = 0$$

$$Y(x) = A_1 \sin\left(\omega\sqrt{\frac{\rho}{T}}x\right) + A_2 \cos\left(\omega\sqrt{\frac{\rho}{T}}x\right) \quad \text{for } 0 < x < L$$

$$\left.\begin{aligned} Y(0) &= A_2 = 0 \\ Y(L) &= A_1 \sin\left(\omega\sqrt{\frac{\rho}{T}}L\right) = 0 \end{aligned}\right\} \Rightarrow \text{non-trivial solutions, } \sin\left(\omega\sqrt{\frac{\rho}{T}}L\right) = 0$$

$$\text{Natural frequencies, } \omega_r^2 = r\pi\sqrt{\frac{T}{\rho L^2}} \quad \text{for integer } r = 1,2,\cdots$$

(3.53)

As before in the discrete case, we have special modal/natural frequencies with their corresponding natural mode shapes. Whereas the discrete modal frequencies were equal to the square root of stiffness divided by inertia, the frequencies in Eq. (3.53) are equal to the square root of tension per unit length divide by the mass of the string. These frequencies and shapes are then substituted into Eq. (3.48) or Eq. (3.51) to obtain the free response solution. Figure 3.10 shows how the free response of a continuous string, which is fixed at both ends, is analyzed using natural frequencies and mode shapes. Some common terminology is introduced in the figure including the notion of fundamental frequencies and *harmonics* or *overtones*.

Musical stringed instruments (e.g., violin, viola, cello, base) are an excellent real-world illustration of the discussion above on the free vibration response of a fixed-fixed string (see Meirovitch, 1986). For example, a standard violin has four strings with four fundamental frequencies, which the musician can change with proper fingering positions along the strings. It is relatively easy to see that changes in L (via fingering on the bridge) or T (via tightening of screws) bring about changes in the fundamental frequencies (see Figure 3.10). It is interesting to note, however, that in musical instruments, the sounds from fundamental frequencies are often not as important as the higher harmonics or overtones. The soundboards of expensive violins (e.g., Stradivarius), for instance, are designed and constructed to produce more pleasing, full sounds than those from a less expensive violin. Likewise, the soundboard of a Steinway grand piano is designed to resonate overtones more effectively than a less expensive instrument.

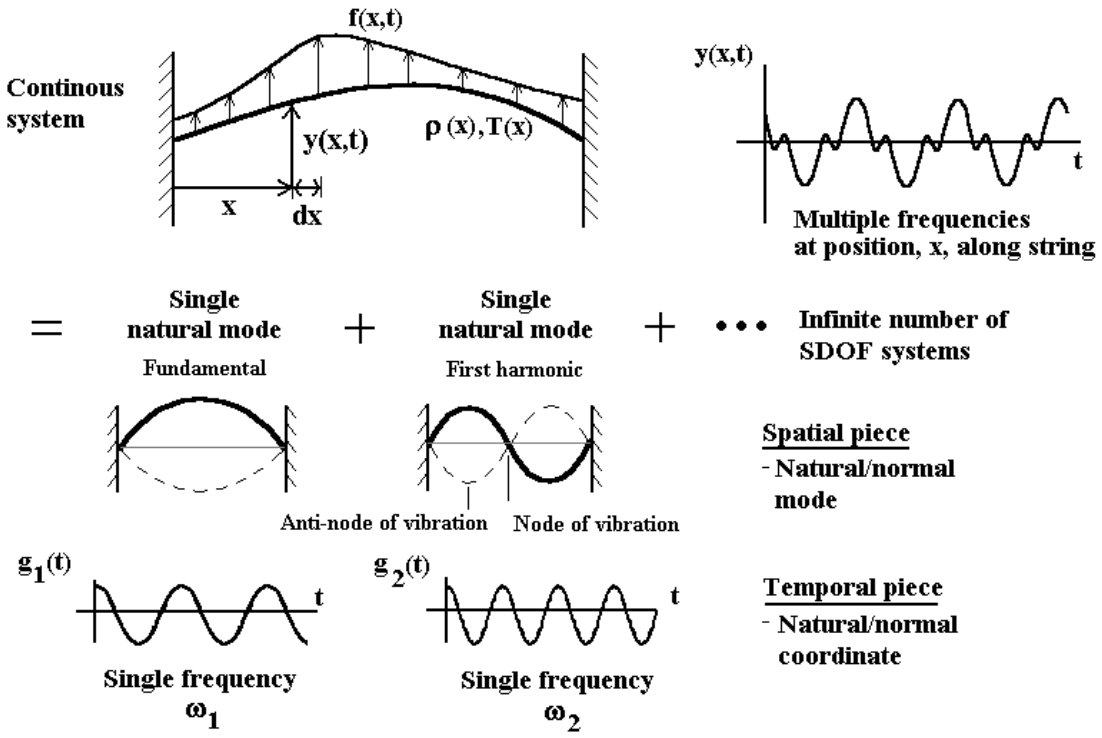

Figure 3.10: Illustration of continuous free vibration solution using modal characteristics

3.7 Fourth order continuous systems and separation of variables

We can proceed in exactly the same way as in Section 3.6 to derive the free response solution for a continuous system of fourth order. Recall the EOM from Eq. (2.53) for the bar undergoing transverse vibration. In the free vibration problem, we set *f(x,t)=0*, and obtain the homogeneous EOM:

$$m(x)\frac{\partial^2 y(x,t)}{\partial t^2} = -\frac{\partial^2}{\partial x^2}\left(EI(x)\frac{\partial^2 y(x,t)}{\partial x^2}\right) \qquad (3.54)$$

We can begin by separating the response *y(x,t)* into spatial and temporal components as before: *y(x,t)=Y(x)G(t)*. After substituting this form into Eq. (3.54) and making the same sort of argument surrounding Eq. (3.45) about equality in space and time functions, we obtain the following two equations:

$$\frac{d^2G(t)}{dt^2} + \omega_r^2 G(t) = 0$$

$$\frac{d^4Y(x)}{dx^4} - \omega_r^2 \frac{m}{EI} Y(x) = 0 \text{ with } Y(0) = 0 = Y(L),\ Y''(x)\big|_{x=0} = 0 = Y''(x)\big|_{x=L}$$

(3.55 a,b)

Note we have assumed that the boundary conditions on the bar are simply supported at both ends producing zero displacements and reactive moments. The natural coordinates are found as before in Eq. (3.47), and the natural modes are found by factoring and then solving the second of Eqs. (3.55 a,b). Note that Eq. (3.55 a,b) is a type of eigen-problem for continuous systems. Moreover, compare this form to the standard form of an eigenvalue problem in discrete systems, *(λI-A)x=0* (Eq. (3.35)). In fact, this expression is often rewritten using operator notation as follows to emphasize this analogy:

$$\left(\frac{d^4}{dx^4} - \omega_r^2 \frac{m}{EI}\right) Y(x) = 0$$

(3.56)

The possible solutions (eigenvectors) for this expression are given below:

$$Y(x) = A_1 \sin\left(\sqrt[4]{\omega^2 \frac{m}{EI}}\, x\right) + A_2 \cos\left(\sqrt[4]{\omega^2 \frac{m}{EI}}\, x\right) + A_3 \sinh\left(\sqrt[4]{\omega^2 \frac{m}{EI}}\, x\right) + A_4 \cosh\left(\sqrt[4]{\omega^2 \frac{m}{EI}}\, x\right)$$

(3.57)

We can apply the boundary conditions in Eqs. (3.55 a,b) to select only those natural modes (eigenvectors) that satisfy the physical constraints on the vibrating bar as follows:

$$\text{Recall } \sinh(x) = \frac{e^x - e^{-x}}{2} \text{ and } \cosh(x) = \frac{e^x + e^{-x}}{2}$$

$$Y(0) = A_2 + A_4 \text{ and } \left.\frac{d^2Y}{dx^2}\right|_{x=0} = \sqrt[2]{\omega^2 \frac{m}{EI}}\left(-A_2 + A_4\right) = 0$$

$$\Rightarrow A_2 = 0 = A_4$$

$$Y(x) = A_1 \sin\left(\sqrt[4]{\omega^2 \frac{m}{EI}}x\right) + A_3 \sinh\left(\sqrt[4]{\omega^2 \frac{m}{EI}}x\right)$$

$$Y(L) = A_1 \sin\left(\sqrt[4]{\omega^2 \frac{m}{EI}}L\right) + A_3 \sinh\left(\sqrt[4]{\omega^2 \frac{m}{EI}}L\right) = 0$$

$$\left.\frac{d^2Y}{dx^2}\right|_{x=L} = \sqrt[2]{\omega^2 \frac{m}{EI}}\left(-A_1 \sin\left(\sqrt[4]{\omega^2 \frac{m}{EI}}L\right) + A_3 \sinh\left(\sqrt[4]{\omega^2 \frac{m}{EI}}L\right)\right) = 0$$

$$\Rightarrow A_3 = 0,\ \sin\left(\sqrt[4]{\omega^2 \frac{m}{EI}}L\right) = 0 \Rightarrow \sqrt[4]{\omega^2 \frac{m}{EI}}L = r\pi \quad \text{for } r = 1,2,\cdots$$

(3.58)

With these natural frequencies and modes, we can expand the free response of the bar as follows:

$$y(x,t) = \sum_{r=1}^{\infty} Y_r(x) g_r(t) = \sum_{r=1}^{\infty} \sqrt{\frac{2}{mL}} \sin\left(\frac{r\pi x}{L}\right) g_r \cos\left(\omega_r t + \phi_r\right)$$

$$\text{where } \int_0^L m Y_r(x) Y_s(x) dx = \delta_{rs} \text{ and } \int_0^L EI \cdot \frac{d^2Y_r(x)}{dx^2} \frac{d^2Y_s(x)}{dx^2} dx = \delta_{rs}\omega_r^2$$

(3.59)

The expansion in Eq. (3.59) assumes that the natural modes have been normalized as defined in the second line of that expression. In order to justify this normalization procedure, we must first prove that natural modes in continuous systems are orthogonal to one another with respect to mass and stiffness just as modal vectors were in discrete systems.

We will proceed in the same way as before. First, we write down the eigen-problem for the natural mode of the bar for two different modes:

$$\frac{d^2}{dx^2}\left[EI(x)\frac{d^2Y_r(x)}{dx^2}\right]=\omega_r^2 m(x)Y_r(x) \quad \text{and} \quad \frac{d^2}{dx^2}\left[EI(x)\frac{d^2Y_s(x)}{dx^2}\right]=\omega_s^2 m(x)Y_s(x)$$

(3.60 a,b)

Then we multiply the *r* eigen-equation by Y_s and integrate by parts over the length of the bar and multiple the *s* eigen-equation by Y_r and integrate by parts. When we do this, subtract the results, and assume that there are boundary conditions like clamped, hinged, and free, then the following orthogonality conditions appear after some calculus:

$$\int_0^L m(x)Y_r(x)Y_s(x)dx=0 \quad \text{for } r\neq s \text{ (Mass orthogonality)}$$

$$\int_0^L EI(x)\cdot\frac{d^2Y_r(x)}{dx^2}\frac{d^2Y_s(x)}{dx^2}dx=0 \quad \text{for } r\neq s \text{ (Stiffness orthogonality)}$$

$$\text{If } \int_0^L m(x)Y_r(x)Y_s(x)dx=\delta_{rs}, \text{ then}$$

$$\int_0^L EI(x)\cdot\frac{d^2Y_r(x)}{dx^2}\frac{d^2Y_s(x)}{dx^2}dx=\omega_r^2\delta_{rs} \text{ (Normalized)}$$

(3.61)

In summary, we have solved a continuous eigenvalue problem to find the natural frequencies and shapes in the same way that we solved the discrete eigenvalue problem in the previous section to find the natural frequencies and vectors. The two differences between the discrete and continuous free vibration problems are that modal vectors are finite dimensional whereas continuous mode shapes are infinite dimensional, and modal frequencies are of finite number whereas continuous modal frequencies are of infinite number.

3.8 Case studies in free vibration

We are now going to study a few examples of free vibrations in real-world systems in order to reinforce the theory that was discussed in this chapter. These examples will be done largely in class; however, the problem statements are given below for reference.

Vehicle suspension vibration in ride:

Vehicle suspension systems can vibrate in a variety of ways. The body and frame can bounce essentially as rigid bodies on the tires and suspension, or the body and frame can vibrate as continuous systems as well. We will model and analyze some of these motions and discuss potential issues to consider when designing a vehicle suspension to avoid noise and vibration problems and maintain handling performance. Because boundary conditions are extremely important in complex, multi-body systems like this one, we will focus much of our discussion on ways to incorporate and examine the effects of different types of boundary conditions.

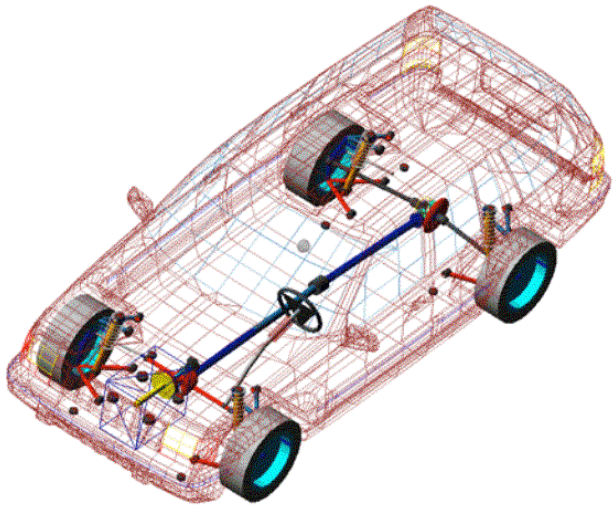

Figure 3.11: Illustration of vehicle suspension model

Equivalent masses in non-ideal springs:

When we discussed MDOF systems, we have modeled mechanical systems using ideal mass, damping, and stiffness elements. Of course, in the real world, mass is compliant to some extent, springs have mass, and dampers have both mass and stiffness. We are going to model and analyze the valve train of an automotive internal combustion engine using an energy-based method (Rayleigh's quotient), which we have not yet discussed.

4 Forced Vibrations

The free response of a mechanical vibrating system only gives us one part of the solution, the complementary solution to the homogeneous equation of motion. In order to find the total solution to the general equation of motion, we must be able to find a solution to the inhomogeneous equation as well, the so-called *particular solution*. Then we just add up the two solutions and apply the initial conditions. This method works, for example, in a forced linear lumped parameter SDOF system with constant coefficients and viscous damping because if $x_c(t)$ is the complimentary solution and $x_p(t)$ is the particular solution, then the sum of these two solutions, $x_d(t)$, satisfies the equation of motion:

$$\begin{aligned} M\ddot{x}_d + C\dot{x}_d + Kx_d &= f(t) \\ M\frac{d^2}{dt^2}\left(x_c + x_p\right) + C\frac{d}{dt}\left(x_c + x_p\right) + K\left(x_c + x_p\right) &= f(t) \\ \left(M\ddot{x}_c + C\dot{x}_c + Kx_c\right) + \left(M\ddot{x}_p + C\dot{x}_p + Kx_p\right) &= f(t) \\ 0 + f(t) &= f(t) \end{aligned} \qquad (4.1)$$

Please note that we CANNOT apply the initial conditions to the complementary solution before adding up the complementary and particular solutions. Our total solution would not satisfy the initial conditions if we did this unless the particular solution were of an unusual form such that $x_p(0)=0=dx_p/dt(0)$. Eq. (4.1) is a direct result of the principle of linear superposition. This additive property of the total response is responsible for most of the techniques that will discuss in this chapter.

4.1 Terminology - steady state and transient response

The terms ‘complementary’ and ‘particular’ have specific physical connotations in vibration analysis: the complementary solution is associated with the free response, which does not depend on the forcing function but does allow us to specify different sets of initial conditions whereas the particular solution describes the specific effects of a given forcing function. We can begin to make the following associations: free response↔complementary solution and forced response↔particular solution.

There is another terminology associated with forced vibration response that is common in the literature. The terms steady state and transient are often used to describe those portions of the total response that remain in the steady state (as $t \to \infty$) and those portions that only last for a finite period of time. Because the complementary solution is always transient as long as the vibration is stable, the particular solution is often all that remains in the steady state. Because of this characteristic, we can also start to make the associations: transient response$\leftrightarrow$complementary solution and steady state response $\leftrightarrow$particular solution. It is also common to refer to steady state and transient forces. For instance, a sinusoidal input (simple harmonic with constant frequency and amplitude) and a broad band random (stationary stochastic) input are both examples of steady state inputs. Likewise, an impulse and a step function are both examples of transient inputs. In general, real-world external inputs contain both steady state and transient parts. For example, an aircraft is subjected to both steady air stream velocities and turbulent (sudden) pockets of air that produce transient responses.

There is also something else special about the additive form of the solution, $x_c(t)+x_p(t)$, which remember is just a consequence of the principle of linear superposition. Specifically, the particular solution is completely decoupled from the complementary solution because $x_p(t)$ is found before the initial conditions are applied. Recall that the complementary solution always contains as many constants as there are initial conditions in the system, but the particular solution does not contain any constants. This result means that the steady state response does not depend on the initial conditions: it is unique. Thus, in linear (or linearized) vibrating systems, the notion of a 'transient' response is reasonable; however, if a system is nonlinear, the complementary and particular solutions are not uncoupled in one direction as they are in linear cases. When the complementary and particular solutions interact, the portion of the response that would be 'transient' in the linear case actually survives into the steady state. This portion is called a *nonlinear resonance* and is an example of how nonlinear systems fail to satisfy the principle of superposition. We will assume here that we are dealing with linear, time-invariant differential equations of motion. This assumption will allow us to apply the principle of superposition in many different ways to simplify our analysis significantly. Figure 4.1 illustrates the additive nature of the forced vibration response in linear systems.

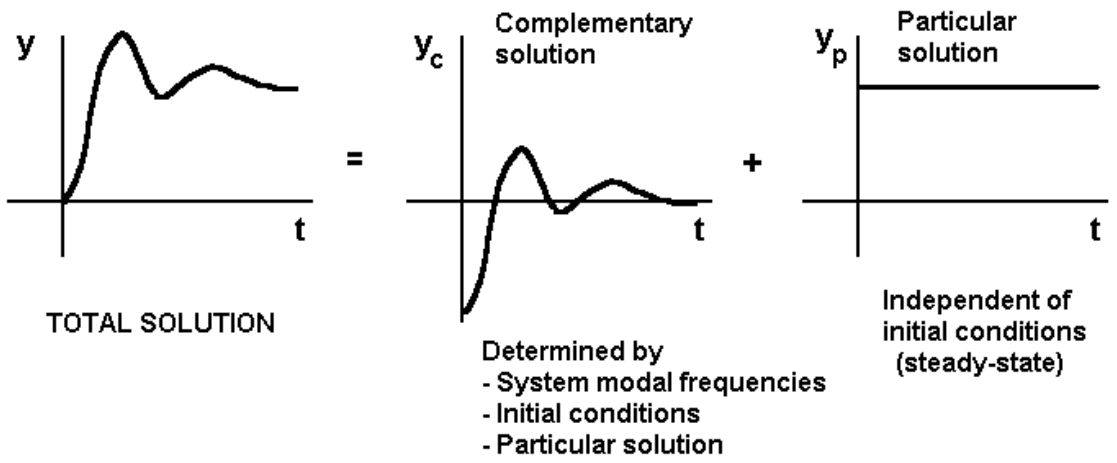

Figure 4.1: Illustration of additive nature of forced vibration response

4.2 Some review of time-frequency signal representation

Forces and responses in real world systems are usually complicated, so we need to understand how to express them in analytical terms. We will focus on deterministic analytical forced vibration response analysis: we assume that we know the excitation or force exactly at any moment in time. In random vibration analysis, we can only describe the statistical properties of the excitation. For example, in vehicle ride analysis, we usually only know that there is a certain probability distribution of wavelengths in a typical road profile. The vehicle is designed to respond well to the distribution rather than to a specific series of deterministic inputs.

An excitation (or response) is said to be harmonic when it contains a single frequency component. A simple harmonic signal is a constant amplitude harmonic. Simple harmonic signals are the simplest kind of periodic signals, which repeat themselves every T seconds. For instance, a linear SDOF vibrating system exhibits a simple harmonic free response to a general set of initial conditions:

$$M\ddot{x}_d + Kx_d = 0$$
$$\text{for } x_d(t) = A\cos(\omega_n t + \varphi) \qquad (4.2)$$

The quantity $\omega_n t+\varphi$ is called the instantaneous phase angle of the signal, $x_d(t)$, and φ is called the initial phase angle. The velocity and acceleration of this system are at +90 and +180 degrees, respectively, with respect to the displacement:

$$\begin{aligned} x_d(t) &= A\cos(\omega_n t+\varphi) \\ \dot{x}_d(t) &= -A\omega_n \sin(\omega_n t+\varphi) = A\omega_n \cos\left(\omega_n t+\varphi+\frac{\pi}{2}\right) \\ \ddot{x}_d(t) &= -A\omega_n^2 \cos(\omega_n t+\varphi) = A\omega_n^2 \cos(\omega_n t+\varphi+\pi) \\ \text{so } \ddot{x}_d &= -\omega_n^2 x_d \end{aligned}$$

(4.3)

Thus, acceleration is proportional to displacement for simple harmonic motion. We can also use complex numbers that rotate in the complex plane (phasors) and Euler's formula to describe harmonic signals. For instance, $x_d(t)$ from the equation above can be rewritten as follows:

$$\begin{aligned} x_d(t) &= A\cos(\omega_n t+\varphi) = \\ &= \mathrm{Re}\left[Ae^{j(\omega_n t+\varphi)}\right] = \mathrm{Re}\left[A\angle\omega_n t+\varphi\right] \\ &= \frac{Ae^{j(\omega_n t+\varphi)}+Ae^{-j(\omega_n t+\varphi)}}{2} \end{aligned}$$

(4.4)

and then the 90 degree phase difference between the displacement-velocity and velocity-acceleration is accounted for with a factor of $j\omega_n$, which introduces a +90 degree rotation in the complex plane:

$$\begin{aligned} x_d(t) &= \mathrm{Re}\left[Ae^{j(\omega_n t+\varphi)}\right] \\ \dot{x}_d(t) &= \mathrm{Re}\left[(j\omega_n)^1 Ae^{j(\omega_n t+\varphi)}\right] \\ \ddot{x}_d(t) &= \mathrm{Re}\left[(j\omega_n)^2 Ae^{j(\omega_n t+\varphi)}\right] \end{aligned}$$

(4.5)

We will develop this idea of using complex numbers to describe two different characteristics in a signal, magnitude and phase (A and $\omega_n t+\varphi$), later on in our discussion about frequency response functions in linear vibrating systems.

The period of oscillation in seconds, T, is inversely proportional to the circular frequency, ω, in radians/second according to $\omega=2\pi/T$. The frequency, f, in Hertz (cycles/second) is the inverse of the period of oscillation, $f=1/T$. When two simple harmonic signals with slightly different frequencies are added, the following result is obtained using trigonometry:

$$\begin{aligned} x_1(t)+x_2(t) &= A\sin(\omega t)+A\sin(\omega t+\Delta\omega t) \\ &= A\left[\sin(\omega t)+\sin(\omega t+\Delta\omega t)\right] \\ &= A\left[2\sin\left(\frac{\omega t+\omega t+\Delta\omega t}{2}\right)\cos\left(\frac{\omega t-\omega t-\Delta\omega t}{2}\right)\right] \\ &= 2A\cos\left(\frac{\Delta\omega t}{2}\right)\sin\left(\omega t+\frac{\Delta\omega t}{2}\right) \end{aligned}$$

(4.6)

which exhibits the so-called *beating* phenomenon. The amplitude slowly varies from 0 to $2A$ according to the small frequency, $\Delta\omega/2$, as the signal frequency remains constant at the larger value $\omega+\Delta\omega/2$. We will discuss this kind of harmonic forced response behavior later on in this chapter when we talk about lightly damped or undamped vibrating systems that are forced at frequencies close to their own natural frequencies of oscillation.

The Fourier series is an important tool for representing excitation and response time histories in analytical vibration analysis. The general idea of Fourier series is to decompose a periodic signal, $x_d(t)$, with period T into a sum of simple harmonic signals with various frequencies. We can also use Fourier series to decompose an aperiodic signal into harmonics over a given time interval, T. The decomposition is given below for real and complex number notations. The response to each term in this series is calculated independently from all the others and then the results are added as shown in Figure 4.2.

$$x_d(t) = \sum_{n=0}^{\infty} \left[a_n \cos(n\omega_o t) + b_n \sin(n\omega_o t) \right]$$

$$\text{where } a_n = \frac{2}{T}\int_{-T/2}^{T/2} x_d(t)\cos(n\omega_o t)dt$$

$$b_n = \frac{2}{T}\int_{-T/2}^{T/2} x_d(t)\sin(n\omega_o t)dt \text{ with } T = \frac{2\pi}{\omega_o}$$

$$x_d(t) = \sum_{n=-\infty}^{\infty} c_n e^{jn\omega_o t}$$

$$\text{where } c_n = \frac{1}{T}\int_{-T/2}^{T/2} x_d(t)e^{jn\omega_o t}dt \text{ with } c_n = \frac{a_n}{2} - j\frac{b_n}{2} \text{ and } c_{-n} = c_n^* = \frac{a_n}{2} + j\frac{b_n}{2}$$

(4.7)

where ω_o is called the fundamental frequency and T is called the fundamental period.

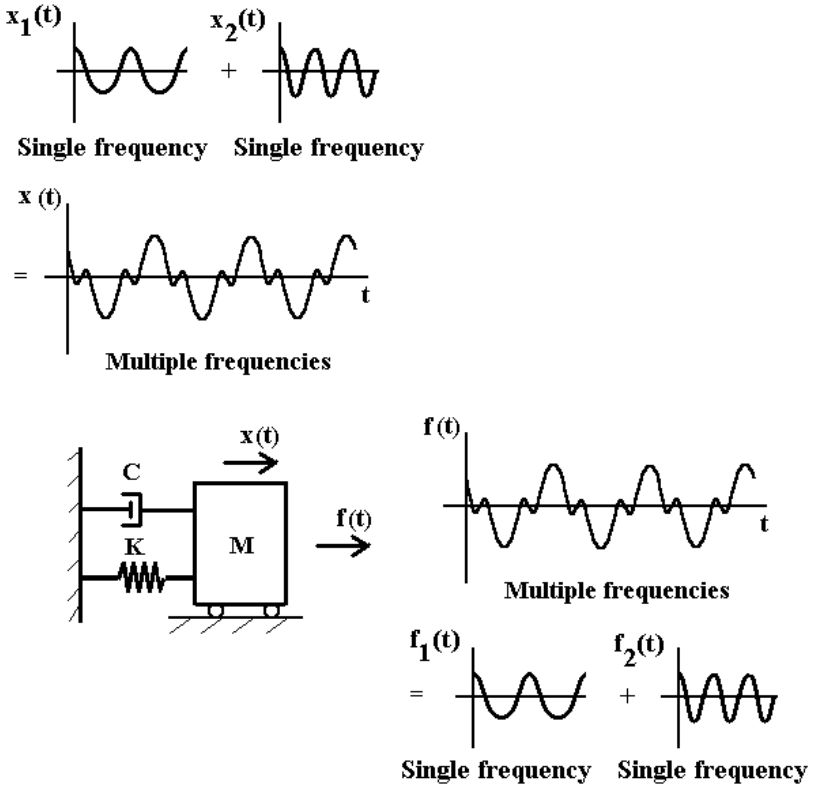

Figure 4.2: Illustration of temporal superposition in forced linear vibrating systems

By decomposing excitations into harmonic components as in Eq. (4.7), solving for the response to each harmonic, and then adding the various harmonic response components, we can deal effectively with many kinds of inputs. Note that linear superposition is what enables us to analyze the forced response of vibrating systems in this way. Superposition holds because stable linear vibrating systems only respond at the excitation frequency in the steady state. Among other things, this guarantees that the response to each harmonic is independent from the response to all other harmonics (see Figure 4.2). In nonlinear systems, two individual response harmonics often conspire to create new harmonic response components, which cannot be explained with linear models. We will limit our analysis primarily to stable linear vibration in which systems only respond at the excitation frequency in the steady state.

Note that periodic signals have discrete frequency spectra (i.e., non-zero coefficients in Fourier series). If we let the period of the periodic signal approach infinity, then we can use the Fourier series to describe any aperiodic signal of 'exponential order' as well. In this case, the fundamental frequency approaches zero and the signal, $x_d(t)$, is decomposed into an infinite series of sinusoids using the Fourier integral:

$$X_d(\omega) = \lim_{T\to\infty} \frac{1}{T}\int_{-T/2}^{T/2} x_d(t)e^{-jn\omega_0 t}dt$$
$$= \int_{-\infty}^{\infty} x_d(t)e^{-j\omega t}dt \qquad (4.8)$$

The function, $X_d(\omega)$, is called the Fourier transform of $x_d(t)$. Thus, aperiodic signals have frequency components (or coefficients) that are continuous in ω. The Fourier integral is one analytical tool that will be used to study frequency response characteristics in linear vibrating systems. Note that the integration limits on the Fourier integral prevent it from being used to study transient response (i.e., it does not take into account the initial conditions). It can only be used to study steady state response behavior.

A close relative of the Fourier integral is the Laplace transform, which can be used to study transient and steady state response behavior in linear vibrating systems. The Laplace transform of a function, $x_d(t)$, is given by the integral below:

$$X_d(s) = \int_0^\infty x_d(t) e^{-st} dt$$

(4.9)

This integral exists if the function, $x_d(t)$, is of exponential order, which is usually true when the function has a finite number of jumps (discontinuities). Note that the limits of integration indicate that the Laplace transform can be used to incorporate initial conditions, which are needed to study transient response behavior. More will be said later about this transform as well.

4.3 Step response: A simple example of forced response analysis

In this section, we will introduce the fundamental ideas of forced response analysis using the sprung disk on the inclined plane problem under the force of gravity (refer to Section 2.1). The illustration is repeated below in Figure 4.3 for reference. The corresponding equation of motion is also repeated below in Eq. (4.10).

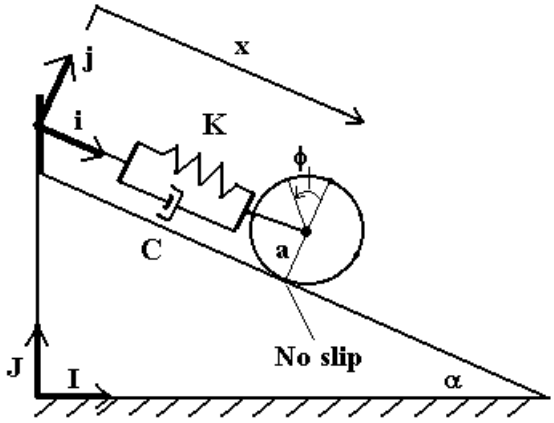

Figure 4.3: Sprung disk on an incline for forced step response analysis

$$\left(M + \frac{I_{CM}}{a^2} \right) \ddot{x} + C\dot{x} + Kx = Mg\sin\alpha + Kx_u$$

(4.10)

Note that gravity is included in the equation of motion as is the undeformed length of the spring. This equation of motion is valid prior to redefinition of the displacement coordinate with respect to the equilibrium position of the disk. We will study the transient and steady state response behavior of the disk when it is released on the incline at $x=0$ (units length) with zero initial velocity. The input in this case is a step equal to the constant on the right hand side of Eq.(4.10).

We begin by finding the form of the complementary (free response) solution, which was already done in Section 3.1. A summary of the results from before are repeated below:

$$\begin{aligned} \text{Characteristic equation}: & \left(M + \frac{I_{CM}}{a^2}\right)s^2 + Cs + K = 0 \\ \text{Modal frequencies}: & \; s_{1,2} = \sigma \pm j\omega_d \\ \text{Complimentary solution}: & \; x_c(t) = A_1 e^{s_1 t} + A_2 e^{s_2 t} = X_o e^{\sigma t}\cos\left(\omega_d t + \phi_o\right) \end{aligned}$$

(4.11)

where the damping factor (σ) and damped natural frequency (ω_d) were previously defined in terms of the inertia, damping, and stiffness parameters for an underdamped system ($\zeta<1$), and the amplitude (X_o) and initial phase angle (φ_o) are to be determined from the initial conditions on the displacement ($x(0)=0$) and velocity ($dx/dt(0)=0$).

The particular solution can be found by any one of a number of different techniques. We will use the method of undetermined coefficients here. In this technique, we assume a form for the particular solution based on the form of the inhomogeneous term (i.e., the excitation) and the modal frequencies. Because the inhomogeneous term in Eq. (4.10) is the constant on the right hand side of that equation, our assumed form will be a constant, $x_d(t)=X_p$ (for $t>0$). If the modal frequencies had been zero instead (i.e., rigid body mode), then it would have been necessary to guess a particular solution of the form $x_d(t)=X_{p1}+ X_{p2}t$. We must include a factor of t with every term that matches in the complementary solution. After substituting our guess into the inhomogeneous equation, we can solve for the single undetermined coefficient, X_p:

$$X_p = \frac{Mg\sin\alpha}{K} + x_u$$

(4.12)

Because Eq. (4.10) is a linear differential equation, we are guaranteed that this is the unique solution. We do not need to look for any other solutions because there are no others.

The total solution is the sum of the complementary and particular solutions:

$$x(t) = X_o e^{\sigma t}\cos(\omega_d t + \phi_o) + \frac{Mg\sin\alpha}{K} + x_u$$
$$= \begin{bmatrix}\text{Transient}\\ \text{Solution}\end{bmatrix} + \begin{bmatrix}\text{Steady - state}\\ \text{Solution}\end{bmatrix}$$

(4.13)

Before applying the initial conditions, note the form of the solution. If the linear system is stable (i.e., M, C, and K positive), then the complementary solution decays after a certain period of time and the particular solution is all that remains. The physical interpretation of this result makes sense because we expect for the disk to come to rest at some position along the plane after it oscillates for a while. In fact, the final position is simply the static equilibrium position, x_e, which we used in Section 3.2 to define the new dynamic coordinate, $x_d=x-x_e$.

After applying the initial conditions, the final solution becomes:

$$x(t) = \frac{Mg\sin\alpha + x_u}{K}\left[1 - \frac{\omega_n}{\omega_d}e^{\sigma t}\cos\left(\omega_d t - \tan^{-1}\frac{\zeta}{\sqrt{1-\zeta^2}}\right)\right] \text{ for } t > 0$$

(4.14)

This solution is plotted in Figure 4.4 below for $Mgsin\alpha/K+x_u=1$ (units length) for three different values of ζ (top) and three different values of ω_n (bottom). Note that less damping produces more overshoot with longer sustained oscillations and more damping produces a faster convergence to the steady state response. Also, larger undamped natural frequencies produce shorter times-to-peak in addition to more rapid oscillations. The effects are both evident in Eq. (4.14) due to the presence of the exponential sinusoid term. Note also that as the system becomes stiffer, K increases and the steady state response amplitude decreases as well. Lastly, note that a step input is equivalent to a co-sinusoidal input with zero frequency, $cos(\omega t)=1$ for $\omega=0$ rad/s, for $t>0$. This equivalence between static and harmonic inputs will become useful later on because we will

associate low-frequency quasi-static response behavior with the stiffness characteristics in the vibrating system.

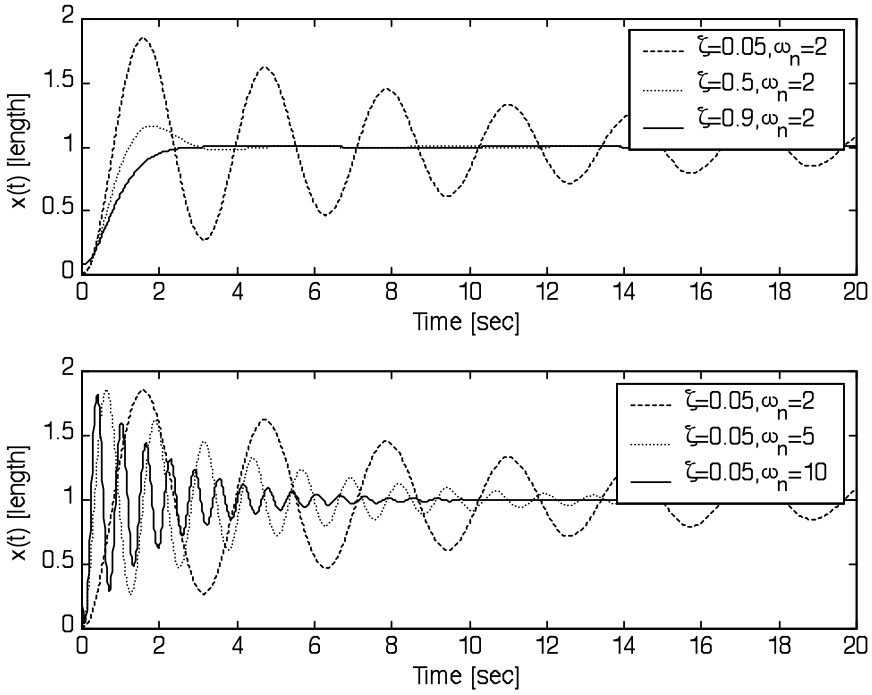

Figure 4.4: Sprung disk step response on an incline showing transient and steady state behaviors

4.4 Harmonic response: relative amplitude and phase relationships

The previous section focused on one special kind of input, the step function $u(t)=1$ for $t>0$. We demonstrated that SDOF mechanical vibrating systems respond in the steady state with a static deflection when forced with a zero frequency excitation. In most cases, the static response of mechanical systems is important but if we ignore the dynamic response to time-varying inputs, systems are not likely to perform the way we expect or would like them to. For instance, if buildings were designed only to support their own weight and not to withstand dynamic excitations, they would fail catastrophically if subjected to base excitations during earthquakes. Why do mechanical systems behave so differently when they are excited with dynamic inputs? In short, mechanical systems 'want' to vibrate at certain frequencies and if we excite them at those frequencies, systems will respond with large amplitudes of vibration. These are called forced resonances and occur when the excitation is driven in phase with the velocity of the

system. We will show later on why this forcing condition produces resonance, but first we must calculate the general solution of a SDOF system to a sinusoidal input.

We will again consider the rolling disk on the incline but choose this time to look only at the dynamic part of the response to a co-sinusoidal input (i.e., we subtract the equilibrium displacement from $x(t)$). The inhomogeneous equation for the dynamic displacement, $x_d(t)$, with a harmonic forcing term is given below:

$$\left(M + \frac{I_{CM}}{a^2}\right)\ddot{x}_d + C\dot{x}_d + Kx_d = F_i \cos(\omega t + \phi_i)$$

(4.15)

As in the previous section, we first find the complementary solution, which is the same as in Eq. (4.11). Then we select a form for the particular solution that is representative of the excitation, $x_p(t)=X_p\cos(\omega t+\varphi_p)$, which assumes that the response is at the same frequency as the input but with a different amplitude and phase. This solution is substituted into Eq. (4.15) as follows:

$$\left[K - \left(M + \frac{I_{CM}}{a^2}\right)\omega^2\right]X_p \cos(\omega t + \phi_p) - \omega C X_p \sin(\omega t + \phi_p) = F_i \cos(\omega t + \phi_i)$$

$$\left(\left[K - \left(M + \frac{I_{CM}}{a^2}\right)\omega^2\right]X_p \cos\phi_p - \omega C X_p \sin\phi_p\right)\cos(\omega t) +$$

$$\left(-\left[K - \left(M + \frac{I_{CM}}{a^2}\right)\omega^2\right]X_p \sin\phi_p - \omega C X_p \cos\phi_p\right)\sin(\omega t) = F_i \cos(\omega t)\cos\phi_i - F_i \sin(\omega t)\sin\phi_i$$

$$\Rightarrow \left[K - \left(M + \frac{I_{CM}}{a^2}\right)\omega^2\right]X_p \cos\phi_p - \omega C X_p \sin\phi_p = F_i \cos\phi_i$$

$$\Rightarrow -\left[K - \left(M + \frac{I_{CM}}{a^2}\right)\omega^2\right]X_p \sin\phi_p - \omega C X_p \cos\phi_p = -F_i \sin\phi_i$$

(4.16)

where the coefficients of the (orthogonal) $\sin(\omega t)$ and $\cos(\omega t)$ terms have been equated from each side of the equation. If the second to the last equation is squared and then added to the last equation, the amplitude of the particular solution can be found. Likewise, if the second to the last

equation is multiplied by $sin\varphi_i$, the last equation is multiplied by $cos\varphi_i$, and then the two are added, the phase of the particular solution can also be found. Both solutions are given below:

$$X_p = \frac{F_i}{\sqrt{\left[K - \left(M + \frac{I_{CM}}{a^2}\right)\omega^2\right]^2 + (\omega C)^2}}$$

$$\phi_p = \phi_i - \tan^{-1}\frac{\omega C}{K - \left(M + \frac{I_{CM}}{a^2}\right)\omega^2}$$

(4.17)

These two equations govern the frequency response of the disk-incline system. The terms 'frequency response' imply that the excitation and particular response are simple harmonic in nature. There are several interesting characteristics to discuss in these solutions. First, note that both the response amplitude and phase are found *relative* to the excitation amplitude and phase. Second, note that the relative phase of the particular response is always less than or equal to zero for all frequencies greater than or equal to zero, respectively. Third, note that there are three frequency ranges over which the particular response behavior is fundamentally different:

- For low frequencies, the relative amplitude and phase of the response are primarily governed by the stiffness of the spring, $X_p \approx F_i/K$ and $\varphi_p \approx \varphi_i + 0\ rad$. Stiffness is said to dominate the frequency response in this frequency range, $0 < \omega << \omega_n$.
- For high frequencies, the relative amplitude and phase of the response are primarily governed by the inertia of the disk, $X_p \approx F_i/M_{eff}\omega^2$ and $\varphi_p \approx \varphi_i - tan^{-1}(-C/M_{eff}\omega)\ rad$. Mass is said to dominate the frequency response in this frequency range, $\omega >> \omega_n$.
- For frequencies near the undamped natural frequency of oscillation, $\sqrt{(K/M_{eff})}$, the relative amplitude and phase of the response are primarily governed by the damper characteristic, $X_p \approx F_i/\omega C$ and $\varphi_p \approx \varphi_i - tan^{-1}(\infty) = \varphi_i - \pi/2\ rad$. Damping is said to dominate the frequency response in this frequency range, $\omega \approx \omega_n$.

In order to summarize these results graphically, we will first rewrite Eq. (4.17) as follows:

$$X_p = \frac{F_i / K}{\sqrt{\left[1 - \left(\frac{\omega}{\omega_n}\right)^2\right]^2 + \left[2\zeta \frac{\omega}{\omega_n}\right]^2}}$$

$$\phi_p = \phi_i - \tan^{-1} \frac{2\zeta \frac{\omega}{\omega_n}}{1 - \left(\frac{\omega}{\omega_n}\right)^2}$$

(4.18)

Figure 4.5 summarizes the discussion above with plots of the relative dynamic amplitude and phase, $X_p/(F_i/K)$ and $\varphi_p - \varphi_i$. Furthermore, it makes sense to plot the amplitude normalized in this way because it indicates how large the dynamic amplitude is relative to the static deflection.

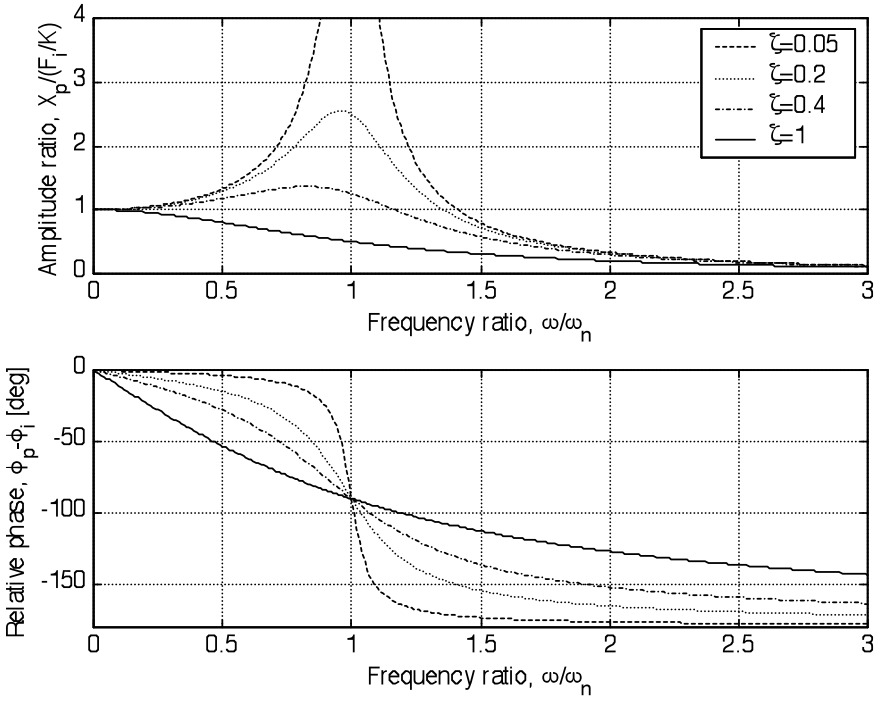

Figure 4.5: Relative amplitude and phase diagrams for damped harmonic frequency response

Figure 4.5 highlights some other interesting characteristics that might not have been obvious in Eq. (4.18). These characteristics are discussed below:

- The maximum value of the relative amplitude does NOT occur at the undamped natural frequency (ω_n) or at the damped natural frequency (ω_d)! Instead, it occurs at $(\omega/\omega_n)_{max} = \sqrt{(1-2\zeta^2)}$. This result is easily shown by differentiating the relative amplitude function with respect to ω and then setting the derivative equal to zero in search of the maximum. The maximum value of the relative amplitude is found by substituting this frequency ratio into Eq. (4.18) (note that the following relationships are valid for $0<\zeta<0.7$):

$$\left(\frac{X_p}{F_i/K}\right)_{\max} = \frac{1}{2\varsigma\sqrt{1-\varsigma^2}}$$
$$\left(\phi_p\right)_{\max} = \phi_i - \tan^{-1}\frac{\sqrt{1-2\varsigma^2}}{\varsigma}$$

(4.19)

- The value of the relative amplitude at the undamped natural frequency is very close to the maximum amplitude above. In fact, if the damping ratio is much less than one ($\zeta<0.1$), the differences are negligible.

$$\left(\frac{X_p}{F_i/K}\right)_{\omega=\omega_n} = \frac{1}{2\varsigma}$$
$$\left(\phi_p\right)_{\omega=\omega_n} = \phi_i - \frac{\pi}{2}$$

(4.20)

- When damping is increased in the system, the amplitude ratio decreases at all excitation frequencies and the relative phase plot changes more gradually. Lightly damped systems exhibit a sharp phase transition, sometimes referred to as a *high quality factor*, $Q=1/2\zeta$. For small damping ratios, the quality factor can be approximated as $\omega_n/(\omega_2-\omega_1)$, in which ω_2 and ω_1 are the half power points ($0.707Q$) above and below, respectively, the undamped natural frequency. Note also that a small change in damping near resonance causes a major change in the amplitude ratio due to the inverse proportionality.

We can also draw conclusions about undamped frequency response characteristics by setting $\zeta=0$ in Eq. (4.17) through (4.20). In this case, the relative amplitude and phase characteristics are given by:

$$\left(X_p\right)_{undamped} = \frac{F_i / K}{\left|1 - \left(\frac{\omega}{\omega_n}\right)^2\right|}$$

$$\left(\phi_p\right)_{undamped} = \phi_i - \tan^{-1}\frac{0}{1 - \left(\frac{\omega}{\omega_n}\right)^2}$$

(4.21)

These characteristics are plotted below in Figure 4.6 in semilogy (top-left), log-log (top-right) and semilogx (bottom) formats. There are a few additional points of interest in these plots:

- Without damping, the relative amplitude between the harmonic response and the excitation is unbounded; damping is the only element that prevents the response from growing continuously at steady state when the system is forced at resonance. Reflect on the meaning of this statement for a moment; it does not mean that the input suddenly jumps to infinity when the excitation frequency is at the undamped natural frequency, rather, the particular response amplitude grows as a linear function of time without end. This undamped resonant forcing condition can be examined by revisiting the form for the total solution (complimentary plus particular) in the case where the system undamped natural frequency is the same as the excitation frequency, $F_i cos(\omega_n t)$. In this case, the particular solution must be expressed as, $x_p(t)=tX_{p1}cos(\omega_n t)+tX_{p2}sin(\omega_n t)$, in order to avoid repetition in the complementary and particular solutions. This substitution into the differential equation of motion yields the following solution (with $X_{p1}=0$):

$$x_p(t) = \frac{F_i}{2\sqrt{KM_{eff}}} t \sin\left(\omega_n t\right)$$

(4.22)

which is plotted in Figure 4.8 when normalized with respect to $F_i/2\sqrt{(KM_{eff})}$ (units length/time) for an undamped natural frequency of 10 rad/s. Note that the amplitude grows linearly with time for linear undamped forced resonance.

- Usually the system begins to behave in a nonlinear way if the amplitude grows to a high enough level as it will in an undamped vibrating system if the excitation frequency is near the resonant frequency. For large motions away from the equilibrium point, linearized models will miss certain nonlinear behaviors.

- The relative phase between the response and the excitation is either zero or -180 degrees away from resonance and equal to -90 degrees at resonance. Moreover, when an undamped SDOF system is forced at resonance, the force leads the displacement by 90 degrees. In other words, the force is in phase with the velocity, which means that the force continually reinforces the vibration of the system.

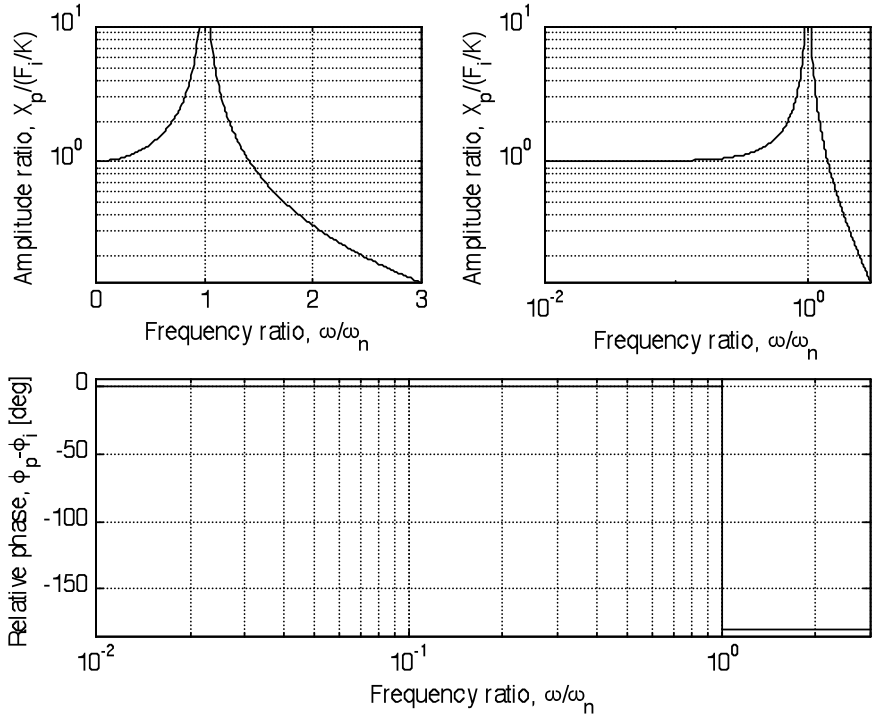

Figure 4.6: Relative amplitude and phase diagrams for undamped frequency response

- If large amplitude particular responses are achieved by forcing a SDOF in phase with its velocity, then small responses must be achieved by forcing a system out of phase with its displacement. Thus, at higher frequencies in Figure 4.6 (mass dominated range), the relative phase is -180 degrees and the amplitude ratio is very small. Think about the physical reasoning behind these comments.

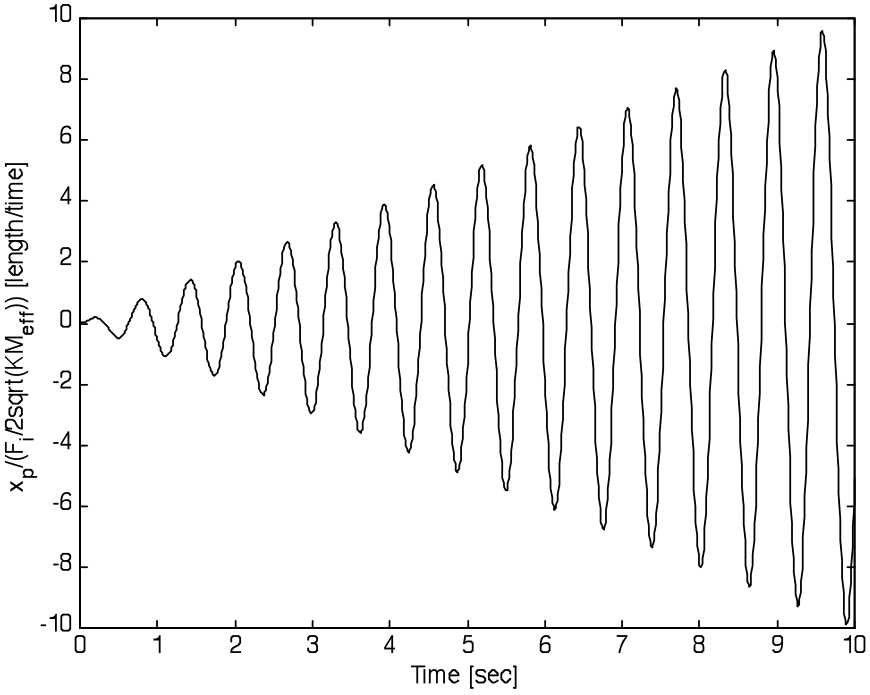

Figure 4.7: Plot of particular solution at undamped forced resonance

4.5 Harmonic response: total solution = transient + steady state

Section 4.4 discussed the particular solution to a simple harmonic input in a SDOF vibrating system in the damped and undamped cases. In order to satisfy system initial conditions, this solution must be added to the complementary solution from Eq. (4.11). Then the initial conditions on displacement and velocity can be satisfied:

$$x_d(t) = x_c(t) + x_p(t)$$
$$= X_o e^{\sigma t}\cos(\omega_d t + \phi_o) + X_p \cos(\omega t + \phi_p)$$

(4.23)

For instance, if a SDOF system with ω_n=*5 rad/s*, ζ=*0.05*, and *K=1 N/m* is forced with an excitation *cos(2t) N* and the initial conditions are chosen such that X_o=X_p and φ_o=*0 rad*, then the total solution is as shown in Figure 4.8 below. Note that two response components are evident during the initial 10 seconds: the complementary solution (transient) is at a higher frequency (5 rad/s) than the particular solution (steady state response at the same frequency as the excitation, 2 rad/s). Beyond *t=20* seconds, however, the complementary solution has vanished and all that remains is the steady state response at 2 rad/s. In fact, if the amplitude ratio and relative phase characteristics are to be measured experimentally, then it is important to wait for a certain period of time before recording the amplitude and phase of the response because the transient will corrupt the steady state measurement otherwise.

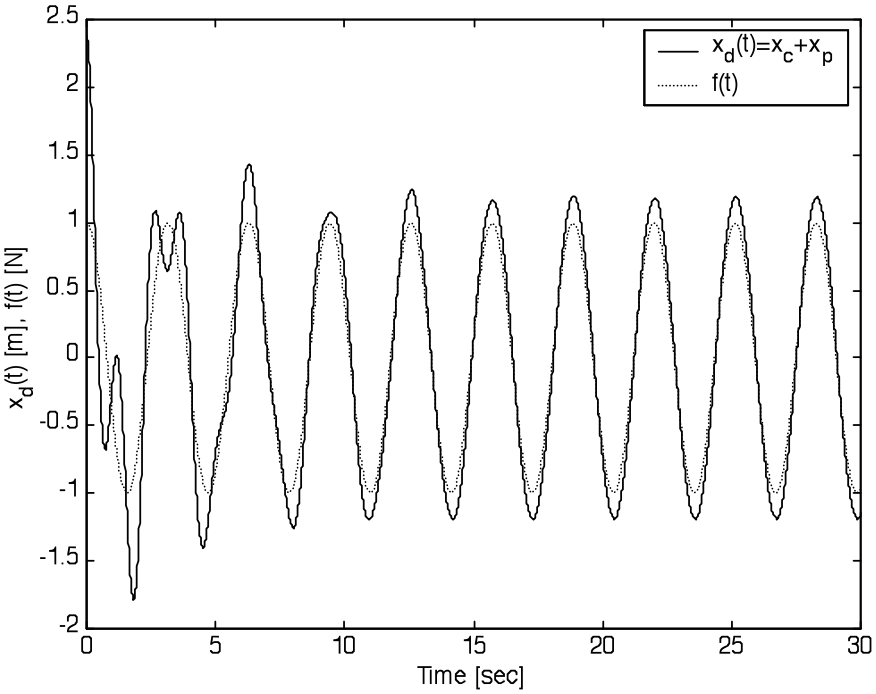

Figure 4.8: Plot of total solution in a SDOF system with transient and steady state components

When undamped systems are forced near resonance, beating can occur as described mathematically in Eq. (4.6). For example, if a SDOF system with $\omega_n=5$ *rad/s*, $\zeta=0.0$, and $K=1$ *N/m* is forced with an excitation *cos(4.8t) N* (i.e., slightly below resonance) and the initial conditions are chosen such that $X_o=X_p$ and $\varphi_o=0$ *rad*, then the total solution is as shown in Figure 4.9 below. Note that the higher frequency in the response is given by $\omega+\Delta\omega/2=4.8+0.1=4.9$ *rad/s* whereas the slower 'beating' of the amplitude is given by $\Delta\omega/2=0.1$ *rad/s*. This type of response behavior is common in twin propeller aircraft because the two blades are rotated slightly out of phase so as to not excite large amplitudes of the airframe. In this case, the two forces on either side of the fuselage conspire to cause beating within the passenger cabin.

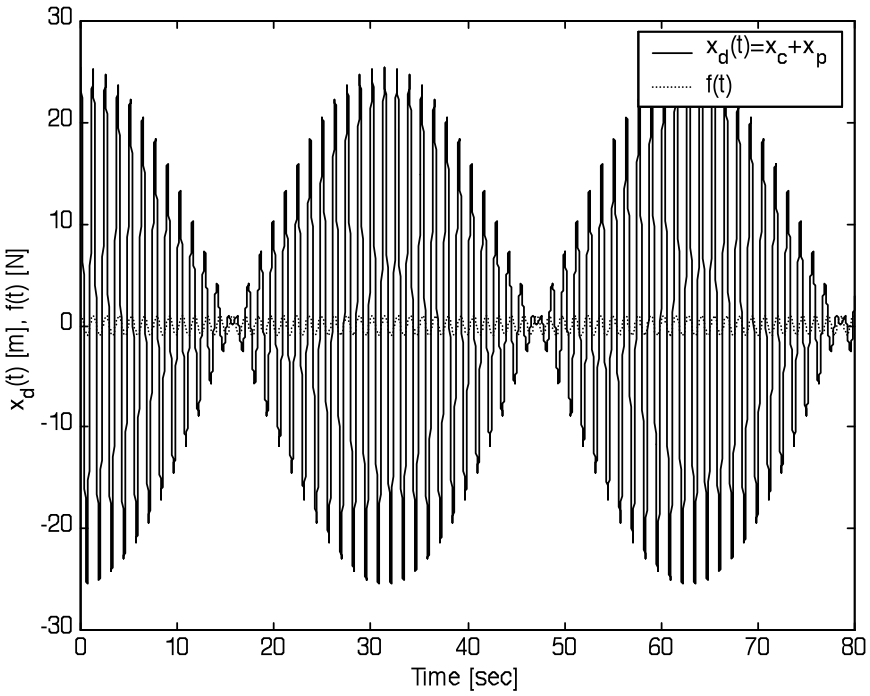

Figure 4.9: Plot of total solution showing beating between complimentary/particular solutions

4.6 Harmonic response with Laplace transforms: frequency response functions

The procedure we used above to find the total solution as a sum of a complementary solution, which depended only on the system characteristics, and a particular solution, which depended on both the system and the type of excitation we considered, is not the only procedure for calculating the total linear forced response. The other common method is to take the Laplace transform of both sides of the inhomogeneous equation of motion (Eq. (4.10) or (4.15)) as indicated before

in Eq. (3.9). This operation is performed below where the Laplace transform of the excitation is written as *F(s)*:

$$\left[\left(M+\frac{I_{CM}}{a^2}\right)s^2+Cs+K\right]X_d(s)=\left(M+\frac{I_{CM}}{a^2}\right)sx_d(0)+Cx_d(0)+\left(M+\frac{I_{CM}}{a^2}\right)\dot{x}_d(0)+F(s)$$

$$X_d(s)=\frac{\left(M+\frac{I_{CM}}{a^2}\right)s+C}{\left(M+\frac{I_{CM}}{a^2}\right)s^2+Cs+K}x_d(0)+\frac{\left(M+\frac{I_{CM}}{a^2}\right)}{\left(M+\frac{I_{CM}}{a^2}\right)s^2+Cs+K}\dot{x}_d(0)+\frac{1}{\left(M+\frac{I_{CM}}{a^2}\right)s^2+Cs+K}F(s)$$

(4.24)

The quantity F(s) could correspond to a step input as in Eq. (4.10) or a sinusoidal input as in Eq. (4.15). For instance, for an input, $f(t)=F_i\cos(\omega t)$, the Laplace transform is $F(s)= s^2F_i/(s^2+\omega^2)$. The solution procedure would then proceed by finding the inverse Laplace transforms of the various terms in Eq. (4.24); however, this is a tedious process for harmonic inputs. The important point to make here is that there is an easier way to derive the amplitude ratio and relative phase expressions in Eq. (4.18). Note that the last term in Eq. (4.24) is equal to the excitation (or input) divided by the so-called *impedance function*. Moreover, the inverse of the impedance function is called the *transfer function*. These definitions are listed below for review:

$$\text{Impedance function: } B(s)=\left(M+\frac{I_{CM}}{a^2}\right)s^2+Cs+K$$

$$\text{Transfer function: } H(s)=\frac{1}{\left(M+\frac{I_{CM}}{a^2}\right)s^2+Cs+K}=\frac{X_d(s)}{F(s)} \text{ for zero I.C.s}$$

(4.25)

We can think of the impedance function as a kind of 'dynamic stiffness'. In other words, if a system only contains springs, then the impedance function is a constant equivalent to the effective stiffness of the system. On the other hand, if a system contains mass and damping, then the impedance will be a function of the complex frequency variable, *s*. Also, note that the transfer function is equal to the ratio of the Laplace transform of the response and the excitation for zero initial conditions.

An inspired choice of s leads to the formulas for the amplitude ratio and relative phase. We choose $s=j\omega$, where ω is the excitation frequency in $F_i cos(\omega t+\varphi_i)$. In other words, we choose to look at slices of the general complex functions, $B(s)$ and $H(s)$, along the imaginary axis. With this choice of s, the transfer function becomes the so-called *frequency response function* (FRF):

$$H(s)\big|_{s=j\omega} = H(j\omega) = \frac{X_d(j\omega)}{F(j\omega)} = \frac{1}{K - \left(M + \frac{I_{CM}}{a^2}\right)\omega^2 + j\omega C}$$

(4.26)

The FRF is a complex number with two parts: real and imaginary (or equivalently, magnitude and phase). The FRF must have two parts because it describes how a linear system responds with a certain amplitude ratio and relative phase angle to a simple harmonic input. Note the similarities between Eq. (4.26) and Eq. (4.17). In fact, if we compute the magnitude of $H(j\omega)$ and the angle (argument), we get precisely the same amplitude ratio and relative phase angle that we computed in Eq. (4.17) and Eq. (4.18):

$$\|H(j\omega)\| = \frac{1}{\sqrt{\left[K - \left(M + \frac{I_{CM}}{a^2}\right)\omega^2\right]^2 + [\omega C]^2}} = \frac{1/K}{\sqrt{\left[1 - \left(\frac{\omega}{\omega_n}\right)^2\right]^2 + \left[2\varsigma\frac{\omega}{\omega_n}\right]^2}}$$

$$\angle H(j\omega) = -\tan^{-1}\frac{\omega C}{K - \left(M + \frac{I_{CM}}{a^2}\right)\omega^2} = -\tan^{-1}\frac{2\varsigma\frac{\omega}{\omega_n}}{1 - \left(\frac{\omega}{\omega_n}\right)^2}$$

(4.27)

In terms of our original differential equation, Eq. (4.15), the excitation and steady state response (particular solution) are of the following form:

$$f(t) = F_i\cos(\omega t + \phi_i) \text{ and } x_p(t) = F_i\|H(j\omega)\|\cos(\omega t + \phi_i + \angle H(j\omega))$$

(4.28)

Again we see that the steady state harmonic response is at the same frequency as the excitation with a different amplitude and phase. Also, remember that this expression is only valid for linear vibrating systems with time-invariant coefficients. The FRF is useful because its form does not change from one moment to another or for different excitation frequencies. The FRF also does not change regardless of how large the response amplitude becomes. This feature is where nonlinear vibrating systems commonly differ from linear vibrating systems, but nonlinear frequency response behavior is beyond the scope of this class.

It is also worthwhile to note the behavior of the FRF for certain frequencies and frequency ranges. The best way to do this is by plotting the magnitude and phase of the FRF, which remember are simply the amplitude ratio and relative phase of the steady state response to a simple harmonic input. In fact, we already did this in Figure 4.5 so there is no need to do it again. You should revisit the discussion preceding Figure 4.5 in light of the FRF in Eq. (4.27) in order to re-examined the forced steady state response behavior at low, middle, and high frequencies.

We could have also used the Fourier transform directly to find the FRF because, recall, Fourier transforms can be used to analyze the steady state input-output behavior of linear systems. In passing, note that the FRF of a given excitation-response pair is sometimes defined as the ratio of the Fourier transform of the steady state response (particular solution) to the Fourier transform of the excitation:

$$H(\omega) = \frac{\mathbf{F}[x_p(t)]}{\mathbf{F}[f(t)]} = \frac{X_p(\omega)}{F(\omega)} = \frac{1}{K - \left(M + \frac{I_{CM}}{a^2}\right)\omega^2 + j\omega C} \qquad (4.29)$$

where **F**[.] denotes the Fourier transform of a function and the *j* in front of the frequency argument is usually removed in this definition. Regardless of how the FRF is derived, it is extremely useful in analytical and experimental mechanical vibrations. Before proceeding, note again that the FRF only exists because the transient and steady-state solutions are decoupled as in Eq. (4.23) and (4.24); therefore, linear superposition is also responsible for the existence of FRFs. Let's continue to study more complicated forces by applying superposition as discussed in Figure 4.2.

4.7 Harmonic response for general periodic inputs using superposition

We have analyzed the forced response of SDOF systems to simple kinds of inputs like step (static) functions and individual harmonics; however, most inputs are more complicated than this. For instance, if we are going to use the accelerometer in Figure 4.10 to measure the acceleration of the surface to which it is attached, then we must be able to compute the response to any combination of harmonics. We follow the procedure in Figure 4.2 in order to do this.

The equation of motion for this system for a base excitation, $x_b(t)$, and a displacement of the piezo element, $x_o(t)$, is given below:

$$M\ddot{x}_o + C\dot{x}_o + Kx_o = C\dot{x}_b + Kx_b$$

(4.30)

An accelerometer uses the relative motion between the base of the accelerometer (i.e., motion of interest) and the piezo crystal/element, $z(t)=x_o(t)-x_b(t)$, to estimate the acceleration of the surface. When this new coordinate is substituted into Eq. (4.30), the nature of the accelerometer as an instrument for sensing acceleration is revealed:

$$M\ddot{z} + C\dot{z} + Kz = -M\ddot{x}_b$$

(4.31)

This equation indicates that the relative displacement, $z(t)$, is the response to an input acceleration at the base of the accelerometer, d^2x_b/dt^2. Because bodies often exhibit periodic acceleration response at multiple frequencies, it is desirable to express the base acceleration as a Fourier series like in Eq. (4.7):

$$x_b(t) = \sum_{n=0}^{\infty}\left[a_n \cos\left(n\omega_o t\right) + b_n \sin\left(n\omega_o t\right)\right]$$

(4.32)

All that remains is to compute the response to this series of harmonics. Because the model in Eq. (4.31) is linear, the responses to each individual harmonic input can be added to give the total response. To that end, the FRF for this system with an input d^2x_b/dt^2 and a response z is given by:

$$H(\omega) = \frac{Z(\omega)}{-\omega^2 X_b(\omega)} = \frac{-M}{K - M\omega^2 + j\omega C}$$

$$\text{where } \|H(\omega)\| = \frac{M}{\sqrt{\left[K - M\omega^2\right] + \left[\omega C\right]^2}} = \frac{1/\omega_n^2}{\sqrt{\left[1 - \left(\frac{\omega}{\omega_n}\right)^2\right]^2 + \left[2\varsigma\frac{\omega}{\omega_n}\right]^2}}$$

$$\text{and } \angle H(\omega) = -180^o - \tan^{-1}\frac{\omega C}{K - M\omega^2} = -180^o - \tan^{-1}\frac{2\varsigma\frac{\omega}{\omega_n}}{1 - \left(\frac{\omega}{\omega_n}\right)^2}$$

(4.33)

Note that the phase of the particular response always starts out at -180 degrees with respect to the base excitation for zero frequency and decreases (loses phase) as the frequency increases. Other interesting remarks can be made after the magnitude and phase of the FRF are plotted (see Figure 4.11 below). The 180 degree phase lag is removed in the signal processing electronics.

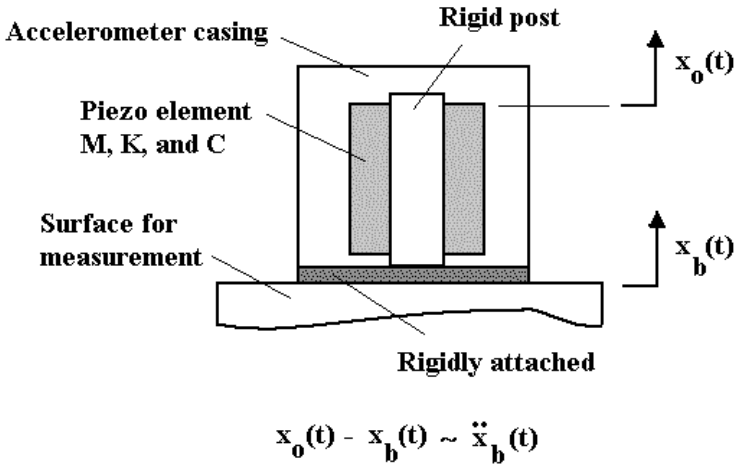

Figure 4.10: Schematic of single degree-of-freedom shear mode piezoelectric accelerometer

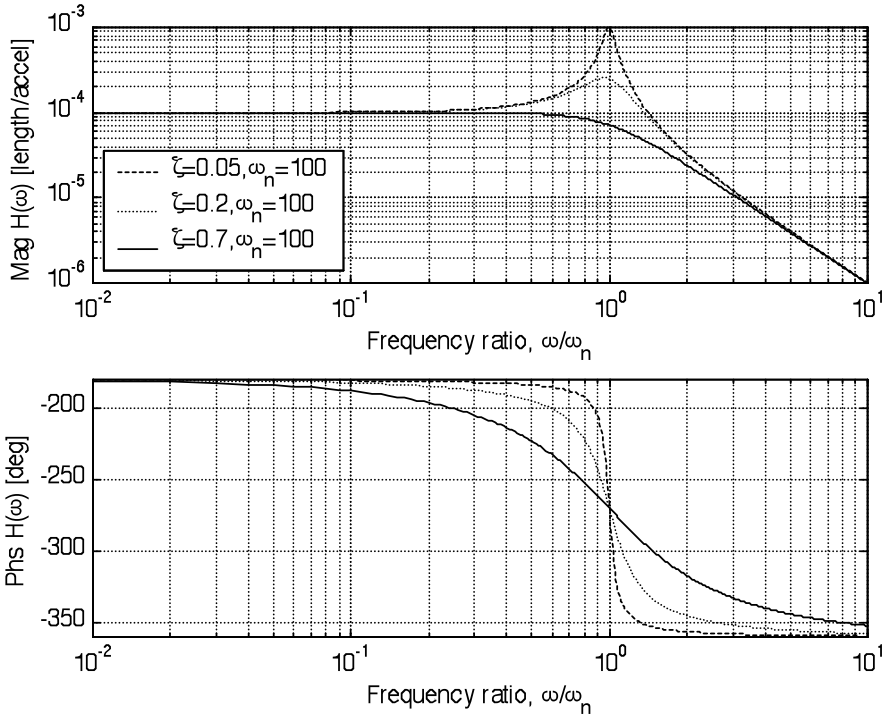

Figure 4.11: Frequency response magnitude and phase characteristics of an accelerometer

First, note that the low frequency (DC) amplitude ratio is $1/\omega^2_n = 1e\text{-}4\ sec^2$ (see Eq. (4.33)). Also note the effects of damping on the frequency response. For large amounts of damping the relative amplitude characteristic is flatter below the undamped resonant frequency, but the phase characteristic drops significantly in that frequency range. This drop in phase produces phase distortion; in other words, each harmonic response component is subjected to a different phase shift so the resultant measured acceleration is quite different from the true acceleration. Likewise, for small damping ratios the phase characteristic is flat nearly all the way out to the undamped resonance, but the amplitude ratio characteristic rises significantly as the resonant frequency is approached. This rise in amplitude produces amplitude distortion; in other words, each harmonic response component is subjected to a different calibration factor (i.e., a certain number of *volts* per *g* of acceleration, for instance). Accelerometers are typically designed to have damping ratios of approximately 0.6 or 0.7 to avoid amplitude distortion. Finally, note that the electronics in an actual accelerometer put an additional gain into the FRF to convert the length/acceleration units to volts/acceleration units. The motion of the piezoelectric element relative to the post produces a certain charge across the element, which is then converted into a voltage for output processing.

Having determined the FRF for the accelerometer, the steady state response to a general periodic input is therefore equal to:

$$z_p(t) = \sum_{n=0}^{\infty} \|H(n\omega_o)\|\left[a_n \cos\left(n\omega_o t + \angle H(n\omega_o)\right) + b_n \sin\left(n\omega_o t + \angle H(n\omega_o)\right)\right]$$

(4.34)

Each harmonic component is amplified and phase shifted according to the characteristic in Figure 4.11. Ideally, the amplitude factor, $||H(\omega)||$, in the frequency range of interest should be approximately flat (i.e., constant) as should the phase characteristic, $\angle H(\omega)$.

4.8 Frequency response functions in systems with non-viscous damping

We said in Chapter 3 that viscous damping is rare in mechanical systems. Other more realistic damping models including quadratic damping, Coulomb damping, and hysteretic/structural damping were discussed at that time. In this section, we will examine how hysteretic damping affects the FRF of the standard SDOF mechanical vibration model. Recall that if we set the viscous damping coefficient to $C_{eq}=h/\omega=\eta K/\omega$, where h is the hysteretic damping coefficient and η is the loss factor, then the SDOF model is slightly modified to:

$$M\ddot{x}_d + \tfrac{\eta K}{\omega}\dot{x}_d + Kx_d = F_i \cos\left(\omega t + \phi_i\right)$$

(4.35)

which is valid for simple harmonic inputs and has the FRF given in Eq. (4.36) below. The magnitude and phase angle of the FRF for this system are plotted in Figure 4.12. There are two main differences between this FRF and that of the corresponding SDOF system with viscous damping (see Figure 4.5):

- The relative phase for zero frequency is not zero; in other words, systems with hysteretic damping are never in phase with the excitation. This behavior is commonly seen in viscoelastics and other elastomers, which exhibit ‘relaxation’ when subjected to DC inputs.

- The low frequency stiffness characteristic changes when the loss factor changes; in other words, hysteretic damping seems to introduce both damping and stiffness-like characteristics into the FRF.

- The peak for all values of η is found at the undamped natural frequency, ω_n.

$$H(\omega) = \frac{1}{K - M\omega^2 + j\eta K}$$

$$\text{where } \|H(\omega)\| = \frac{1}{\sqrt{\left[K - M\omega^2\right]^2 + \left[\eta K\right]^2}} = \frac{1/K}{\sqrt{\left[1 - \left(\frac{\omega}{\omega_n}\right)^2\right]^2 + \left[\eta\right]^2}}$$

$$\text{and } \angle H(\omega) = -\tan^{-1}\frac{\eta K}{K - M\omega^2} = -\tan^{-1}\frac{\eta}{1 - \left(\frac{\omega}{\omega_n}\right)^2}$$

(4.36)

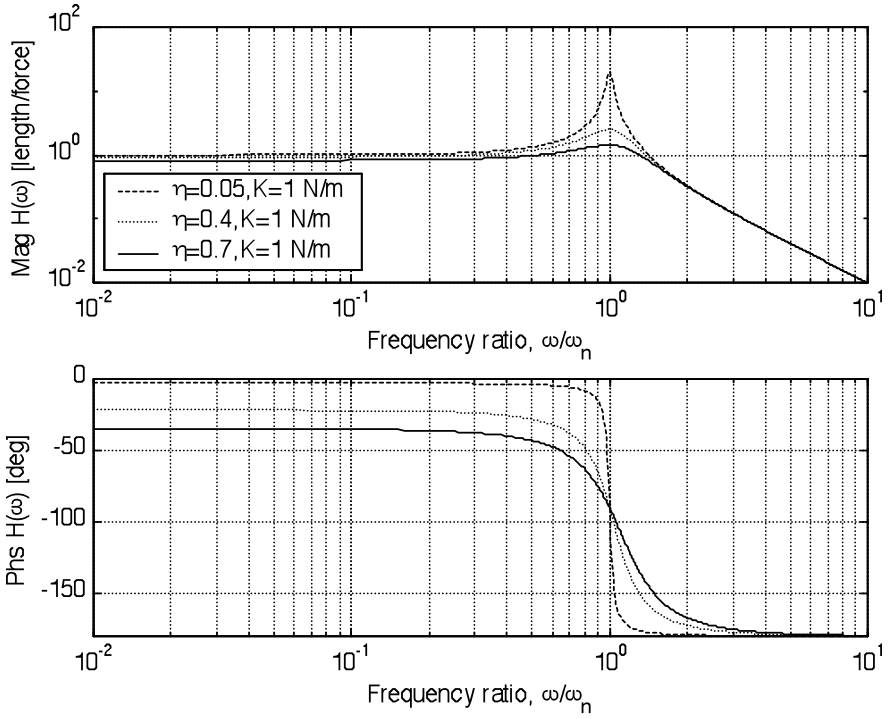

Figure 4.12: Frequency response magnitude and phase characteristics for hysteretic damping

Note that only the stiffness and damping-dominated regions of the FRF are affected by the change to hysteretic damping. The mass-dominated region is completely unaffected by this change because the inertia term is the same as in the viscous damping case.

4.9 Forced response to general inputs and transients through convolution

Even though we are now equipped to use Fourier series to describe general periodic excitations, we are still unable to describe inputs like potholes, for instance, in roads. Potholes and other transient-type excitations are not periodic, so they are not amenable to Fourier series analysis. We conclude that we need to find a different, more general, approach to forced response than the FRF. The approach we need is actually intimately related to the FRF approach as we will now explain.

Why was the FRF so useful? The answer is because its form did not change when the excitation frequency changed. But the FRF was applied in the frequency domain, that is, for excitations that are described as a series of harmonics. We want to find an expression in the time domain that can be used in a similar way with arbitrary types of excitations. Superposition will again be the basis of our approach. Consider the illustration in Figure 4.13. If we could develop a procedure for decomposing an arbitrary excitation, *f(t)*, into a sum of impulse functions and calculating the response to each impulse, then we could obtain the total forced response by simply adding up the responses to the individual impulses. This approach is only valid for linear vibrating systems (and time varying systems if we account for the variation with time of the response characteristic). This method is known as convolution and it works for any type of input.

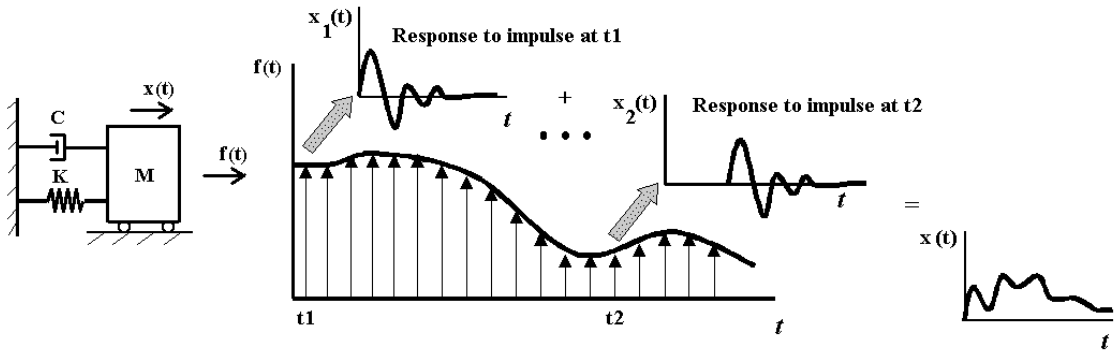

Figure 4.13: Illustration of impulse response convolution method for forced response analysis

The process of convolution begins by decomposing the excitation into an infinite train of impulses functions. This decomposition is accomplished using the special sieve property of the impulse function, $\delta(t)$, which is given by $\int\delta(t-a)f(t)dt=f(a)$. Each impulse has a strength equal to the value of $f(t)$ at the particular value of time, $t=n\Delta t$, times the time interval, Δt. The excitation can then be rewritten as follows:

$$f(t) = \sum_{n=0}^{+\infty} \delta\left(t - n\Delta t\right) f(n\Delta t)\Delta t$$

(4.37)

where it is assumed that the excitation is applied at $t=0$ and is zero before that time. Now we will find the particular solution to each of these impulses separately and then sum the results. First, we can find the impulse response of the SDOF vibrating system by applying the Fourier transform definition of the FRF given that the Fourier transform of $\delta(t)$ is 1:

$$X_p(\omega) = H(\omega)F(\omega) = \frac{1}{K - M\omega^2 + j\omega C} \cdot 1$$
$$\text{so that } x_p(t) = h(t) = \mathbf{F}^{-1}\left[H(\omega)\right]$$

(4.38)

where $\mathbf{F}^{-1}[.]$ denotes the inverse Fourier transform and $h(t)$ is called the unit impulse response function (IRF). Consequently, we see that the inverse Fourier transform of the FRF plays an important role in the forced response to arbitrary excitations.

If we want to avoid introducing Fourier transform theory, then we can use Eq. (4.24) and Laplace transforms instead. That equation is repeated below for a linear SDOF vibrating system:

$$X_d(s) = \frac{Ms + C}{Ms^2 + Cs + K} x_d(0) + \frac{M}{Ms^2 + Cs + K} \dot{x}_d(0) + \frac{1}{Ms^2 + Cs + K} F(s)$$

(4.39)

The important thing to notice is that the second term and the last term in this equation are almost identical when $F(s)=1$, which corresponds to an impulsive input, $\delta(t)$; therefore, we can say that

impulsive excitations introduce initial conditions on the velocity. Furthermore, the general form of the complementary solution for any set of initial conditions (see Eq. 3.15),

$$\begin{aligned} x_d(t) &= X_o e^{\sigma t}\cos(\omega_d t + \phi_o) \\ &= X_o e^{-\zeta\omega_n t}\cos\left(\sqrt{1-\zeta^2}\,\omega_n t + \phi_o\right) \\ \text{where } x_d(0) &= X_o\cos\phi_o \\ \dot{x}_d(0) &= \sigma X_o\cos\phi_o - \omega_d X_o\sin\phi_o \end{aligned}$$

can be used to solve for the impulse response by using the correct initial conditions corresponding to the impulsive excitation: $x_d(0)=0$ and $dx_d(0)/dt=1/M$, chosen to make the second and third terms of Eq. (4.39) match. Thus, $\varphi_o=-\pi/2$ and $X_o=1/M\omega_d$, which yield the following impulse response function:

$$x_p(t) = h(t) = \frac{1}{M\omega_d}e^{\sigma t}\sin(\omega_d t) \text{ for } t > 0$$

(4.40)

Note that the IRF is zero at time zero, has a finite initial velocity, and oscillates and decays as before. Finally, we can add up each of the impulse responses to the series of impulses in Eq. (4.37) by shifting the IRF to the times at which the impulses are applied and then integrating to obtain the particular response to an arbitrary excitation, $f(t)$:

$$\begin{aligned} x_p(t) &= \sum_{n=0}^{+\infty} h(t-n\Delta t)f(n\Delta t)\Delta t \\ \text{Let } \Delta t \to 0 \text{ then } x_p(t) &= \int_0^t h(t-\tau)f(\tau)d\tau \end{aligned}$$

(4.41)

Eq. (4.41) is profound because it suggests that if we know the IRF, which is determined solely by the system, then the particular response to any excitation can be found by convolving the excitation with the IRF. The integral in Eq. (4.41) is called a *convolution integral* for that reason. This development is valid for linear, time-invariant SDOF systems and provides the particular solution for zero initial conditions. As before, the total solution is equal to the sum of the complementary solution and the particular solution from Eq. (4.41).

As an example of how to apply the convolution integral, consider the system forced by a static input from Section 4.3. The equation under consideration there is repeated below:

$$\left(M + \frac{I_{CM}}{a^2} \right) \ddot{x} + C\dot{x} + Kx = Mg\sin\alpha + Kx_u$$

In this case, the input is a step function so $f(t)=(Mgsin\alpha+Kx_u)u_s(t)$, where $u_s(t)$ is called the unit step function and is zero before $t=0$ and 1 for $t>0$. The particular solution for zero initial conditions is found by substituting this excitation into Eq. (4.41):

$$\begin{aligned} x_p(t) &= \int_0^t h(t-\tau) f(\tau) d\tau \\ &= \int_0^t \frac{1}{M_{ef} \omega_d} e^{\sigma(t-\tau)} \sin(\omega_d (t-\tau)) (Mg\sin\alpha + Kx_u) d\tau \\ &= \frac{Mg\sin\alpha + Kx_u}{M_{ef} \omega_d} \int_t^0 e^{\sigma\theta} \sin(\omega_d \theta) d\theta \\ &= \frac{Mg\sin\alpha + x_u}{K} \left[1 - \frac{\omega_n}{\omega_d} e^{\sigma t} \cos\left(\omega_d t - \tan^{-1} \frac{\varsigma}{\sqrt{1-\varsigma^2}} \right) \right] \text{ for } t > 0 \end{aligned}$$

(4.42)

which was the same result we found in Section 4.3. In general, the calculus and algebra required to analytically calculate the convolution integral is unwieldy, so these integrations are done numerically instead.

4.10 Some common applications of forced vibration response analysis

The material in the previous sections is applied throughout many industries on a daily basis, so there are many different applications to discuss. Automotive engineers are continuing to develop new ways to minimize vibration and noise in their products, while micro-chip manufacturers are working diligently to develop sophisticated vibration isolation environments in which to assemble their products with precision. We will focus on a few traditional examples involving rotating (reciprocating) unbalance, vibration isolation, shaft whirl, and elastomeric mounts and bushings. See any textbook on vibration for discussions of these problems (e.g., Morse *et al*).

Reciprocating unbalance in rotating machinery produces oscillating (harmonic) inputs that, in turn, introduce unwanted (usually) vibration into systems. There are many good example of when the resulting vibration is actually desired. For instance, many baby bassinets are instrumented with inertial exciters that have small rotating inertias, which produce vibration that is supposed to 'sooth' babies. A basic rotating system with an eccentric mass is illustrated in Figure 4.14. This system could represent a clothes washer or dryer with an imbalance in how the clothes are distributed, a lathe or rotating machine tool with a slight imbalance, or any other rotating system in which the center of rotation does not coincide with the center of mass (e.g., fan, disk drive, etc.). M is the total mass of the system, m is the eccentric mass, e is the eccentricity, and ω is the frequency of operation. The system is supported by a linear spring and viscous damper. The equation of motion for the system by Newton's method is:

$$M\ddot{x} + C\dot{x} + Kx = me\omega^2 \sin(\omega t) \tag{4.43}$$

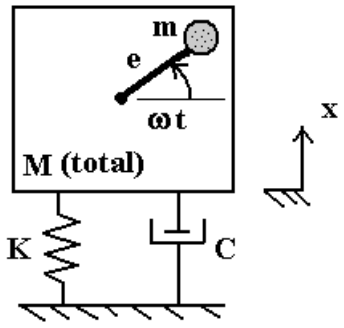

Figure 4.14: Schematic of SDOF system with rotating unbalance (eccentric oscillating mass)

Because the excitation is harmonic, we can use Eq. (4.26) to find the FRF as long as the dependence on frequency is included in the excitation:

$$\text{If } f(t) = me\omega^2 \sin(\omega t) = F_i \sin(\omega t), \text{ then } x_p(t) = X_p \sin(\omega t + \phi_p) \text{ where}$$

$$H(j\omega) = \frac{X(j\omega)}{F(j\omega)} = \frac{1/K}{1 - \left(\frac{\omega}{\omega_n}\right)^2 + j2\zeta\left(\frac{\omega}{\omega_n}\right)} \text{ and}$$

$$\frac{MX_p}{me} = \frac{\left(\frac{\omega}{\omega_n}\right)^2}{\sqrt{\left[1 - \left(\frac{\omega}{\omega_n}\right)^2\right]^2 + \left[2\zeta\left(\frac{\omega}{\omega_n}\right)\right]^2}} \qquad (4.44)$$

The phase of the particular solution can also be found, but we will focus on the magnitude characteristic. The last line of Eq. (4.44) is plotted in Figure 4.15 below. There are several interesting characteristics to note in this FRF magnitude plot:

- First, we notice that although there is still a peak in the FRF magnitude plot for the reciprocating unbalance problem as there was in previous Bode magnitude plots for forced SDOF systems, the shape of the FRF seems to be the mirror image of the one in Figures 4.5, 4.6, 4.11, and 4.12. More specifically, the flat stiffness region seems to have shifted to high frequencies (high operating speeds) and the steep mass region seems to have shifted to low frequencies (low operating speeds). This switch occurs because there is now a factor of ω^2 in the numerator of the FRF that 'cancels' the ω^2 in the denominator. Physically, the flat characteristic at high operating speeds implies that the center of mass of the rotating system is stationary.

- Second, note that if the goal is to have as little vibration as possible, then it is best to operate at speeds (frequencies) below the resonant frequency (i.e., $r<1$) because the amplitude is smaller in this region. This result is in contrast to the SDOF FRF characteristic.

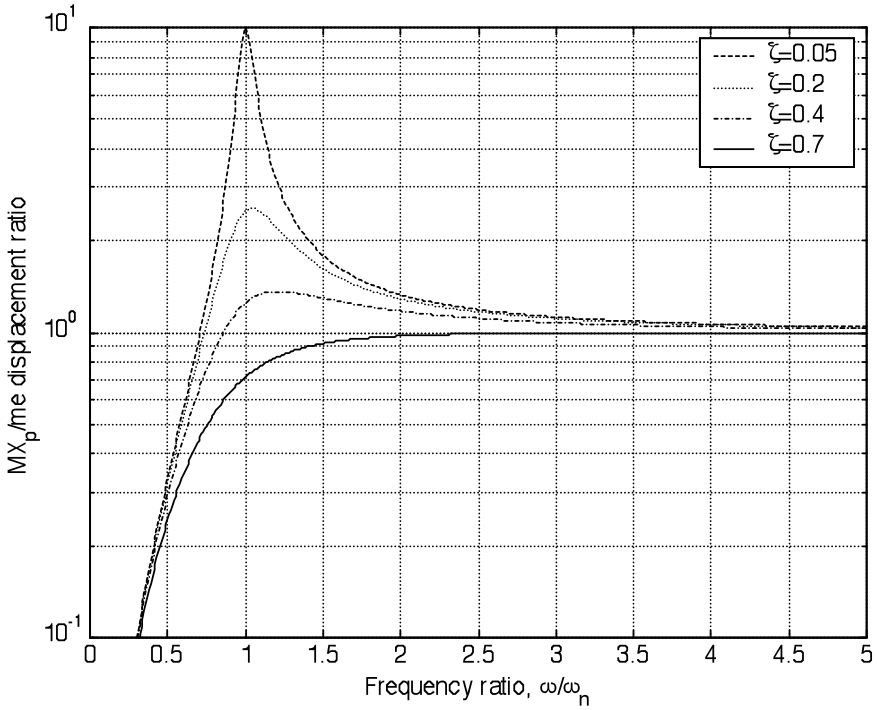

Figure 4.15: Amplitude of response due to reciprocating unbalance

Whirling shafts are also an important application for vibration analysis in rotating systems. Figure 4.16 is an illustration of the simplified problem involving shaft whirl. The shaft (assumed massless) and bearings both provide stiffness via a restoring force to the disk as it rotates about the axis through point *P*. The axis through point *O* passes through the two fixed bearing supports and is a reference for motion of points *P* and the disk center of mass, *G*. The rotational velocity of the line segment *OP* is called the whirl velocity and the distance *OP* is the whirling amplitude. Note that the whirl speed and direction are not always the same as the shaft speed and direction. The rotational speed of the shaft is prescribed and the equations of motion in the *x* and *y* directions are assumed to be uncoupled. Newton's method produces the following results:

$$M\ddot{x} + K_x x = Me\omega^2 \cos\omega t$$
$$M\ddot{y} + K_y y = Me\omega^2 \sin\omega t \qquad (4.45)$$

Note that the stiffness in the *x* and *y* directions are taken to be different, and the damping in both directions is set to zero; this result makes the problem less complicated and the results more easily interpreted. Also, note that the excitations for each direction are 90 degrees apart.

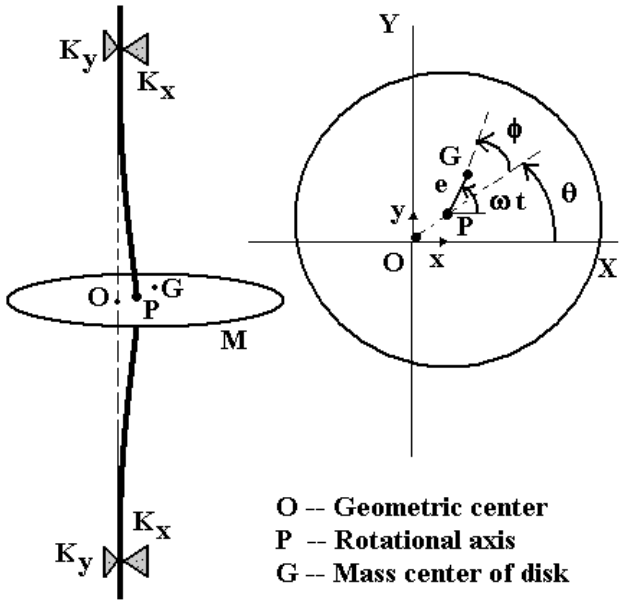

Figure 4.16: Illustration of shaft whirl geometry for equation of motion derivation

In the steady state, the magnitudes and phases of the *x* and *y* responses can be shown to be governed by the following FRFs:

$$\frac{X(j\omega)}{e} = \frac{\left(\frac{\omega}{\omega_{nx}}\right)^2}{1-\left(\frac{\omega}{\omega_{nx}}\right)^2} \text{ and } \frac{Y(j\omega)}{e} = \frac{\left(\frac{\omega}{\omega_{ny}}\right)^2}{1-\left(\frac{\omega}{\omega_{ny}}\right)^2} e^{-j\pi/2} \tag{4.46}$$

Again, we can note several interesting things about these FRFs and then relate these characteristics to the physical nature of the response:

- The amplitudes of $x_p(t)$ and $y_p(t)$ are not equal; thus, the motion of the point P cannot describe a circle but instead describes an elliptical shape. Because there is no damping, this ellipse has its major (or minor) axis aligned with the vertical (or horizontal).

- There are three regions of operation similar to those already discussed for the SDOF system above in Section 4.4. In the first region, $\omega < \omega_x$ and $\omega < \omega_y$, the x and y motions are 90 degrees out of phase and the disk and the point P rotate in the same direction. We assume here that the y motion is 90 degrees lagging the x motion because the y motion is forced with a sinusoid while the x motion is forced with a co-sinusoid. Think about this and make sure you understand why the two motions follow the path they do in Figure 4.17. Carefully consider the rotations of the line segments OP and PG.

- In the second region, $\omega > \omega_y$ and $\omega < \omega_x$ (or vice versa depending on whether or not $\omega_y <$ *or* $> \omega_x$), the x and y motions are 270 degrees out of phase so the disk and point P rotate in opposite directions because the $Y(j\omega)$ phase is -270 degrees whereas the $X(j\omega)$ phase is zero. The shaft speeds in this region are called *critical speeds* for two reasons: first, the amplitudes are rather large when the speed of rotation is near one of the undamped resonances; and second, the resultant phase shift between the disk rotation and rotation of point P introduces stress reversals in the shaft. These stress reversals can and often do result in fatigue failures under the right conditions.

- In the third and final region, $\omega > \omega_y$ and $\omega > \omega_x$, the x and y motions are again 90 degrees out of phase so the disk and the point P rotate in the same direction because the $Y(j\omega)$ phase is -270 degrees and the $X(j\omega)$ phase is -180 degrees. This region is the safest operating region with the smallest x and y amplitudes and no stress reversals. Finally, note that for high operating speeds, the center of mass of the disk, G, aligns itself with the center of rotation, O. Why is this? Think about the phase angle, φ, of the line segment OP with respect to PG.

- The whirl angle and speed are found by combining the x-y coordinates as follows:

$$\theta = \tan^{-1}\frac{y}{x}, \qquad \omega_{whirl} = \frac{d\theta}{dt} = \left(\sec^2\frac{y}{x}\right)\left(\frac{\dot{y}x - \dot{x}y}{x^2}\right)$$

(4.47)

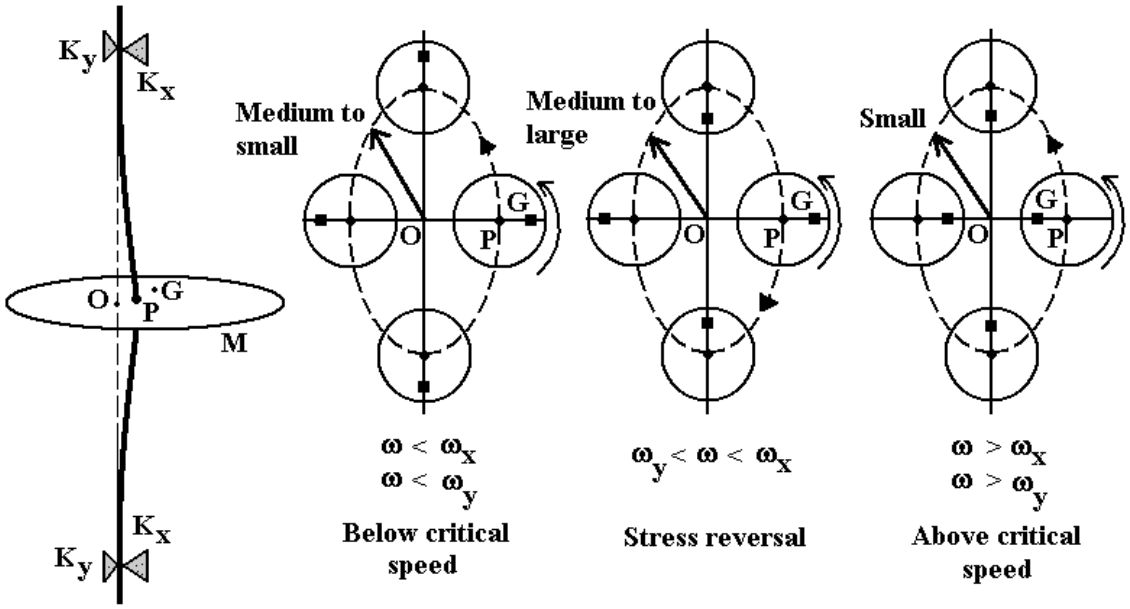

Figure 4.17: Illustration of shaft whirl geometry modes of vibration

Isolation and transmissibility reduction are also important applications in mechanical vibration analysis. The standard SDOF models for studying isolation and transmissibility characteristics of mounting systems are shown in Figure 4.18. In the model on the left, we are interested in how much of the excitation force, *f(t)*, is transmitted to the foundation, whereas in the model on the right, we are interested in how much of the base displacement is transmitted through to the isolated mass. The equations of motion for these two systems and the transmitted forces are given below:

$$\begin{aligned} &\text{LEFT}: \; M\ddot{x} + C\dot{x} + Kx = f(t) \;\text{ and }\; f_T(t) = C\dot{x} + Kx \\ &\text{RIGHT}: \; M\ddot{x}_2 + C\dot{x}_2 + Kx_2 = C\dot{x}_1 + Kx_1 \end{aligned}$$

(4.48)

The associated FRFs can be computed directly from these equations of motion. In the first case, the 'input' is the excitation force, $f(t)$, and the 'output' is the transmitted force, $f_T(t)$, and in the second case the 'input' is the base displacement, $x_1(t)$, and the 'output' is the mass displacement, $x_2(t)$. The FRFs are given below for these input-output pairs:

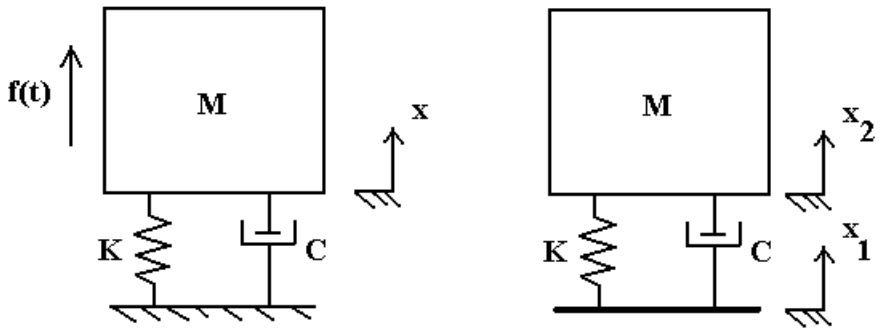

Figure 4.18: Single degree-of-freedom model for isolation and transmissibility analysis

$$\frac{F_T(j\omega)}{F(j\omega)} = \frac{1 + j2\zeta\left(\frac{\omega}{\omega_n}\right)}{1 - \left(\frac{\omega}{\omega_n}\right)^2 + j2\zeta\left(\frac{\omega}{\omega_n}\right)} = \frac{X_2(j\omega)}{X_1(j\omega)} \qquad (4.49)$$

Note that the FRFs are equal for the force transmissibility and motion transmissibility cases. The magnitude of this function is shown below in Figure 4.19. Note the following key characteristics:

- At low frequency, the transmission is one-to-one and at $\omega/\omega_n=\sqrt{2}$ it is also unity.

- Near resonance, $\omega/\omega_n=1$, the ratio is approximately a maximum; thus, we do not typically want to operate below the frequency, $\omega/\omega_n=\sqrt{2}$, because the best we can do in terms of isolation is one-to-one. For example, if we are trying to isolate a micro-chip bonding station and the floor is vibrating at 0.1 mm due to HVAC-related excitations, then the best we could do is to isolate the bonding operation to 0.1 mm displacement, which is clearly too large to obtain good repeatability and precision at the micro-scale.

- Above $\omega/\omega_n=\sqrt{2}$, the transmission ratio is less than one; this range is where isolation systems are designed to operate most effectively. Also note that isolation is actually BETTER for more lightly damped systems! This result is counterintuitive because we always think about damping as a way to reduce vibration, but in this case less damping actually provides better isolation.

- In practice, damping is not usually chosen too small because the speed must pass through resonance during 'start-up' procedures. If damping is too small, then the lightly damped response is quite high and can damage the isolation system if the speed dwells at resonance for too long.

- In summary, the resonant frequency of a force or motion isolation system is chosen much lower (1/10) than the frequency or frequencies of operation. This operating frequency provides better isolation as indicated by the comments above.

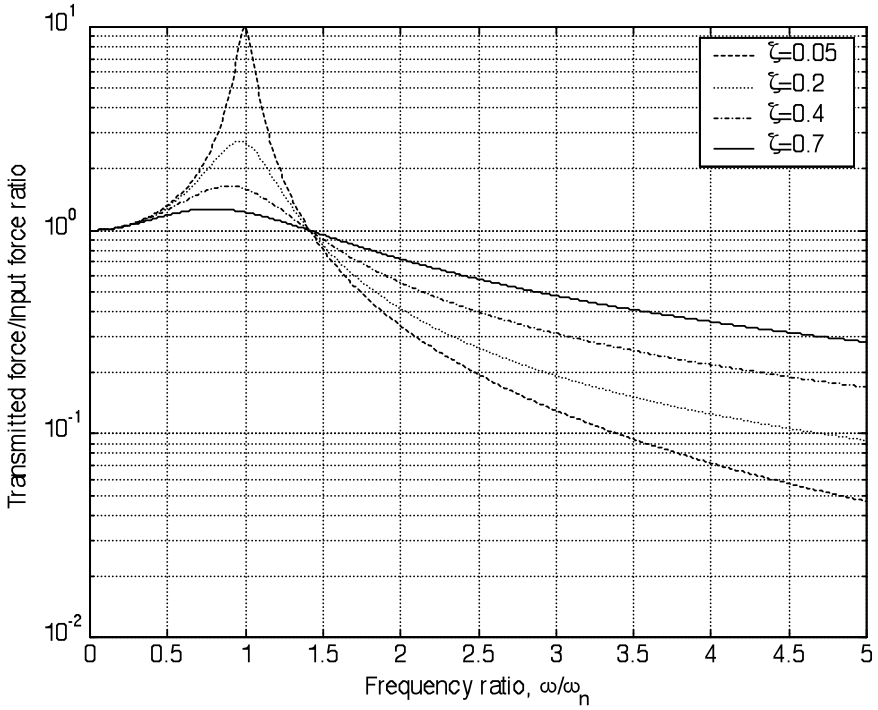

Figure 4.19: Isolation and transmissibility magnitude characteristic for SDOF systems

4.11 Forced response in multiple degree-of-freedom systems

Nothing changes from our previous forced response analysis when we add DOFs. We still use FRFs, except now we need more of them to account for the multiple inputs and multiple outputs we might have. We still use convolution integrals, except again we need more IRFs because there are more inputs and outputs to consider. Furthermore, we should expect from our discussion of modal decompositions in Chapter 3 that MDOF forced response analysis can be thought of as a group of SDOF forced response problems, and this is exactly the case. Superposition will play a new role in MDOF forced response analysis by giving us the capability to add the forced response results not only from various input harmonics but also from various inputs as well. This kind of spatial superposition is illustrated in Figure 4.20.

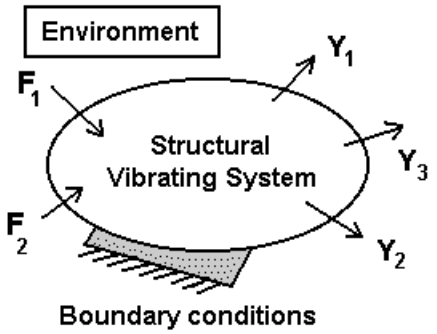

Total response = Sum of responses to individual forces at each frequency

$$Y_1 = H11 * F_1 + H12 * F_2$$

$$Y_2 = H21 * F_1 + H22 * F_2$$

$$Y_3 = H31 * F_1 + H32 * F_2$$

Figure 4.20: Illustration of spatial superposition in multiple degree-of-freedom systems

We will use the two DOF system from Eq. (3.21) to study the forced response of MDOF systems. For arbitrary forcing conditions, that system of equations is repeated below:

$$\begin{bmatrix} M & 0 \\ 0 & M \end{bmatrix} \begin{Bmatrix} \ddot{x}_1 \\ \ddot{x}_2 \end{Bmatrix} + \begin{bmatrix} 2C & -C \\ -C & C \end{bmatrix} \begin{Bmatrix} \dot{x}_1 \\ \dot{x}_2 \end{Bmatrix} + \begin{bmatrix} 2K & -K \\ -K & K \end{bmatrix} \begin{Bmatrix} x_1 \\ x_2 \end{Bmatrix} = \begin{Bmatrix} f_1(t) \\ f_2(t) \end{Bmatrix} \tag{4.50}$$

where $f_1(t)$ is applied to body 1 and $f_2(t)$ is applied to body 2. Since we saw in previous sections that step responses are a special case of harmonic responses at zero frequency, we will focus on the harmonic response problem. Instead of a transfer function, Eq. (4.50) produces a transfer function matrix after taking the Laplace transform and setting the initial conditions to zero. The impedance matrix and transfer function matrix are both computed below along with the characteristic polynomial, $\Delta(s)$.

$$
\begin{aligned}
[B(s)] &= \begin{bmatrix} Ms^2 + 2Cs + 2K & -Cs - K \\ -Cs - K & Ms^2 + Cs + K \end{bmatrix} \\
[H(s)] &= [B(s)]^{-1} \\
&= \frac{1}{\Delta(s)} \begin{bmatrix} Ms^2 + Cs + K & Cs + K \\ Cs + K & Ms^2 + 2Cs + 2K \end{bmatrix} \\
\text{where } \Delta(s) &= \left(Ms^2 + 2Cs + 2K\right)\left(Ms^2 + Cs + K\right) - \left(Cs + K\right)^2
\end{aligned}
$$

(4.51)

The transfer function matrix relates the responses to the excitations as follows:

$$
\begin{aligned}
[B(s)] \begin{Bmatrix} X_1(s) \\ X_2(s) \end{Bmatrix} &= \begin{Bmatrix} F_1(s) \\ F_2(s) \end{Bmatrix} \\
&\text{and} \\
\begin{Bmatrix} X_1(s) \\ X_2(s) \end{Bmatrix} &= [H(s)] \begin{Bmatrix} F_1(s) \\ F_2(s) \end{Bmatrix} \\
&= \begin{bmatrix} H_{11}(s) & H_{12}(s) \\ H_{21}(s) & H_{22}(s) \end{bmatrix} \begin{Bmatrix} F_1(s) \\ F_2(s) \end{Bmatrix} \\
\text{where } H_{11}(s) &= \left(Ms^2 + Cs + K\right) / \Delta(s) \\
H_{12}(s) &= H_{21}(s) = \left(Cs + K\right) / \Delta(s) \\
H_{22}(s) &= \left(Ms^2 + 2Cs + 2K\right) / \Delta(s)
\end{aligned}
$$

(4.52)

Eq. (4.52) is the basis for frequency response analysis in MDOF systems. The following comments summarize the most important characteristics in this expression:

- Each response has two components: one due to the first excitation and another due to the second excitation. This is the spatial superposition highlighted in Figure 4.20.

- Each transfer function, $H_{pq}(s)$, describes the effects that $F_q(s)$ has on $X_p(s)$. Stated differently: if $F_2(s)=0$ then the response at $X_1(s)$ is solely due to $F_1(s)$ and is equal to $H_{11}(s)F_1(s)$.

- Each transfer function has the same denominator, which is a reflection of our earlier discussion about how the system alone (and B.C.s) determines the modal frequencies because the modal frequencies are found by setting this denominator equal to zero, $\Delta(s)=0$ (the characteristic equation). This result implies that no matter what the input is or what the output is, the modal frequencies that govern the complementary and particular solutions will be identical.

- Although there are four transfer functions, only three of them are unique because the mass, damping, and stiffness matrices are symmetric. Likewise, there are four FRFs and four IRFs, but only three of each of them are unique.

The FRFs associated with the transfer functions in Eq. (4.52) are found by letting $s=j\omega$, which produces the following set of frequency domain equations of motion:

$$\begin{Bmatrix} X_1(j\omega) \\ X_2(j\omega) \end{Bmatrix} = \begin{bmatrix} H_{11}(j\omega) & H_{12}(j\omega) \\ H_{21}(j\omega) & H_{22}(j\omega) \end{bmatrix} \begin{Bmatrix} F_1(j\omega) \\ F_2(j\omega) \end{Bmatrix}$$

$$\text{where } H_{11}(j\omega) = \left(K - M\omega^2 + j\omega C\right) / \Delta(j\omega)$$

$$H_{12}(j\omega) = H_{21}(s) = \left(K + j\omega C\right) / \Delta(j\omega)$$

$$H_{22}(j\omega) = \left(2K - M\omega^2 + j\omega 2C\right) / \Delta(j\omega)$$

(4.53)

It is worthwhile to reflect on the meaning of Eq. (4.53) for a moment. If DOF 1 is forced with a simple harmonic input at a frequency, ω_1, and DOF 2 is forced with a simple harmonic input at frequency, ω_2, then the response at either one of the DOFs contains two components in the steady state, which are at the same frequency as the inputs but have different amplitudes and phases. In

equation form, the two time domain excitations and particular (steady state) responses are written as follows using FRF notation:

$$\text{If } f_1(t) = F_{1i}\cos(\omega_1 t + \phi_{i1}) \text{ and } f_2(t) = F_{2i}\cos(\omega_2 t + \phi_{i2})$$
$$\text{then,}$$
$$x_{1p}(t) = \|H_{11}(j\omega_1)\|F_{1i}\cos(\omega_1 t + \phi_{i1} + \angle H_{11}(j\omega_1)) + \|H_{12}(j\omega_2)\|F_{2i}\cos(\omega_2 t + \phi_{i2} + \angle H_{12}(j\omega_2))$$
$$x_{2p}(t) = \|H_{21}(j\omega_1)\|F_{1i}\cos(\omega_1 t + \phi_{i1} + \angle H_{21}(j\omega_1)) + \|H_{22}(j\omega_2)\|F_{2i}\cos(\omega_2 t + \phi_{i2} + \angle H_{22}(j\omega_2))$$

(4.54)

Therefore, the total responses of the two DOF system to any set of initial conditions are:

$$\begin{Bmatrix} x_1(t) \\ x_2(t) \end{Bmatrix} = X_{1o}\begin{Bmatrix} \psi_{11} \\ \psi_{21} \end{Bmatrix} e^{\sigma_1 t}\cos(\omega_{d1}t + \phi_{1o}) + X_{2o}\begin{Bmatrix} \psi_{12} \\ \psi_{22} \end{Bmatrix} e^{\sigma_2 t}\cos(\omega_{d2}t + \phi_{2o}) + \begin{Bmatrix} x_{1p}(t) \\ x_{2p}(t) \end{Bmatrix}$$

(4.55)

This equation is applied in the same way as Eq. (4.23) by applying the initial conditions to calculate the unknown parameters in the complementary solution.

Now consider the form of the four FRFs in Eq. (4.54). Each of the complex $H_{pq}(j\omega)$ has a magnitude and phase (argument) that vary as a function of frequency, but the nature of these functions is quite different and more 'complex' than those for the SDOF in Figure 4.5. The four Bode diagrams for these FRFs are plotted in Figure 4.21. The physical meaning of these functions can be described as follows:

- First note that there are two resonances in each FRF and that these damped natural frequencies are the same in each of the plots because modal frequencies do not depend on the location of the excitation or response. When the system is excited at each of its undamped natural frequencies, it exhibits a particular mode shape of vibration. Figure 4.22 illustrates this frequency response behavior for the modes at 6.2 rad/s and 16.2 rad/s with the following inputs at DOF 1: $cos(6.2 \cdot t)$ and $cos(16.2 \cdot t)$ (force units).

- $H_{11}(j\omega)$ and $H_{22}(j\omega)$ are *driving point* FRFs because they describe the sinusoidal response amplitude and phase when the excitation and response are at the same DOF in the system. Note that the phase in each of these FRFs 'recovers' following the so-called *antiresonances*, which are the frequencies at which the FRF magnitude drops suddenly (also called complex zeroes). Therefore, an N DOF system exhibits a -180 degree phase shift in its driving point FRFs over the entire frequency range. Intuitively, this is because driving point responses 'want' to follow their respective inputs at each mode of vibration. Mathematically, 180 degrees of phase is added at the antiresonances due to the numerator dynamics in the FRFs (i.e., Ms^2+Cs+K in $H_{11}(j\omega)$).

- All of the FRFs (magnitude and phase) are flat towards zero frequency because for smaller frequencies (near zero), the system behaves like a group of static springs according to:

$$\begin{Bmatrix} X_1(j0) \\ X_2(j0) \end{Bmatrix} = \frac{1}{K^2}\begin{bmatrix} K & K \\ K & 2K \end{bmatrix}\begin{Bmatrix} F_1(j0) \\ F_2(j0) \end{Bmatrix} \tag{4.56}$$

- $H_{12}(j\omega)$ and $H_{21}(j\omega)$ are equal, so the system is said to exhibit Maxwell-Beti reciprocity, which always holds when the mass, viscous damping, and stiffness matrices are symmetric. Also, note that although the phase in each of these so-called 'cross-point' FRFs fails to recover after the resonances because there are no antiresonances (for this two DOF case), an N DOF system does not exhibit a $-N*180$ degree phase shift over the entire frequency range, rather a $-N*180+90$ degree shift. Intuitively, this result is obtained because cross-point responses tend to lag behind their respective inputs at each mode of vibration.

- Three sets of FRF are shown for varying mass, varying damping, and varying stiffness in Figures 4.23, 4.24, and 4.25, respectively. Think about the changes in the resonances and antiresonances and try to develop explanations for these shifts in the FRFs.

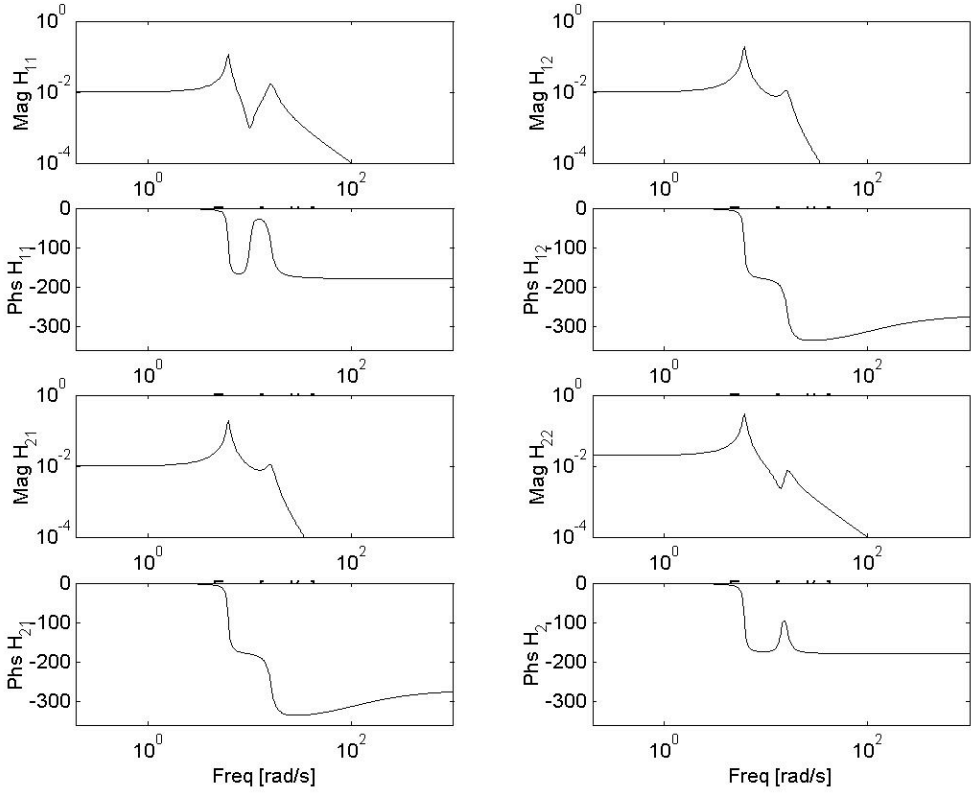

Figure 4.21: FRF Bode diagrams for two degree-of-freedom system

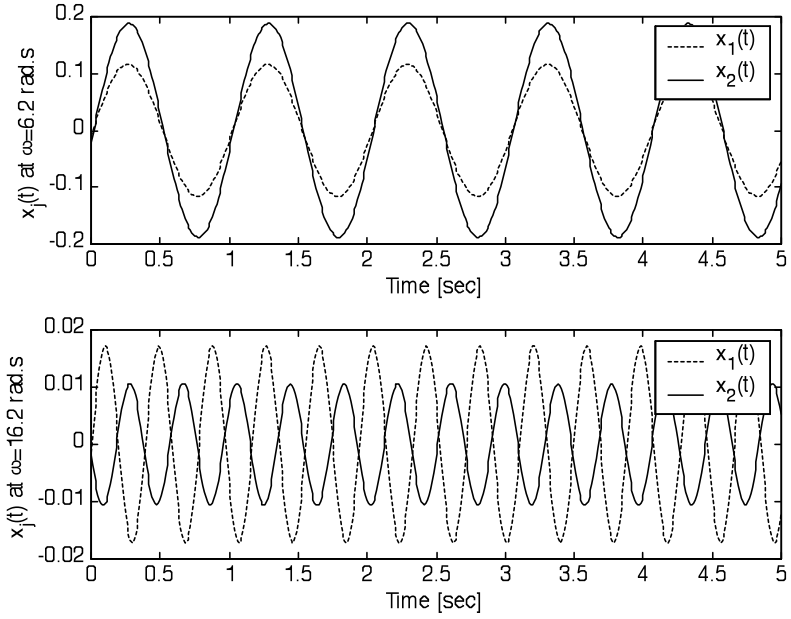

Figure 4.22: Steady state responses of two DOF system for excitations at two resonances

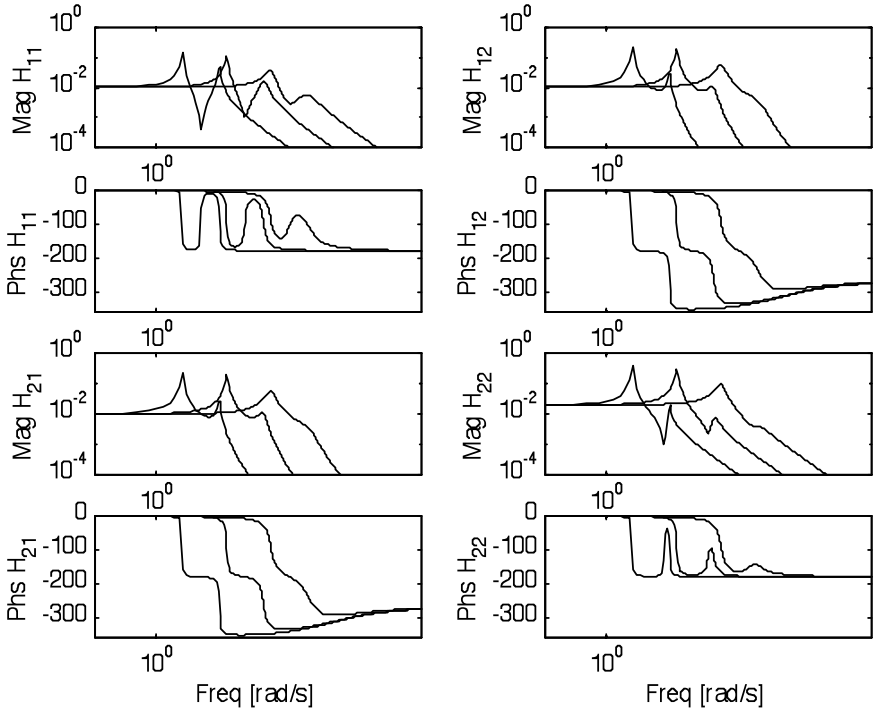

Figure 4.23: FRF Bode diagrams for two degree-of-freedom system (variable *M*)

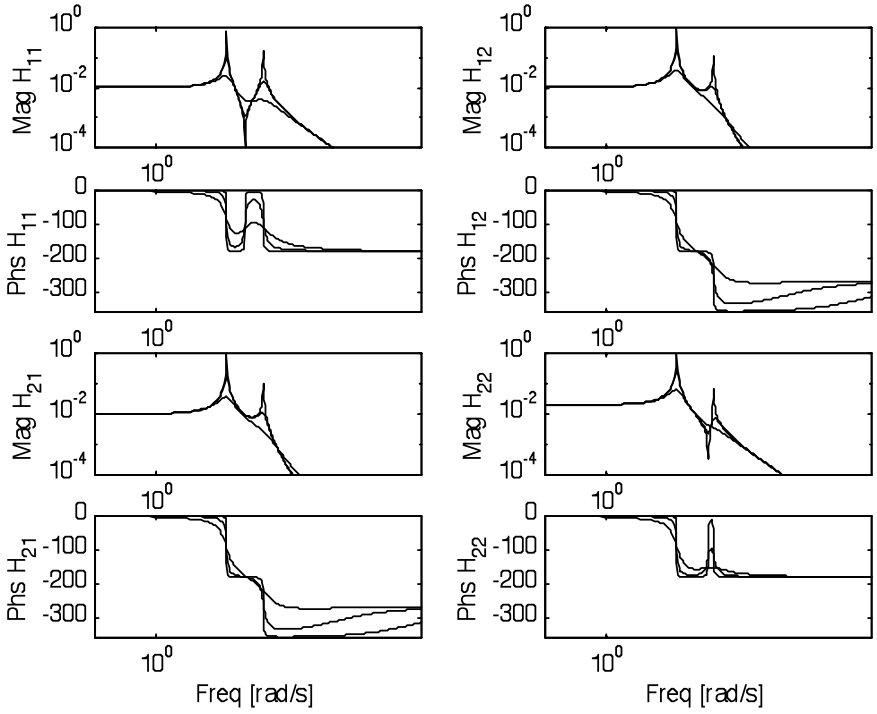

Figure 4.24: FRF Bode diagrams for two degree-of-freedom system (variable *C*)

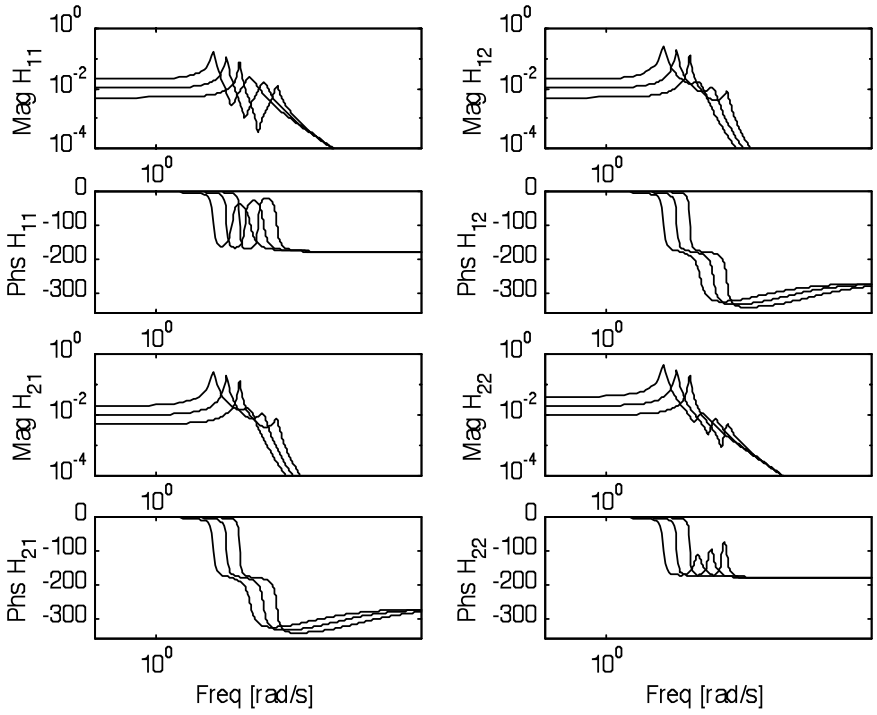

Figure 4.25: FRF Bode diagrams for two degree-of-freedom system (variable *K*)

4.12 Common applications in multiple degree-of-freedom forced analysis

In many vibration isolation systems, elastomers are used as the primary building block. Examples of elastomers include engine and powertrain mounts and bushings in linkage mechanisms. Because elastomers have both stiffness and damping, and because they exhibit special characteristics, they require a slightly different modeling approach. Figure 4.26 illustrates one type of model for an elastomer that includes a linear spring in parallel with a series damper-spring. The purpose of this model is to describe the frequency-dependent nature of the damping and stiffness characteristics of the elastomer. In other words, the stiffness of the elastomer is not simply, *K*, but instead is dependent on the frequency of excitation. Likewise, the damping also depends on frequency. The two equations of motion that describe the system in Figure 4.26 are given below:

$$\begin{aligned} M\ddot{x} + C\left(\dot{x} - \dot{x}_o\right) + Kx &= F_i \sin \omega t \\ C\left(\dot{x} - \dot{x}_o\right) &= K_e x_o \end{aligned} \qquad (4.57)$$

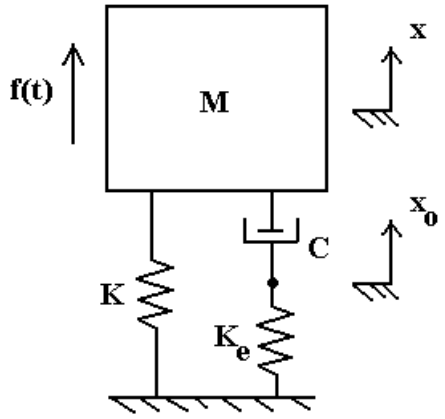

Figure 4.26: Model of linear elastomeric damper

For zero initial conditions, the Laplace transforms of both sides of these equations are,

$$\begin{aligned} \left(Ms^2 + Cs + K\right)X(s) - CsX_o(s) &= F(s) \\ CsX(s) - CsX_o(s) &= K_eX_o(s) \end{aligned}$$

(4.58)

After solving the second of these equations for $X_o(s)$ and substituting the result into the first equation, the following transfer function between $X(s)$ and $F(s)$ is obtained:

$$\text{With } X_o(s) = \frac{Cs}{Cs + K_e}X(s), \text{ we have}$$

$$\begin{aligned} \frac{X(s)}{F(s)} &= \frac{Cs + K_e}{\left(Ms^2 + Cs + K\right)\left(Cs + K_e\right) - C^2s^2} \\ &= \frac{Cs + K_e}{MCs^3 + MK_es^2 + CKs + CK_es + KK_e} \end{aligned}$$

(4.59)

The corresponding frequency response function is rewritten in the following way,

$$\frac{X(j\omega)}{F(j\omega)} = \frac{j\omega C + K_e}{KK_e\left(1-\frac{\omega^2}{\omega_n^2}\right) + j\omega C\left(K + K_e - M\omega^2\right)}$$

$$= \frac{K_e\left(\frac{j\omega C}{K_e}+1\right)}{KK_e\left(1-\frac{\omega^2}{\omega_n^2}\right) + j\omega CK\left(1+\frac{K_e}{K}-\frac{\omega^2}{\omega_n^2}\right)}$$

$$= \frac{\frac{1}{K}\left(\frac{j\omega C}{K_e}+1\right)}{\left(1-\frac{\omega^2}{\omega_n^2}\right) + j\frac{\omega C}{K_e}\left(1+\frac{K_e}{K}-\frac{\omega^2}{\omega_n^2}\right)}$$

$$= \frac{\frac{1}{K}\left(j2\varsigma_e\frac{\omega}{\omega_{ne}}+1\right)}{\left(1-\frac{\omega^2}{\omega_n^2}\right) + j2\varsigma_e\frac{\omega}{\omega_{ne}}\left(1+N-\frac{\omega^2}{\omega_n^2}\right)}, \text{ where } \omega_n^2 = \frac{K}{M},\ N = \frac{K_e}{K},\ \frac{2\varsigma_e}{\omega_{ne}} = \frac{C}{K_e}$$

(4.60)

We could have also obtained this FRF by describing the responses, $x(t)$ and $x_o(t)$, as the imaginary parts of the rotating phasors, $Xe^{j\omega t}$ and $X_oe^{j\omega t}$, where X and X_o are complex amplitudes, and the excitation, $f(t)$, as the imaginary part of the rotating phasor, $F_ie^{j\omega t}$, where F_i is the real amplitude of the excitation. This approach would have led to the exact same FRF as in Eq. (4.60). The magnitude and phase of this FRF are plotted in Figure 4.27 below. Note the following characteristics of this plot:

- The SDOF FRF for an elastomer support has the same low frequency (stiffness) characteristics as the SDOF FRF for viscous damping. This result is obtained because the damper in Figure 4.26 cannot support any static load, so all of the static support comes from the stiffness, K.

- The SDOF FRF for viscous damping passes through -90 degrees phase at the undamped natural frequency, $\omega_n=\sqrt{(K/M)}$, but the SDOF FRF with an elastomer support does not. This result is obvious from Eq. (4.60) and means that resonance is delayed to a slightly higher frequency.

- Even though the elastomer support has the same damping coefficient, C, and same mass, M, it has a smaller damping ratio, ζ, because the effective stiffness near resonance is $K+K_e$ (i.e. $\zeta=C/2\sqrt{(K_{eff}M)}$).

- As K_e increases, the system in Figure 4.26 approaches the system in Figure 4.18 (left).

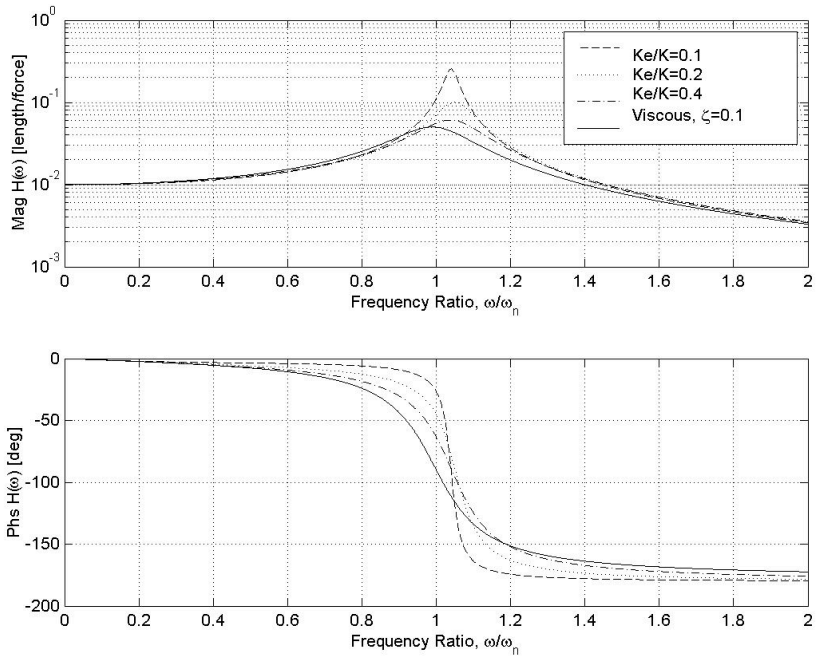

Figure 4.27: Frequency response function for SDOF system with elastomer support

The differences mentioned above become important when discussing vibration (force and motion) isolation systems as described before (see Figure 4.19). The transmissibility function across an elastomer is derived below and plotted in Figure 4.28 for *M=1 kg*, *K=100 N/m*, *C=2 N-s/m*, and variable K_e. Note that there is little difference between the reduction in transmissibility achieved when using a viscous or elastomer isolation system in the low-to-mid frequency range; however, there is a substantial difference above $\omega/\omega_n>5$. Also, the relative phase approaches -180 degrees for the elastomer but only -90 degrees for the system with viscous damping as frequency increases. Intuitively, this phase difference means that the elastomer is more effective

at blocking higher frequencies because it has an additional power of $j\omega$ in the denominator of its FRF that helps to cause a $1/\omega^2$ decrease in amplitude rather than just a $1/\omega$ decrease due to this additional loss in phase.

$$\frac{F_T(j\omega)}{F(j\omega)} = \frac{K\frac{1}{K}\left(j2\zeta_e\frac{\omega}{\omega_{ne}}+1\right)+K_e\left(\frac{1}{K}j2\zeta_e\frac{\omega}{\omega_{ne}}\right)}{\left(1-\frac{\omega^2}{\omega_n^2}\right)+j2\zeta_e\frac{\omega}{\omega_{ne}}\left(1+N-\frac{\omega^2}{\omega_n^2}\right)}$$

$$= \frac{1+j2\zeta_e\frac{\omega}{\omega_{ne}}(N+1)}{\left(1-\frac{\omega^2}{\omega_n^2}\right)+j2\zeta_e\frac{\omega}{\omega_{ne}}\left(1+N-\frac{\omega^2}{\omega_n^2}\right)} \qquad (4.61)$$

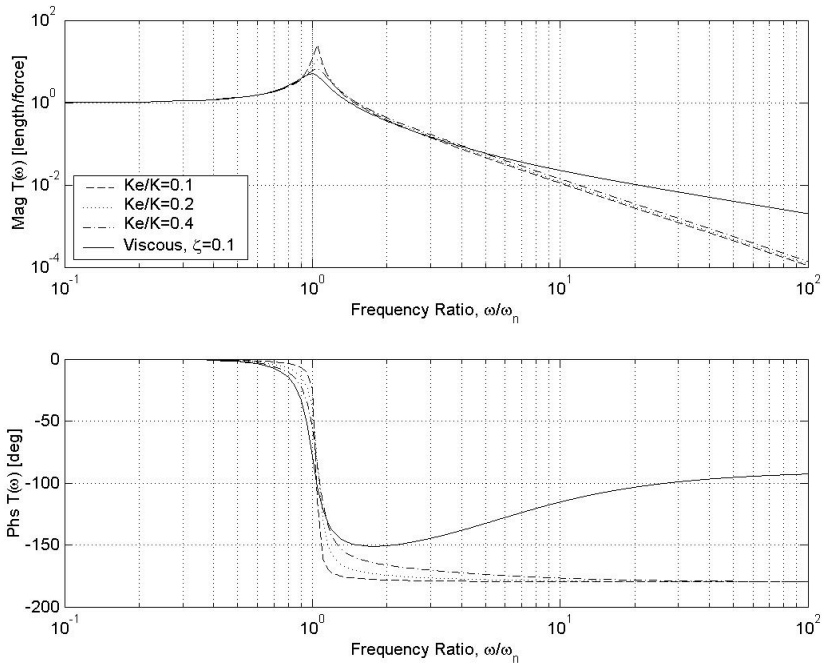

Figure 4.28: Transmissibility function for SDOF system with elastomer support

If a SDOF system is forced near its resonant frequency, it will vibrate with large amplitudes. If the damping is increased, its steady state amplitude will decrease considerably; however, damping is usually very difficult to introduce into systems either in the original design or with a retrofitted damper of some kind. For that reason, a different type of vibration reduction mechanism is often used: the vibration absorber. Vibration absorbers do not dissipate energy like damping does; rather, they absorb energy that would otherwise be imparted to the original system by the excitation. Figure 4.29 is a schematic of an undamped SDOF system with and without a vibration absorber.

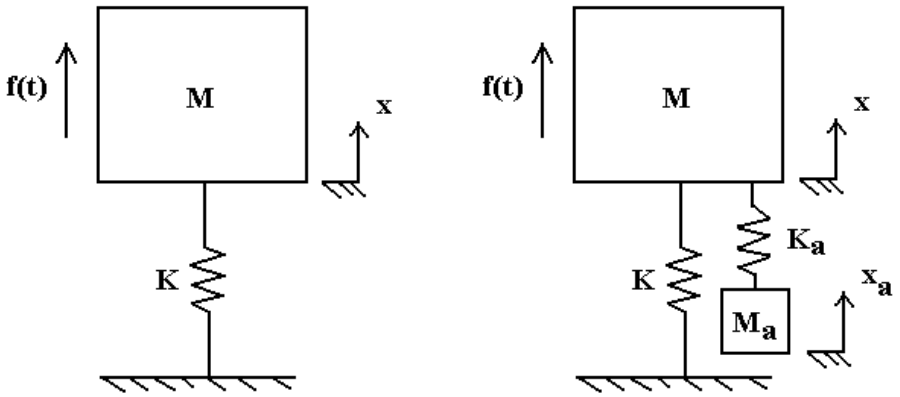

Figure 4.29: SDOF undamped system with (right) and without (left) a vibration absorber

The equations of motion of these systems derived using Newton's laws are given below:

$$\text{WITHOUT}: \; M\ddot{x} + Kx = F_i \sin \omega t$$
$$\text{WITH}: \; M\ddot{x} + (K + K_a)x - K_a x_a = F_i \sin(\omega t) \text{ and } M_a \ddot{x}_a + K_a x_a - K_a x = 0 \qquad (4.62)$$

and the associated FRF and FRF matrix are:

$$\text{WITHOUT}: \frac{X(\omega)}{F(\omega)} = \frac{1}{K - M\omega^2}$$

$$\text{WITH}: \quad \begin{Bmatrix} X(\omega) \\ X_a(\omega) \end{Bmatrix} = \begin{bmatrix} K + K_a - M\omega^2 & -K_a \\ -K_a & K_a - M_a\omega^2 \end{bmatrix}^{-1} \begin{Bmatrix} F(\omega) \\ 0 \end{Bmatrix}$$

$$= \frac{1}{\Delta(\omega)} \begin{bmatrix} K_a - M_a\omega^2 & K_a \\ K_a & K + K_a - M\omega^2 \end{bmatrix} \begin{Bmatrix} F(\omega) \\ 0 \end{Bmatrix}$$

where

$$\Delta(\omega) = \left(K + K_a - M\omega^2\right)\left(K_a - M_a\omega^2\right) - K_a^2$$

(4.63)

Note the form of these two sets of equations. First, the equations in Eq. (4.62) are differential equations and the equations in Eq. (4.63) are algebraic equations, yet they describe the same exact systems. This transformation from differential to algebraic equations is the main benefit of using Laplace (and Fourier) transforms for solving vibrations problems. Instead of having to integrate the time domain equations of motion, we can look directly at the algebraic equations in the frequency domain and solve the problem almost by inspection.

In this case, we would like to design the absorber so that the response of the system near resonance, $\omega=\sqrt{(K/M)}$, is reduced. If we force the system with a harmonic excitation at resonance, then energy will continually be added to the system because we are exciting the system in phase with its velocity. This resonant forcing causes the amplitude of the displacement response to grow linearly without bound. Our goal is to design a vibration absorber so this does not happen. In other words, we want the energy we put into the system to be absorbed by the mass M_a instead of mass M. The question is: What should the absorber mass and stiffness be in order to produce the minimum motion of mass M at the resonant frequency $\omega=\sqrt{(K/M)}$? The answer is in the 1-1 element of the FRF matrix in Eq. (4.63). If we design the absorber such that $\sqrt{(K_a/M_a)}=\omega_n=\sqrt{(K/M)}$, then the mass M does not move at all in the steady state because:

$$\begin{Bmatrix} X(\omega) \\ X_a(\omega) \end{Bmatrix} = \left(\frac{1}{\Delta(\omega)} \begin{bmatrix} K_a - M_a\omega^2 & K_a \\ K_a & K + K_a - M\omega^2 \end{bmatrix} \right) \Bigg|_{\omega=\omega_n=\sqrt{K_a/M_a}} \begin{Bmatrix} F(\omega) \\ 0 \end{Bmatrix}$$

$$= \frac{-1}{K_a^2} \begin{bmatrix} 0 & K_a \\ K_a & K_a \end{bmatrix} \begin{Bmatrix} F(\omega) \\ 0 \end{Bmatrix}$$

$$= \begin{Bmatrix} 0 \\ \frac{-1}{K_a} F(\omega) \end{Bmatrix} \Leftrightarrow \begin{cases} x_p(t) = 0 \\ x_{ap}(t) = \frac{F_i}{K_a} \sin(\omega t - \pi) \end{cases}$$

(4.64)

The original FRFs between the excitation, *f(t)*, and response, *x(t)*, and modified FRFs with the absorber included are shown in Figure 4.30. Note that the particular response is zero at resonance when the absorber is perfectly tuned and very small when the absorber is mistuned by 10% to either side of the resonance. In the presence of damping, the tuning requirements are more complicated but are easily determined as well.

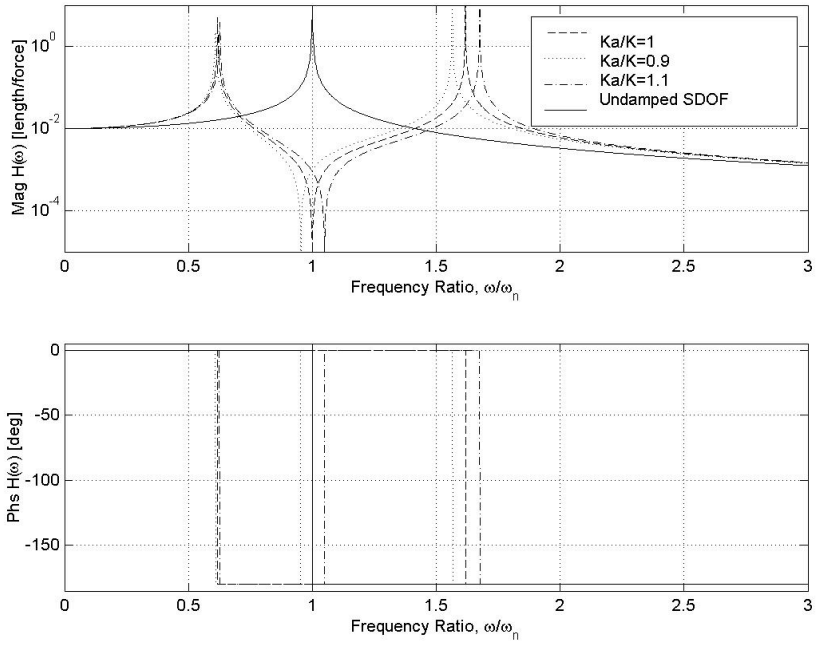

Figure 4.30: FRFs for undamped SDOF system and system with absorber